

The Large Scale Structure of the Universe 4: Redshift Space Distortions and New observables

Eusebio Sánchez Álvaro
CIEMAT

UniCamp Winter School on Observational Cosmology
Sao Paulo
July 2018

RSD, combined probes and future projects

Redshift Space Distortions. Modelling and measurement
Cosmology with RSD

Combined probes: cross-correlations

Brief intro to Weak Gravitational Lensing

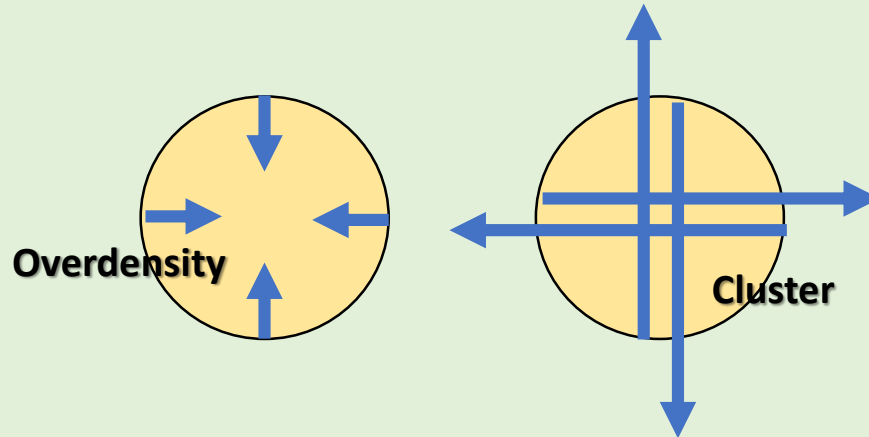
Cosmology results from DES 3x2pt (combining probes)

Very brief description of future experiments on LSS (DES, DESI, Euclid, LSST)

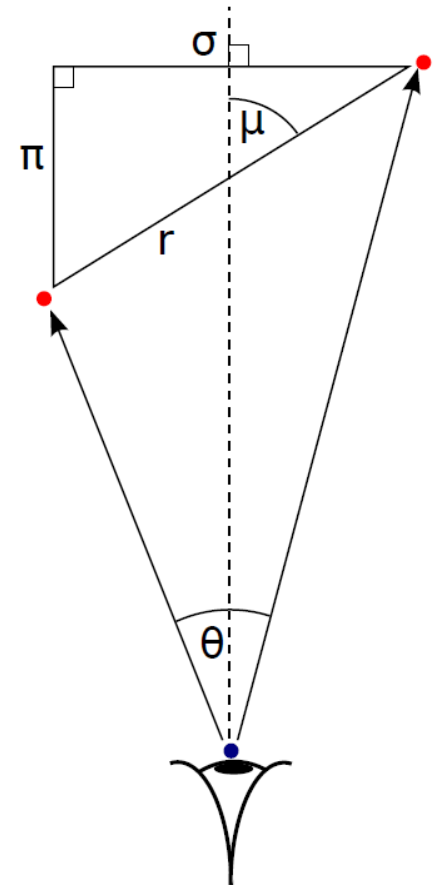
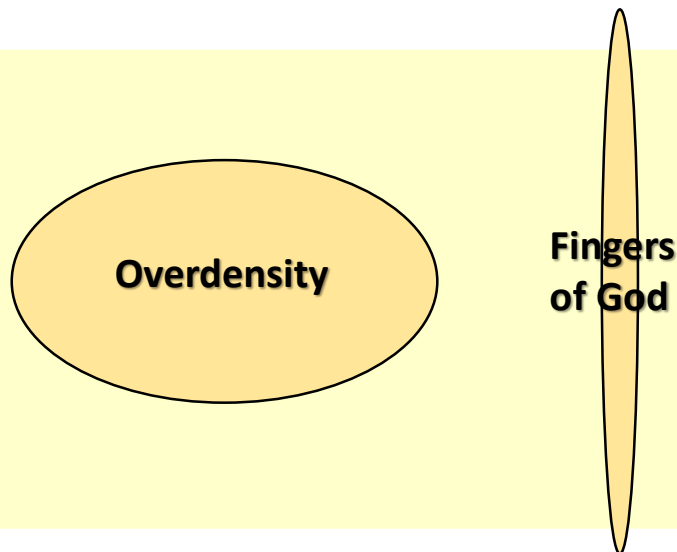
REDSHIFT SPACE DISTORTIONS

The spatial distribution of galaxies appears squashed and distorted when studied in the redshift space. But we only measure redshift, not distances. The RSD are always present

**Real
Space**



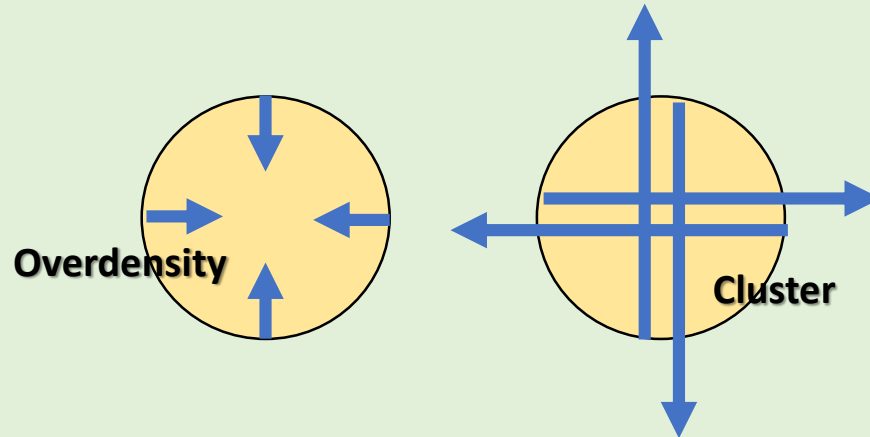
**Redshift
Space**



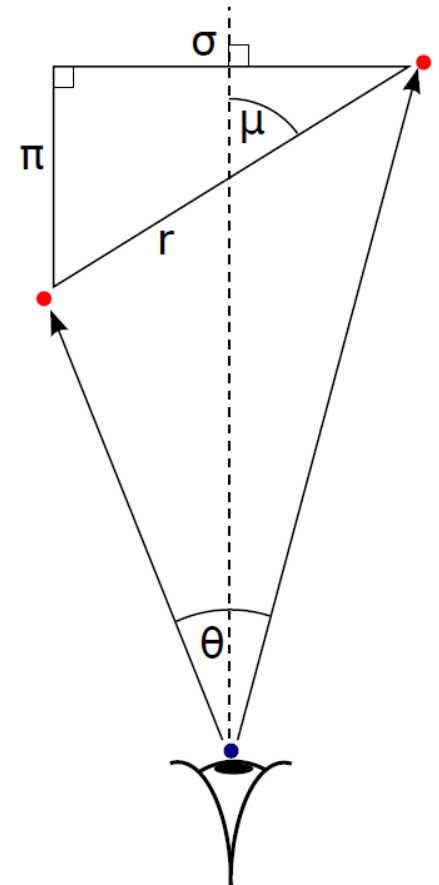
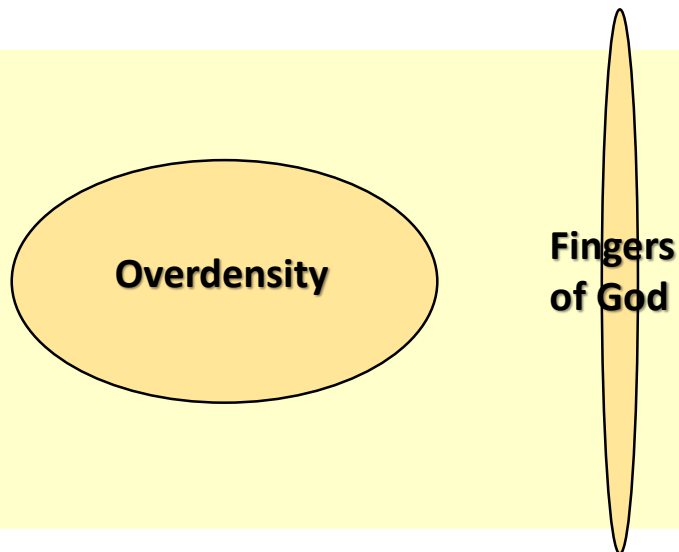
REDSHIFT SPACE DISTORTIONS

They are a consequence of peculiar velocities → Coming from structure
They carry very valuable information about cosmology

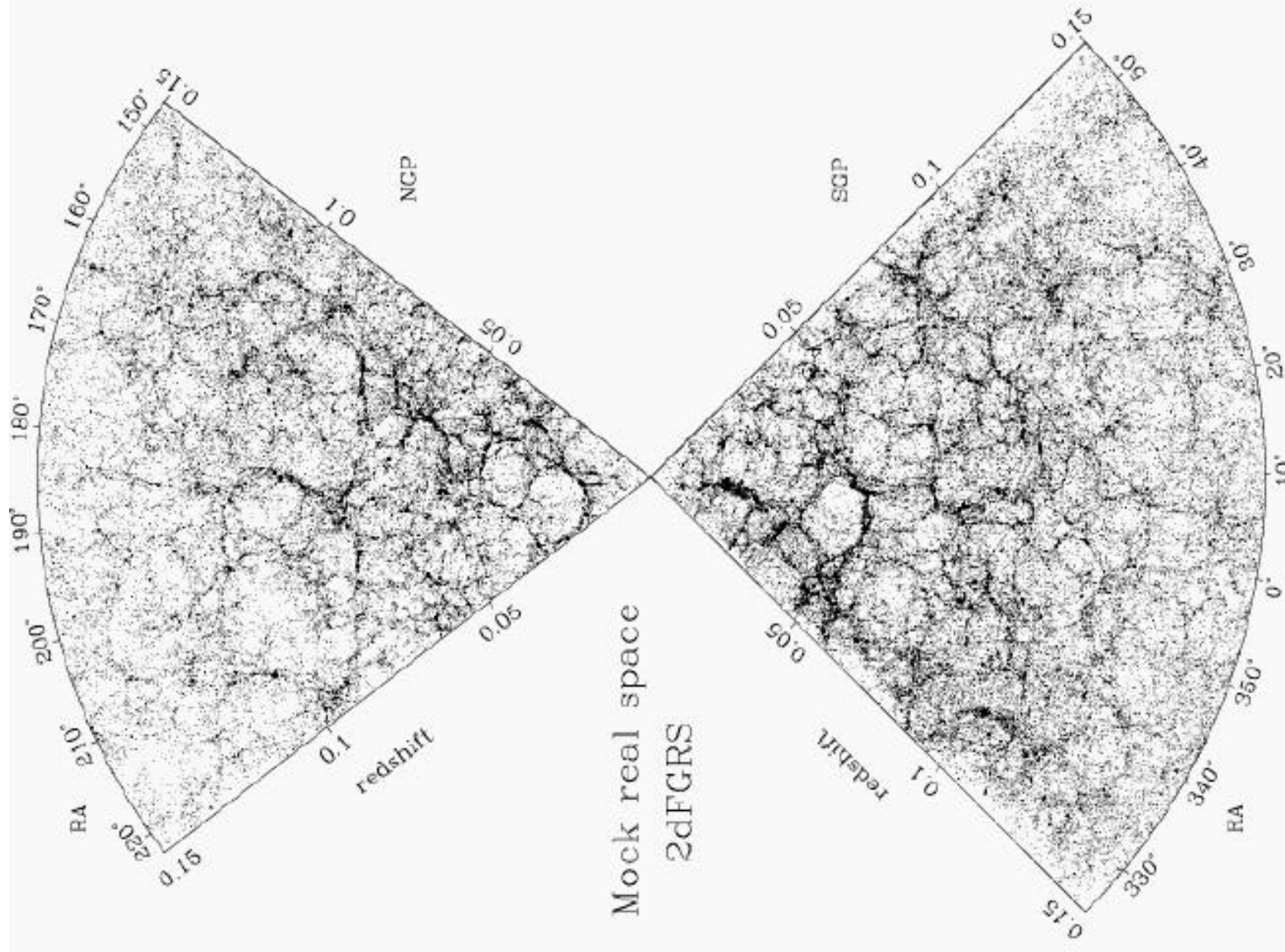
**Real
Space**



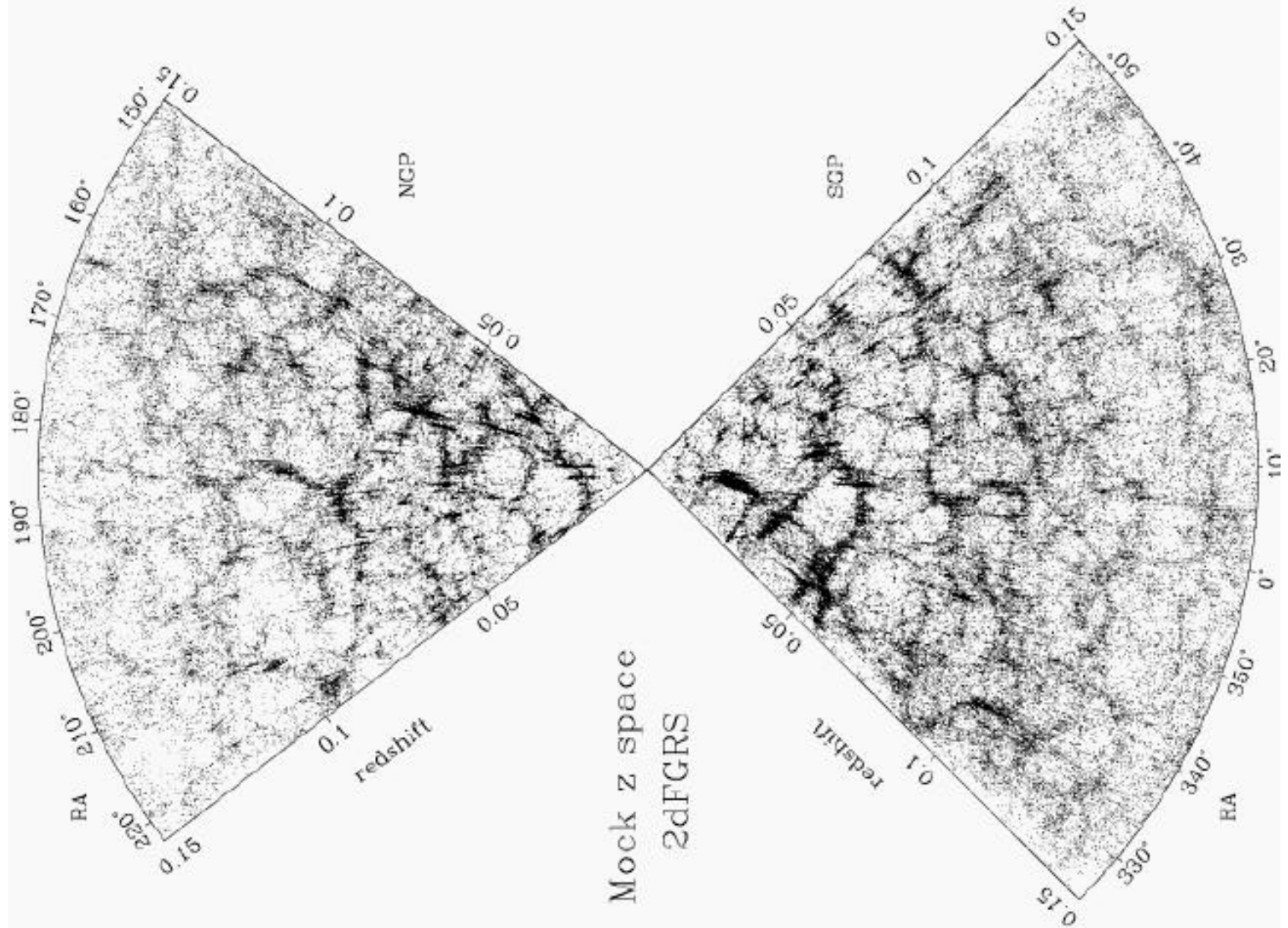
**Redshift
Space**



REDSHIFT SPACE DISTORTIONS



REDSHIFT SPACE DISTORTIONS



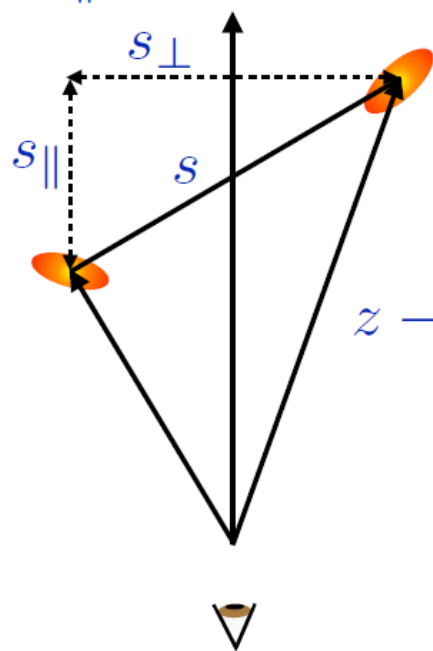
The full BAO power

Anisotropic clustering

Measuring angular and
radial BAO separately

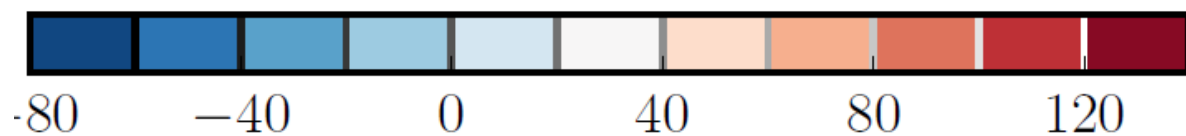
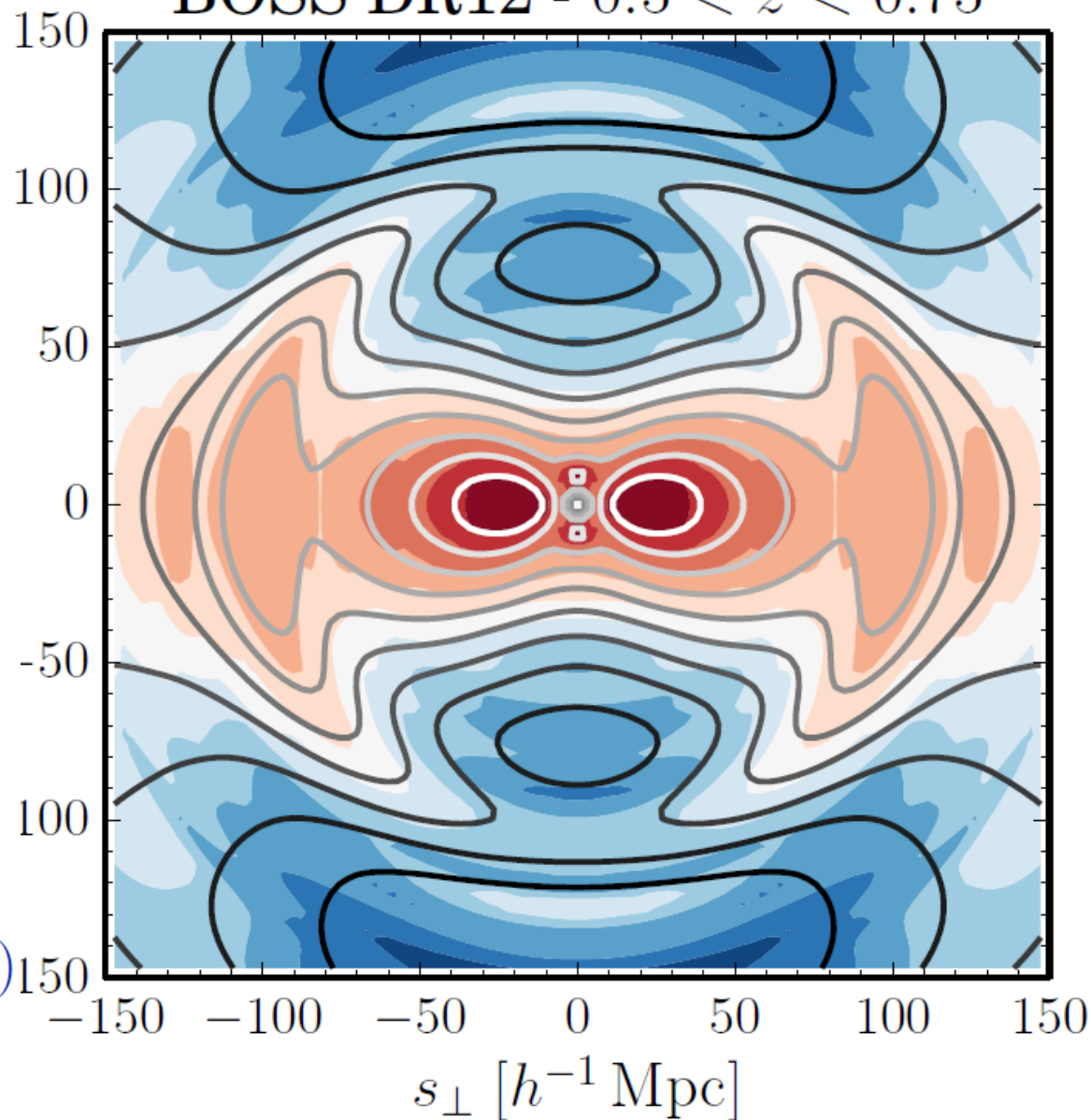
Redshift space distortions

$\xi(s_{\perp}, s_{\parallel})$



BOSS DR12 - $0.5 < z < 0.75$

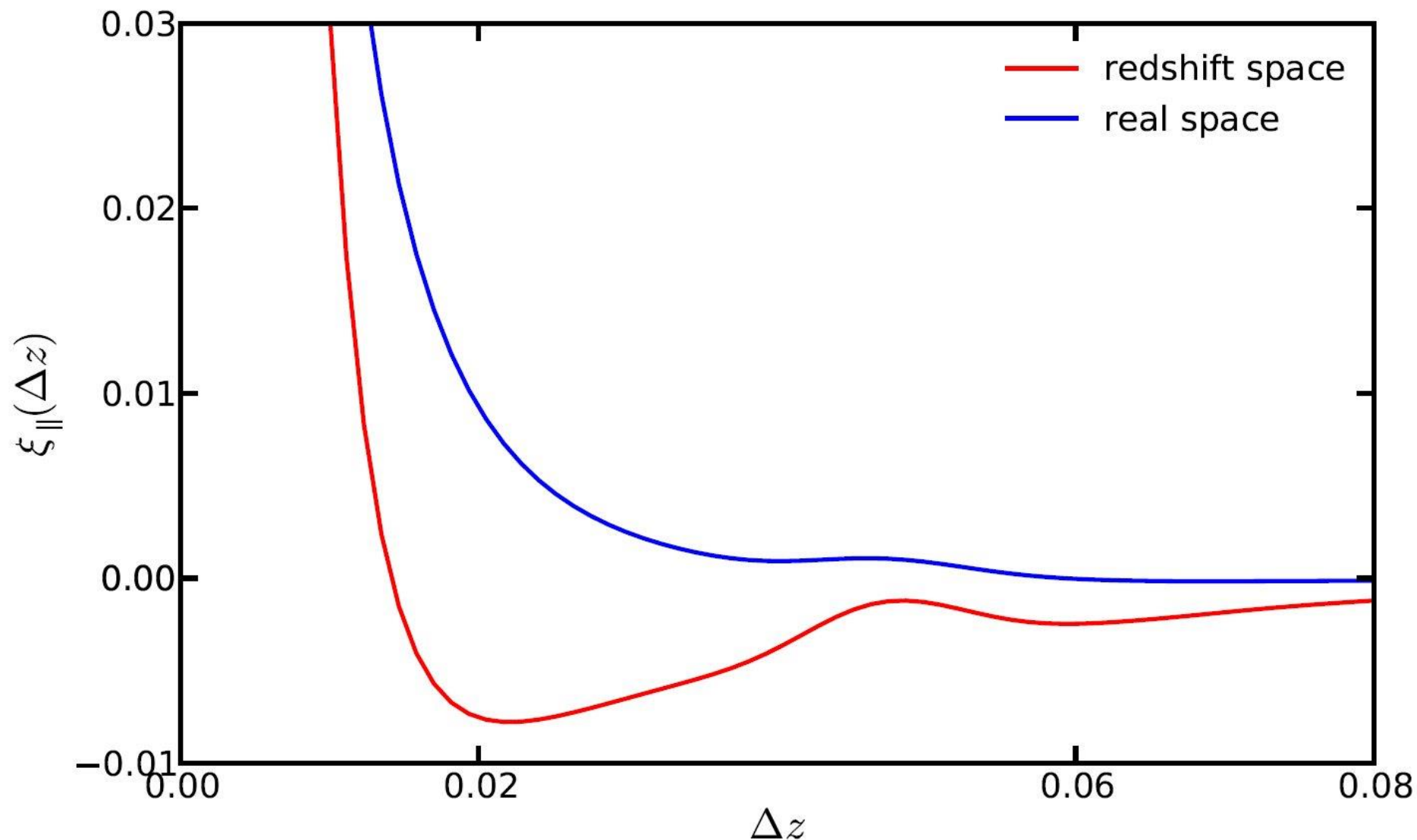
$[h^{-1} \text{ Mpc}]$



The shape of the correlation function changes dramatically when RSD are included

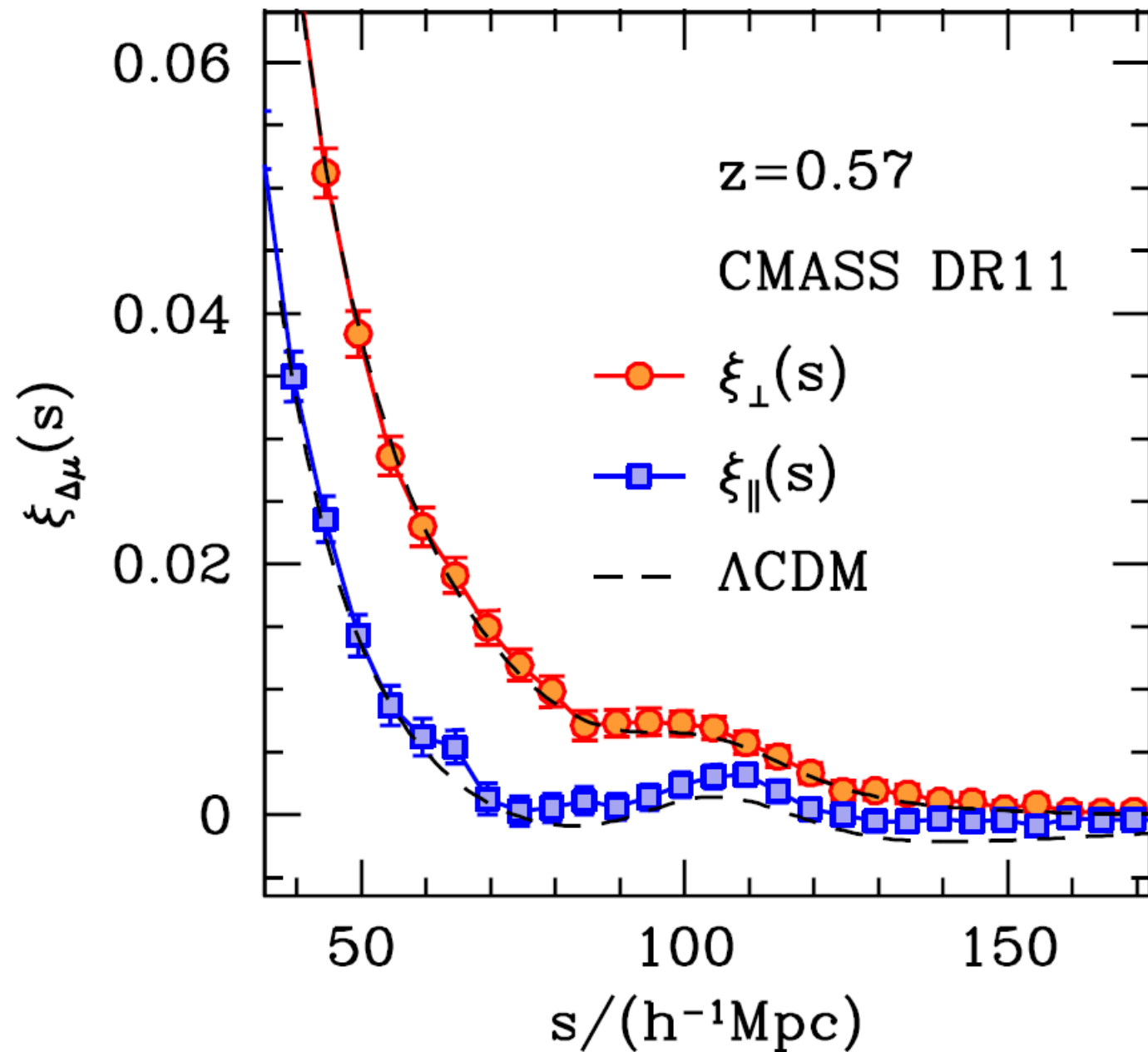
However the BAO peak position does not change

BAO is very robust against systematic errors

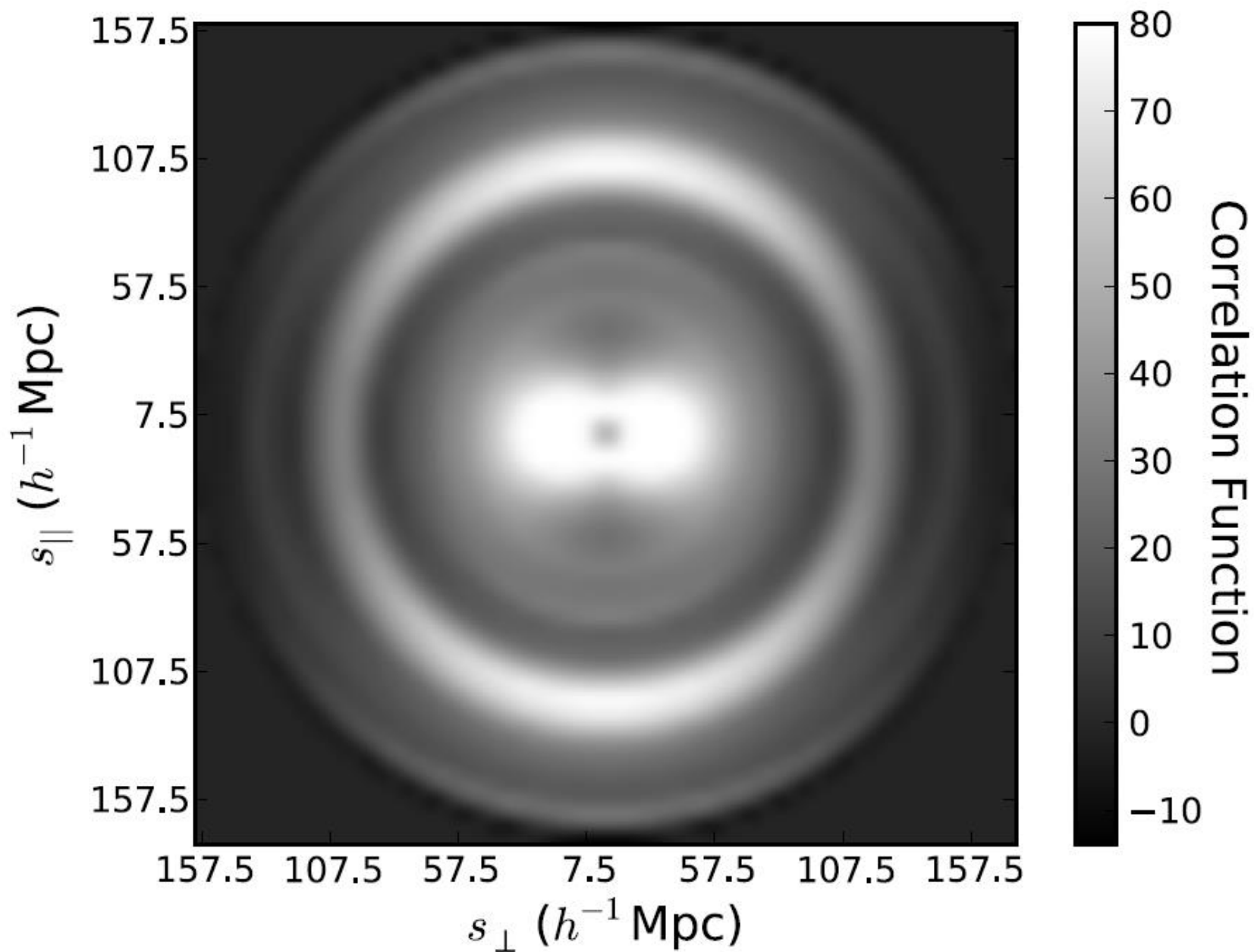


The RSD have
been
measured
many times

RSD are one
of the
cosmological
probes
sensitive to
the growth of
structure that
are used
today



RSD effect is concentrated in intermediate scales of the correlation function
BAO is seen as an excess in a ring with radius $\sim 110 h^{-1} \text{ Mpc}$



$$\delta_{s,\mathbf{k}} = (1 + \beta \mu_{\mathbf{k}}^2) \delta_{r,\mathbf{k}} \quad \mu_{\mathbf{k}} \equiv \mathbf{k} \cdot \hat{\mathbf{n}}_z / k$$

$$\beta = \frac{f}{b} \approx \frac{\Omega_{m0}^{0.6}}{b} \quad \beta = \frac{\Omega_M^\gamma}{b}$$

Hence, redshift-space distortions induce an anisotropy in the observed power spectrum, which now is a function of both k and μ_k

$$P_s(k, \mu_{\mathbf{k}}, z) = (1 + \beta(z) \mu_{\mathbf{k}}^2)^2 P_r(k, z)$$

Redshift space distortions are sensitive to the growth of structures in the Universe

Provide a good test for modified gravity theories through the determination of the growth factor and the growth index

Power spectrum is normalized using the variance of Galaxy distribution smoothed on a scale of $8h^{-1}$ Mpc or

$$\sigma_8(z) = \sigma_{8,0} D(z)$$

What we really measure from RSD are $f\sigma_8$ and $b\sigma_8$

$$P_s(k, \mu_{\mathbf{k}}, z) = (1 + \beta(z) \mu_{\mathbf{k}}^2)^2 P_r(k, z)$$

$$\mu_{\mathbf{k}} \equiv \mathbf{k} \cdot \hat{\mathbf{n}}_z / k \qquad \beta = \frac{\Omega_M^\gamma}{b}$$

A very common way of studying RSD is by the use of the multipole expansion

$$(1 + \beta \mu_k^2)^2 = \left(1 + \frac{2}{3}\beta + \frac{1}{5}\beta^2\right) \mathcal{P}_0(\mu_k) + \left(\frac{4}{3}\beta + \frac{4}{7}\beta^2\right) \mathcal{P}_2(\mu_k) + \frac{8}{35}\beta^2 \mathcal{P}_4(\mu_k)$$

Each term can be independently measured due to the different angular dependence

$$\xi(r, \mu) = \sum_l \xi_l(r) \mathcal{P}_l(\mu) \qquad \xi_l(r) = \frac{i^l}{2\pi^2} \int dk P(k) k^2 j_l(kr)$$

$$\xi_s(r, \mu) = b(z)^2 \left\{ \left[1 + \frac{2}{3}\beta + \frac{1}{5}\beta^2\right] \mathcal{P}_0(\mu) \xi_0(r) + \left[\frac{4}{3}\beta + \frac{4}{7}\beta^2\right] \mathcal{P}_2(\mu) \xi_2(r) + \frac{8}{35}\beta^2 \mathcal{P}_4(\mu) \xi_4(r) \right\}$$

Non-Linear Effects: Fingers of God

On small (non-linear) scales these velocities are large enough to compensate Hubble's law and the spheres are turned inside out and deformed in shape, forming structures that point towards the observers, commonly known as fingers of God

Difficult to model. In general:

$$P_s(k, \mu_{\mathbf{k}}, z) = (1 + \beta(z) \mu_{\mathbf{k}}^2)^2 F(k, \mu_{\mathbf{k}}) P_r(k, z)$$

CfA: $0^\circ < \delta < 30^\circ$

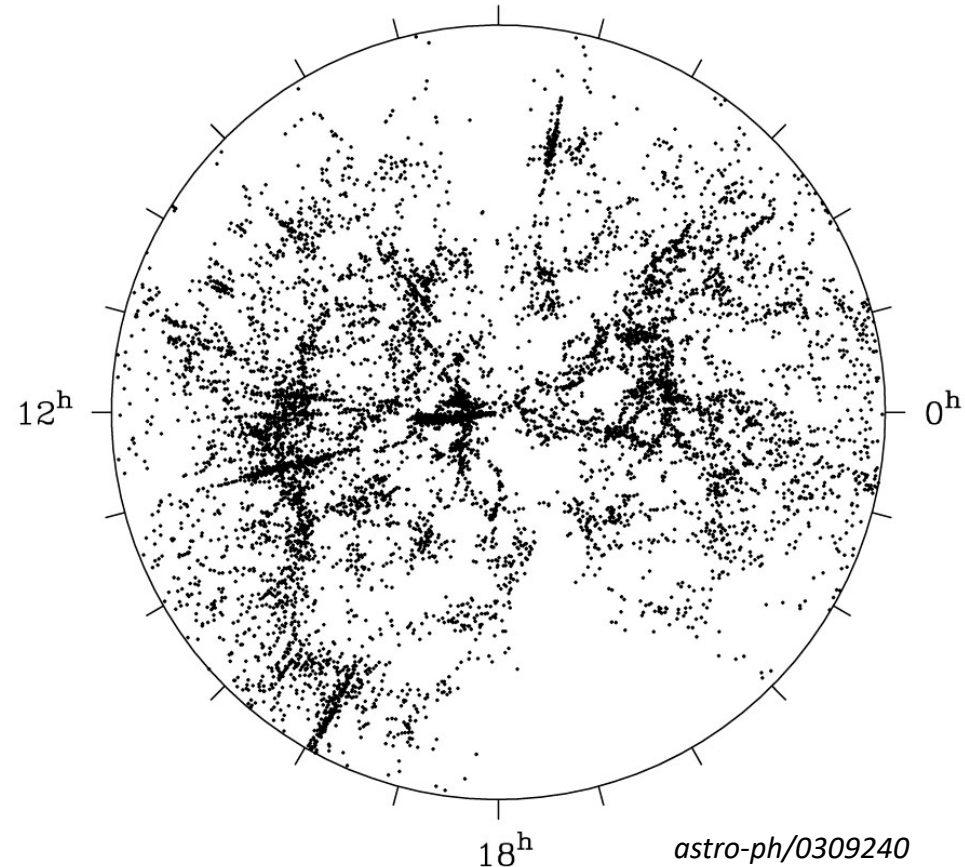
6^h

$v < 12\,000 \text{ km s}^{-1}$

A usual $F(k, \mu)$ is

$$F(k, \mu_{\mathbf{k}}) = \frac{1}{(1 + k^2 \mu_{\mathbf{k}}^2 \Sigma_v^2)^2}$$

Streaming model



SUMMARY

- What we observe in a redshift survey is the density field in redshift space. A combination of density and velocity fields
- The 3rd dimension of 3D maps is obtained from redshift, that is a combination of Hubble recession and peculiar velocity
- Distortion is correlated with the density field and can be used to test its growth
- Constrain $dD/d\ln a \sim f\sigma_8$
- 2 regimes: Coherent infall (RSD) or random motion (FoG)

Measurements of RSD in Galaxy surveys: BOSS

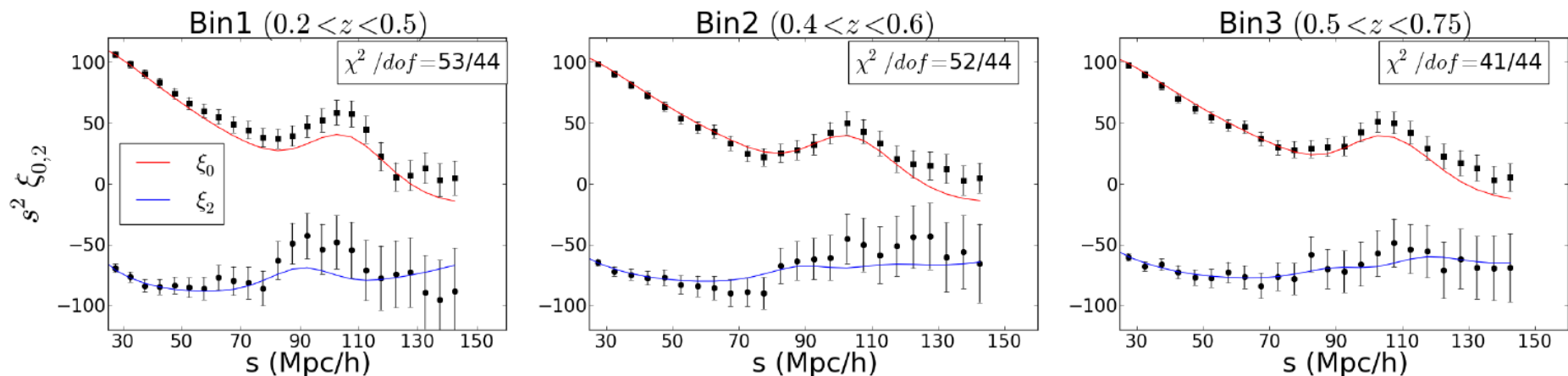
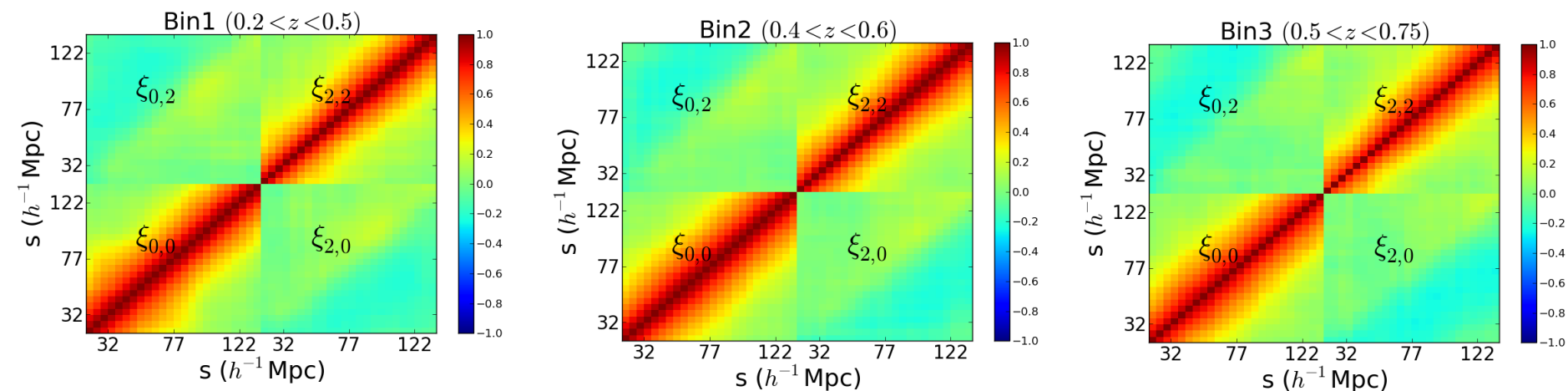


Figure 1. The black dots in the plots of this figure represent monopole (■) and quadrupole (●) for BOSS DR12 galaxy sample evaluated at different values of s . The error bars are obtained from the diagonal elements of the covariance matrices corresponding to mocks in the three redshift bins. The red and the blue lines denote the best fit models of monopole and quadrupole of the galaxy data. The analysis assumes a fitting range $25 \, h^{-1} \text{Mpc} \leq s \leq 150 \, h^{-1} \text{Mpc}$ with a bin size of $5 \, h^{-1} \text{Mpc}$.



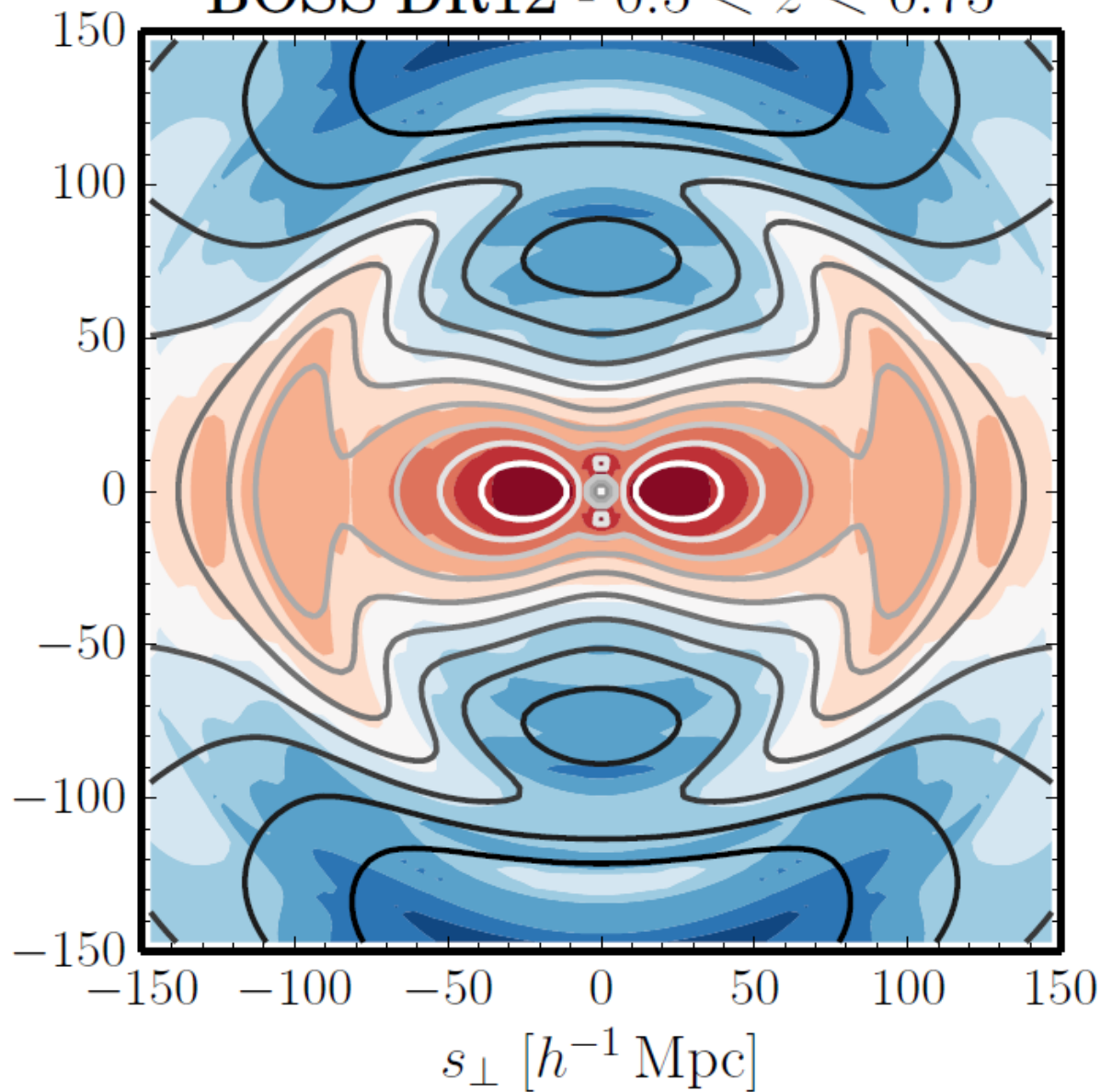
Correlation matrices obtained from MD-P mocks with $z_e = 0.38$, $z_e = 0.51$, $z_e = 0.61$.

BOSS DR12 - $0.5 < z < 0.75$

The measured pre-reconstruction correlation function in the directions perpendicular and parallel to the line of sight, in the redshift range $0.50 < z < 0.75$.

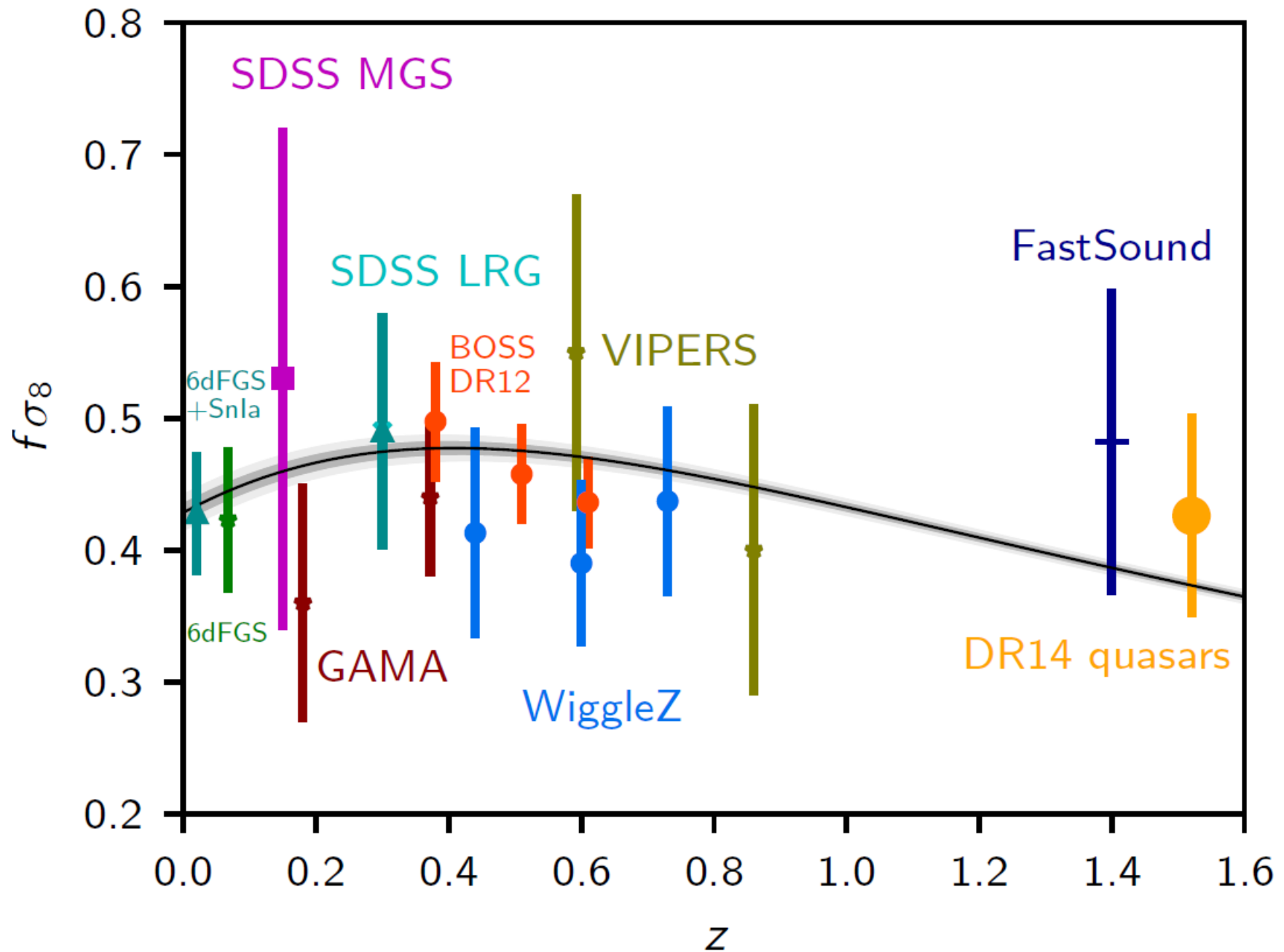
The color scale shows the data and the contours show the prediction of the best-fit model

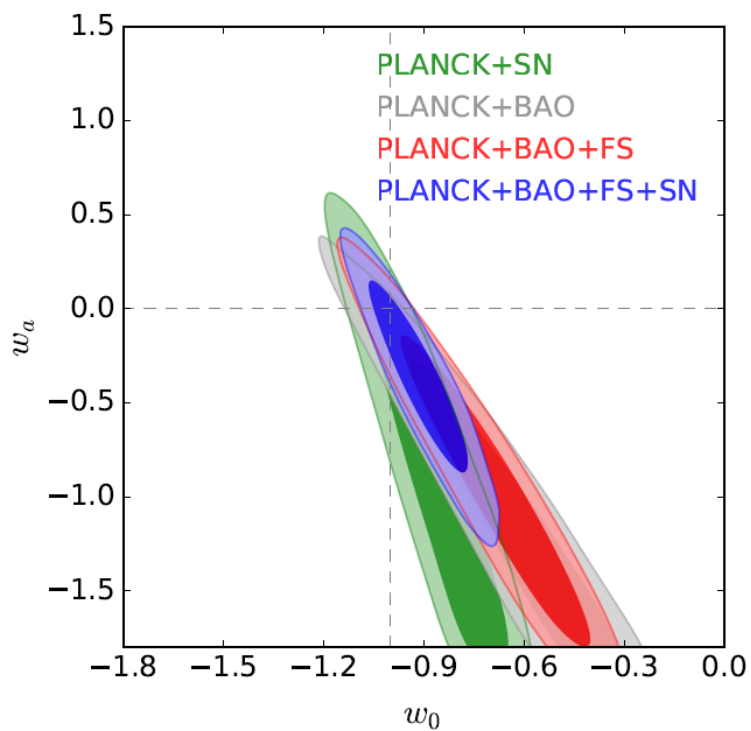
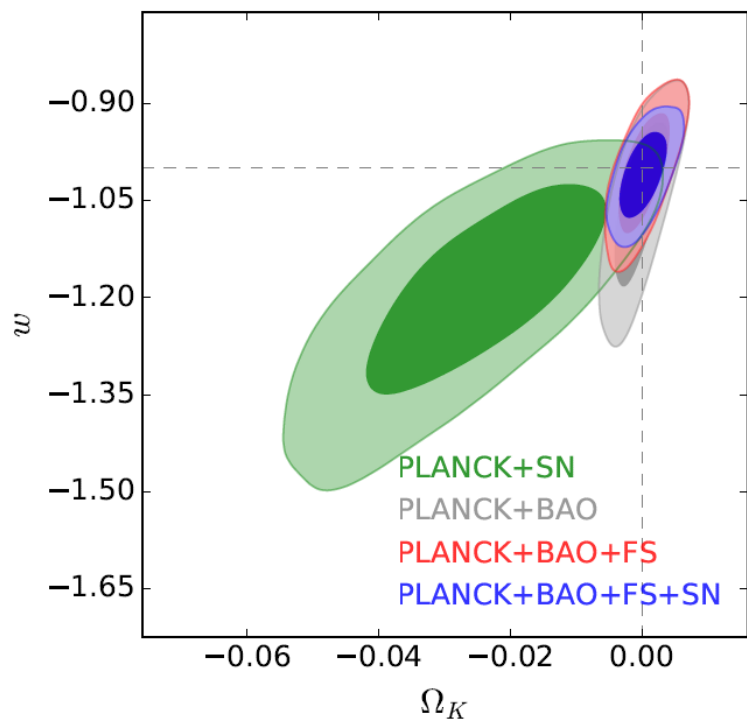
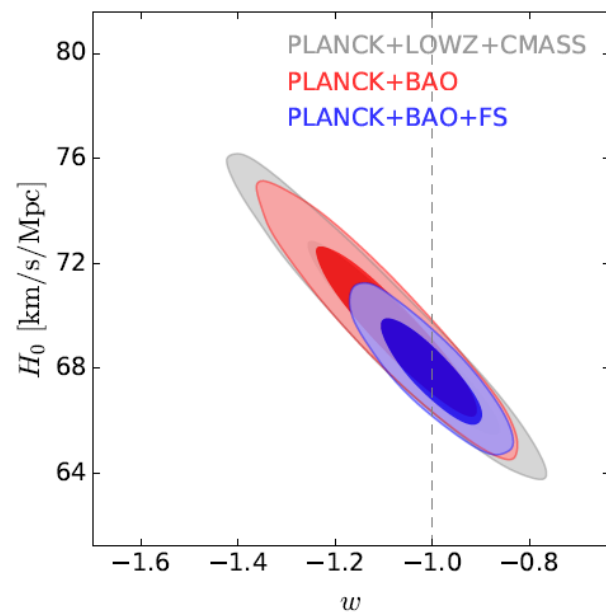
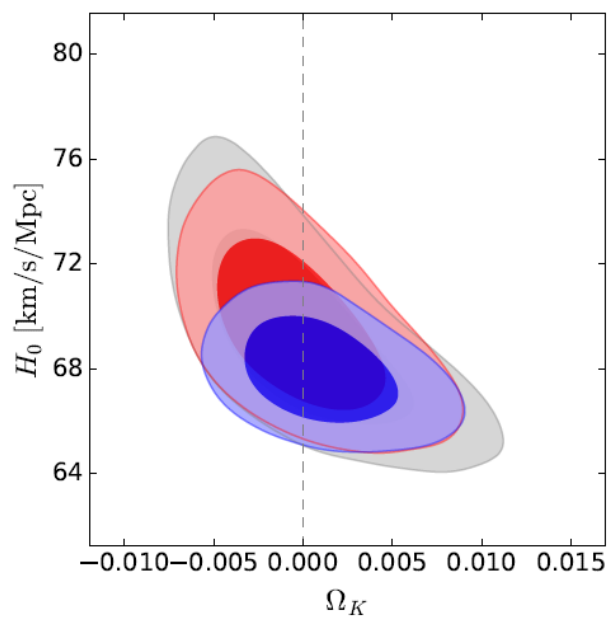
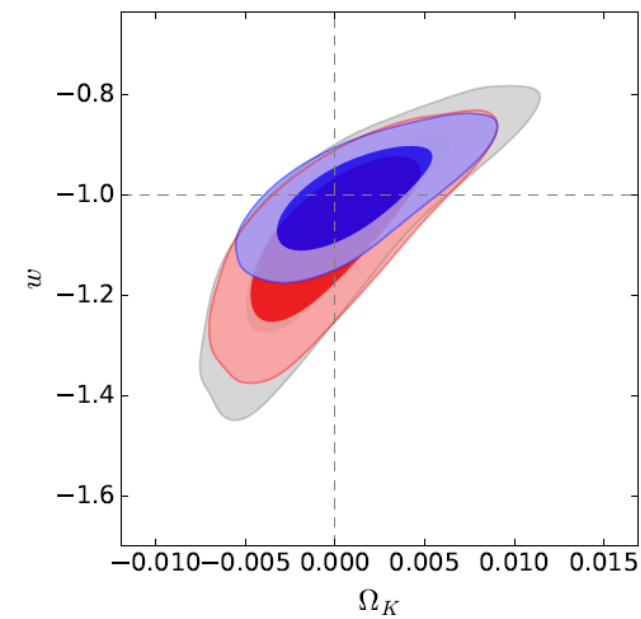
$s_{\parallel} [h^{-1} \text{ Mpc}]$



-80 -40 0 40 80 120

Current status of Growth Factor Measurements





Beyond individual probes

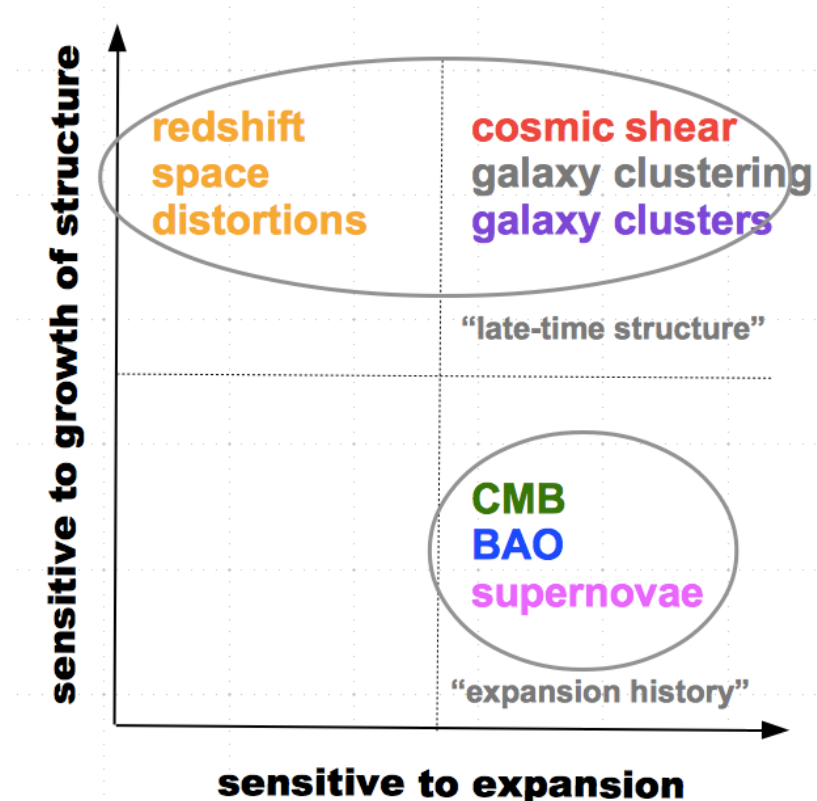
There are many observational probes for dark energy:

Distance probes: *SN1a, BAO, CMB, weak lensing, galaxy clusters...*

Growth of structure probes: *CMB, RSD, weak lensing, galaxy clusters...*

No single technique is sufficiently powerful to improve the current knowledge on dark energy by one order of magnitude →

COMBINATION OF TECHNIQUES

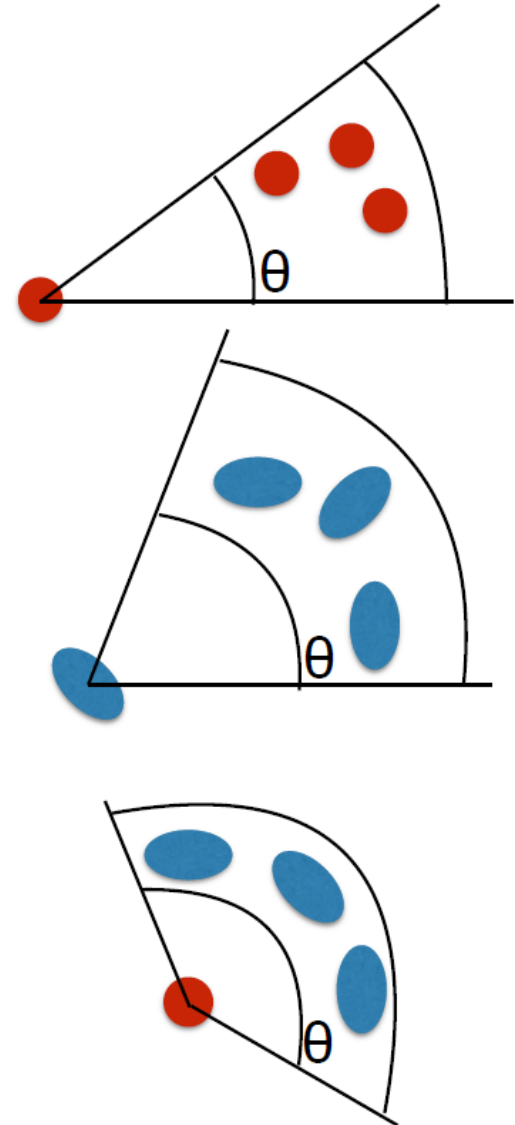


Beyond individual probes

We can measure more properties of galaxies than only their positions: colors, spectra, shape and we can correlate them

Correlations

- $w(\theta)$
Galaxy density (position) correlation function
- $\xi_+(\theta)$, $\xi_-(\theta)$
Shear (shape) correlation functions
- $\gamma_T(\theta)$
Shear around galaxies
(galaxy-galaxy lensing)

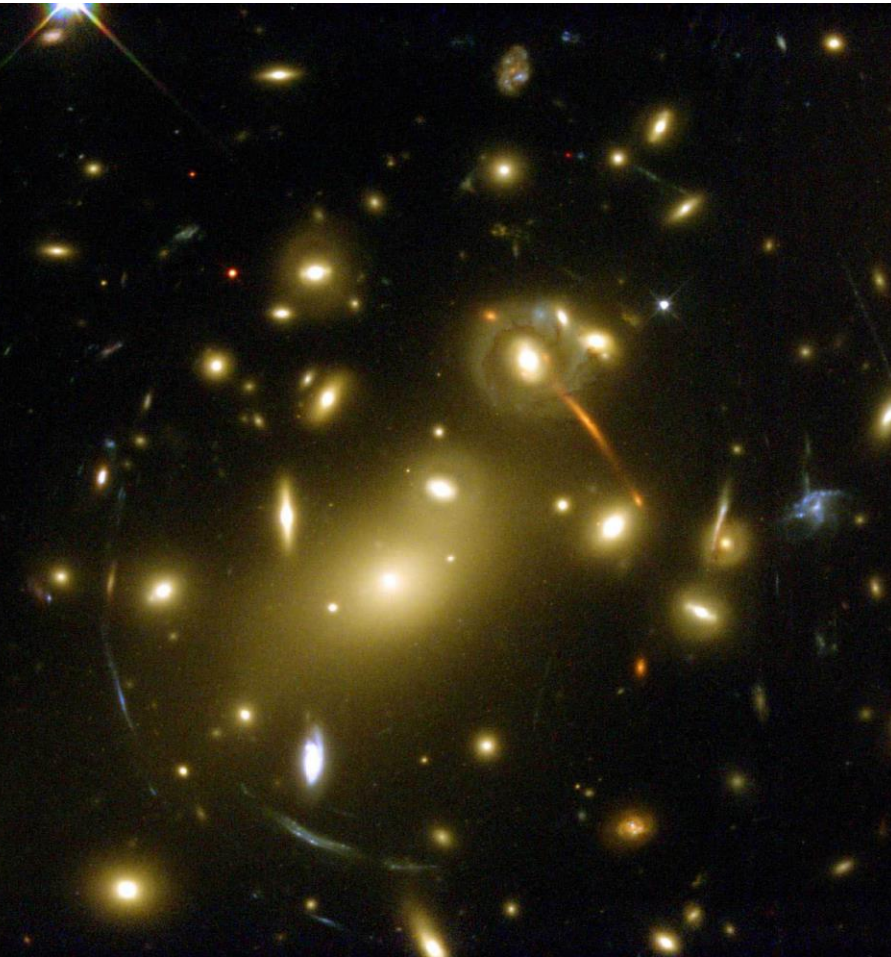


Weak Gravitational Lensing

Radiation is deflected in gravitational fields → Image distortion

Since the effect comes from the gravitational field, it is sensitive to all matter/ energy, including dark matter and dark energy

STRONG LENSING



WEAK LENSING



Weak Gravitational Lensing

The effect depends on the lens mass and the distances between observer, lens and source:

Window to the mass (mostly dark matter) distribution in the lenses

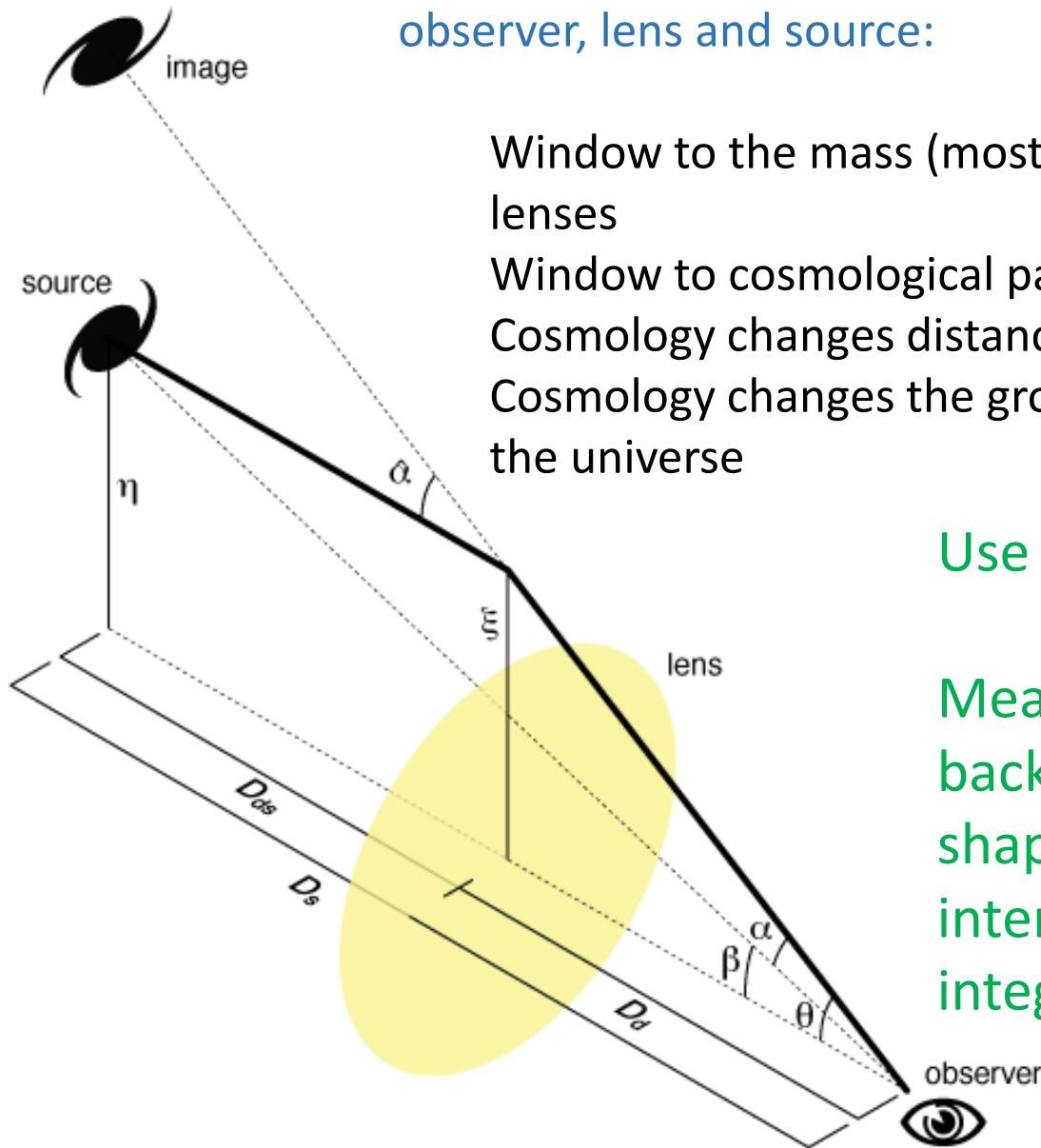
Window to cosmological parameters:

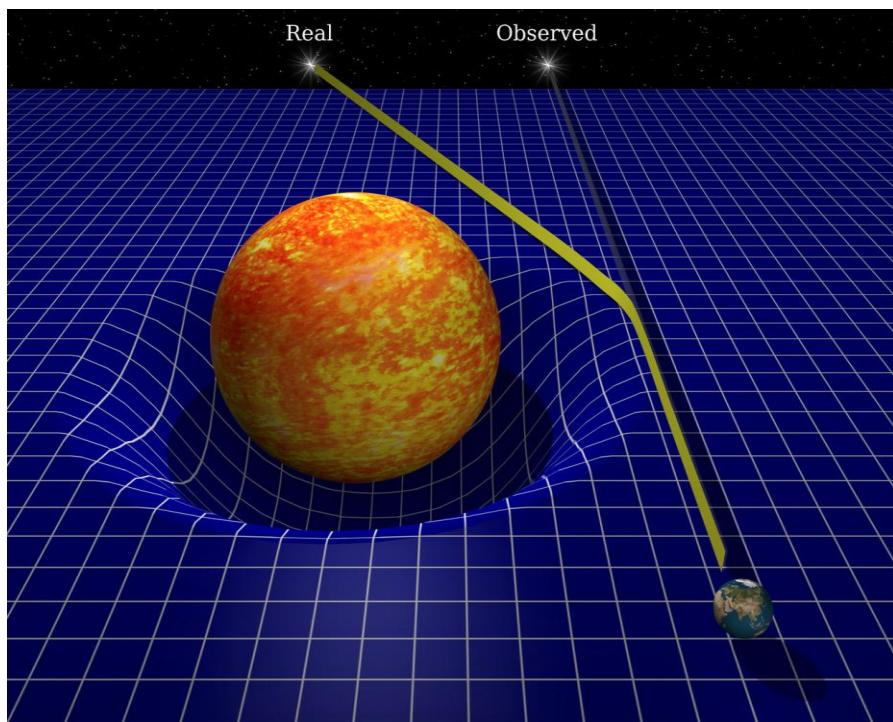
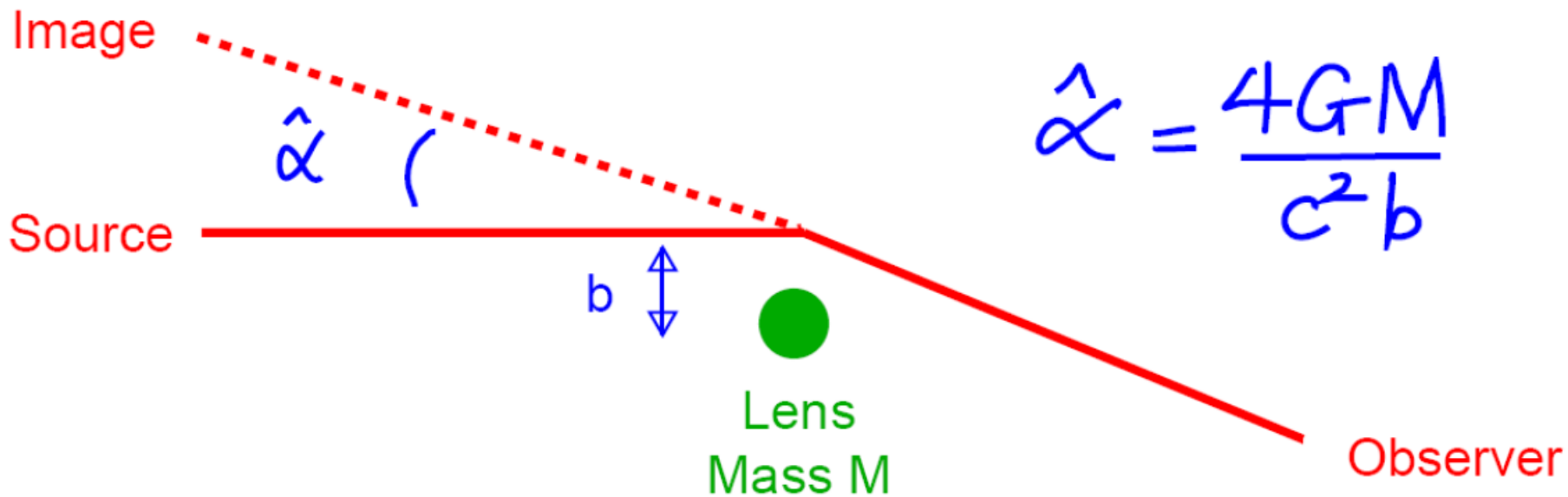
Cosmology changes distances **D_d** , **D_s** , **D_{ds}**

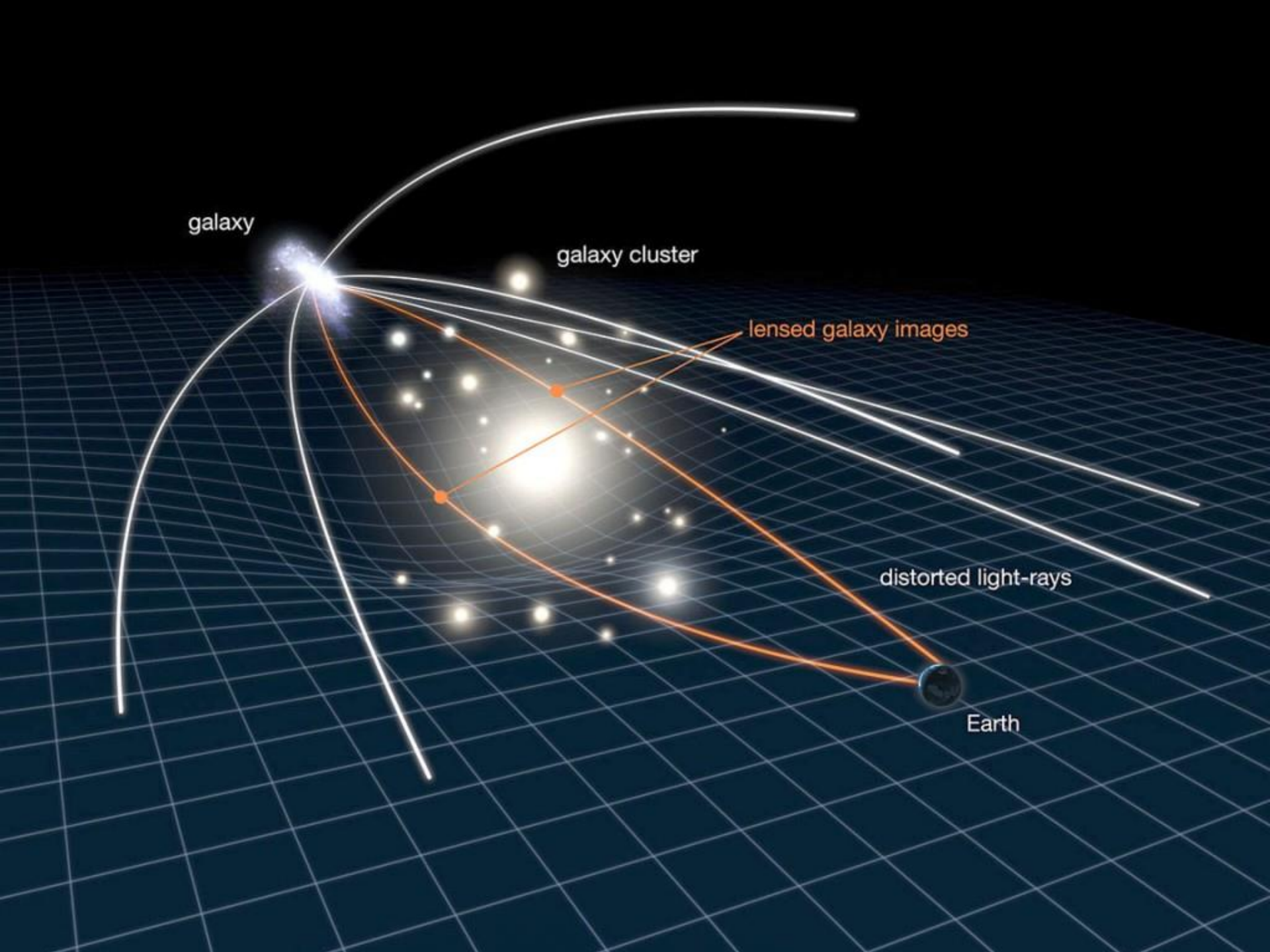
Cosmology changes the growth rate of mass structures in the universe

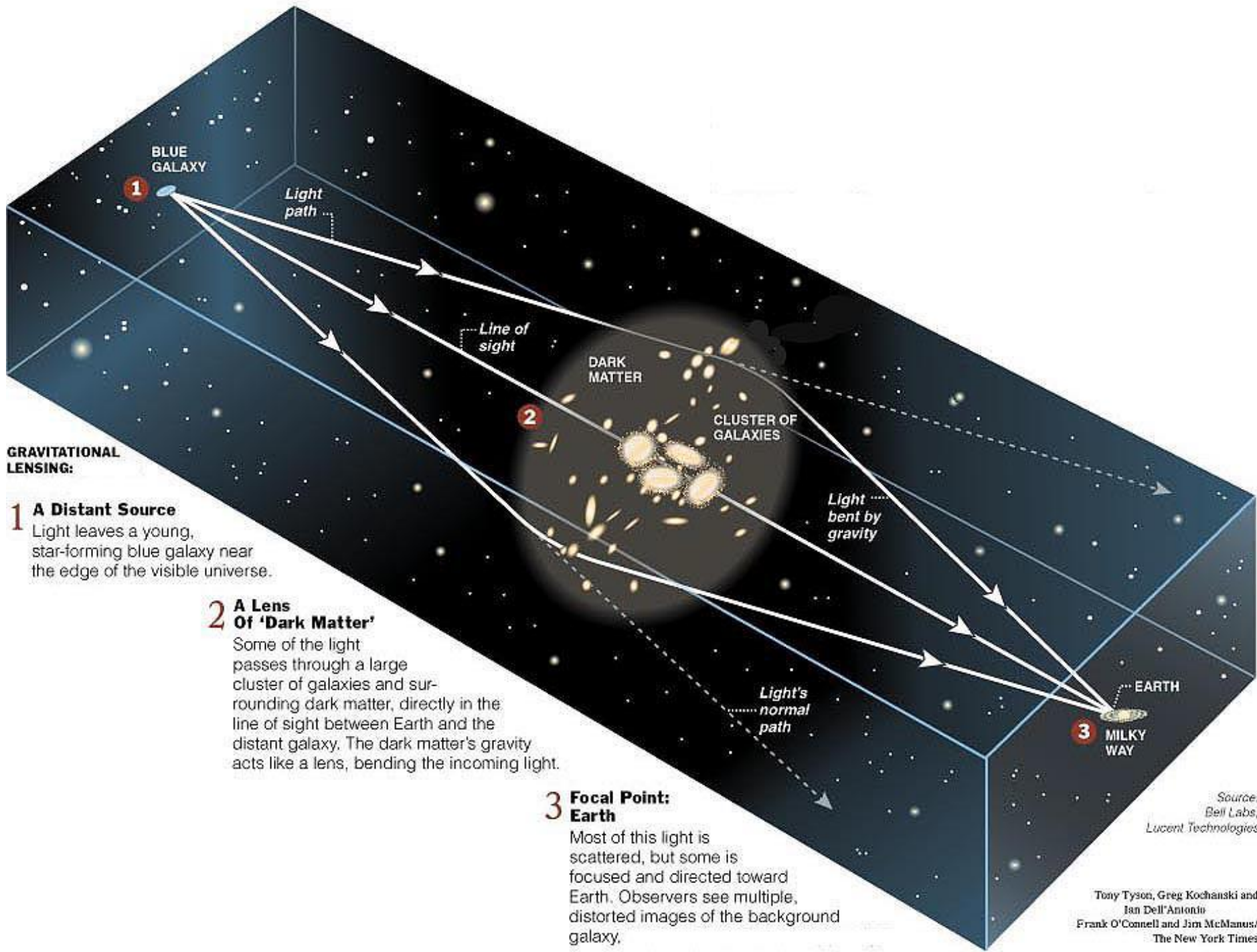
Use galaxies as tracers

Measure the shapes of background galaxies → Galaxy shapes are distorted by intervening mass → Infer mass integrated along the line of sight









GRAVITATIONAL LENSING:

1 A Distant Source

Light leaves a young, star-forming blue galaxy near the edge of the visible universe.

2 A Lens Of 'Dark Matter'

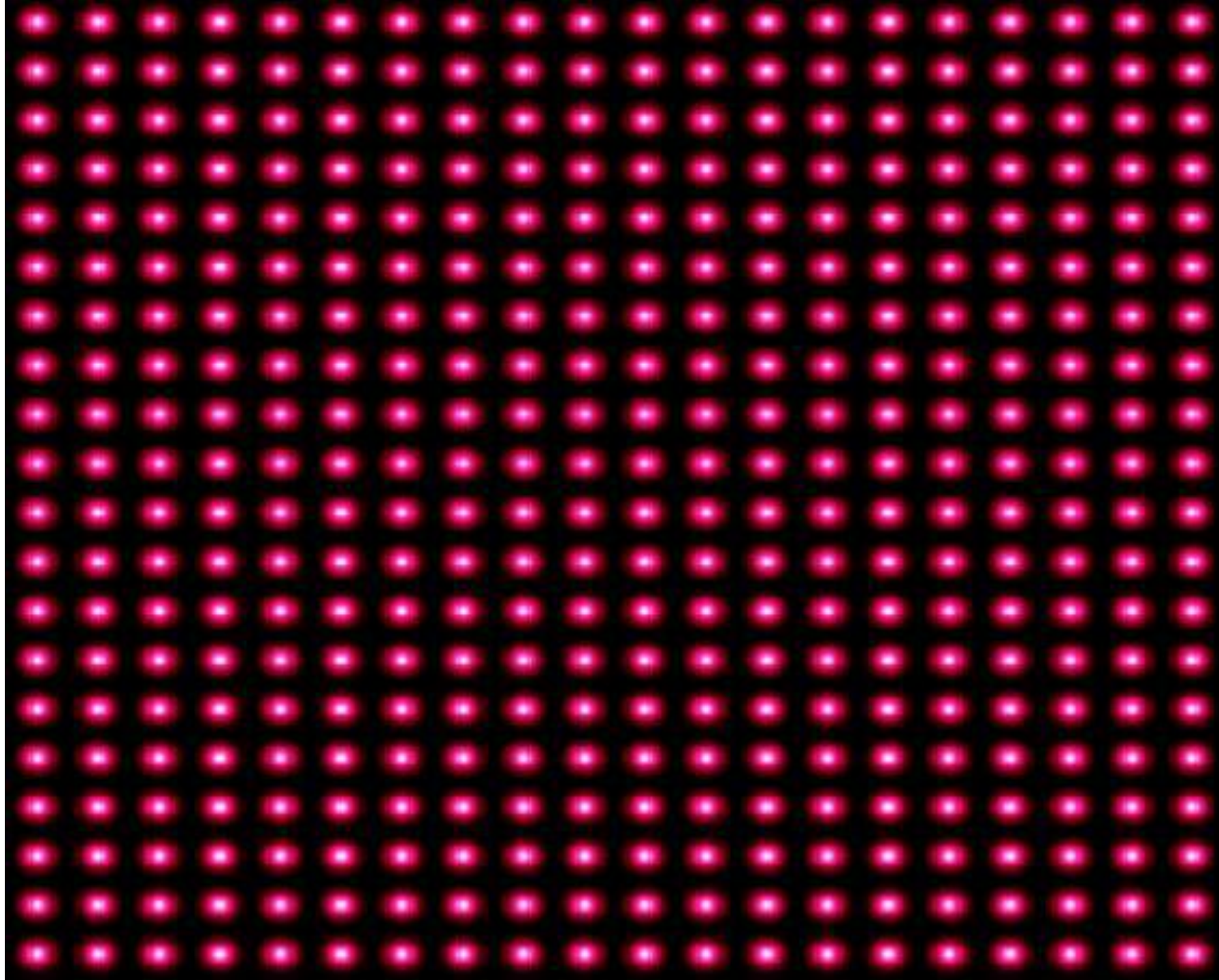
Some of the light passes through a large cluster of galaxies and surrounding dark matter, directly in the line of sight between Earth and the distant galaxy. The dark matter's gravity acts like a lens, bending the incoming light.

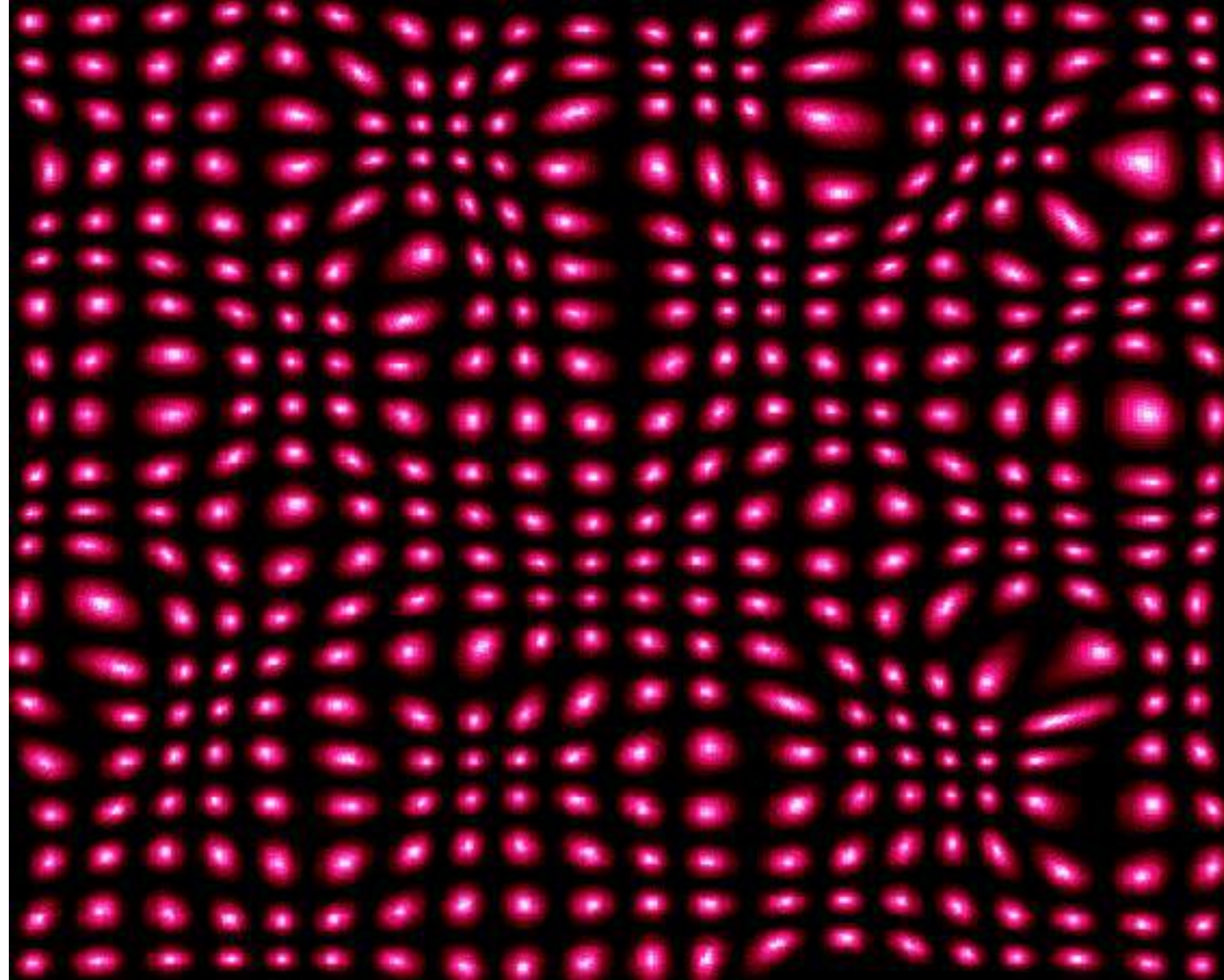
3 Focal Point: Earth

Most of this light is scattered, but some is focused and directed toward Earth. Observers see multiple, distorted images of the background galaxy.

Source:
Bell Labs,
Lucent Technologies

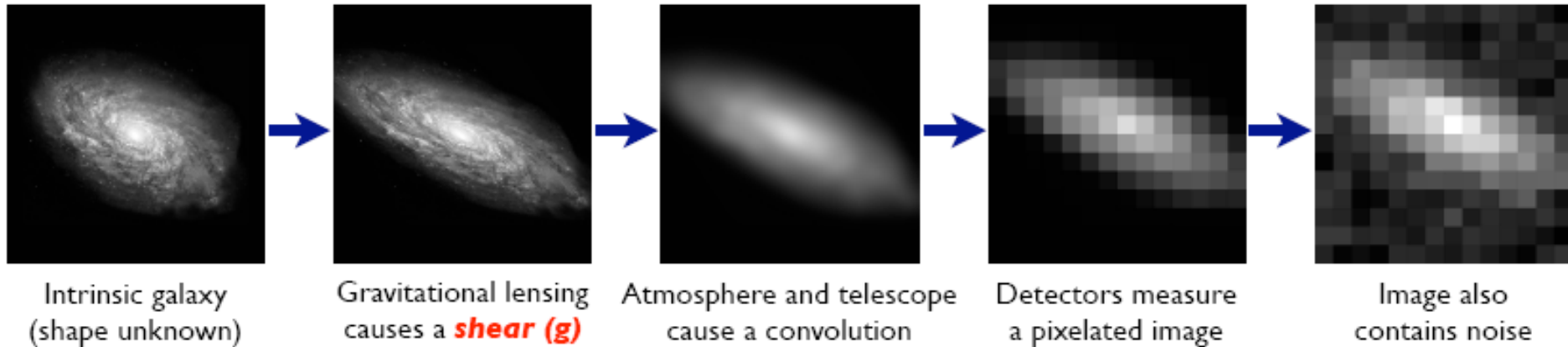
Tony Tyson, Greg Kochanski and
Ian Dell'Antonio
Frank O'Connell and Jim McManus/
The New York Times





Weak Gravitational Lensing

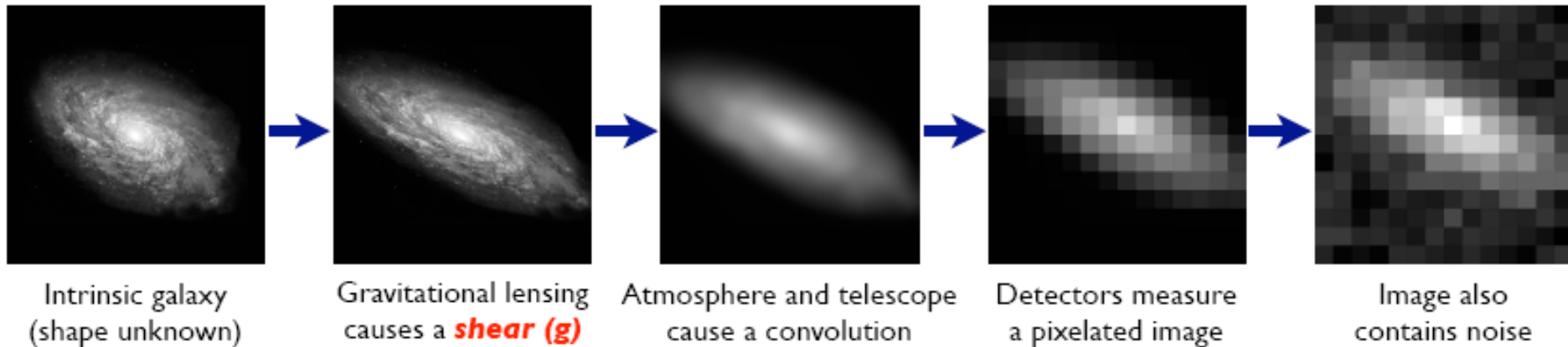
Effect exaggerated by x20



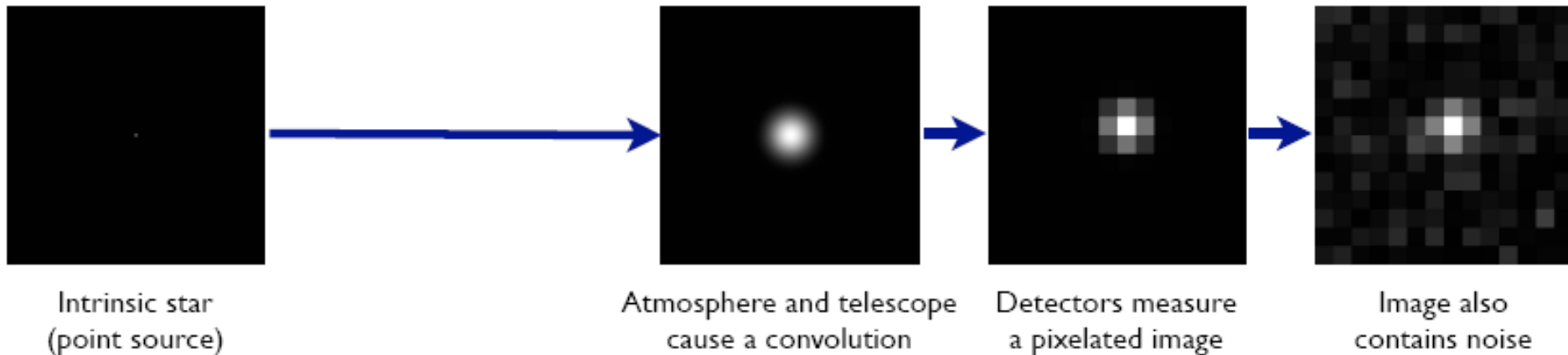
Small and difficult to measure effect, but observable

Weak Gravitational Lensing

Effect exaggerated by x20



Stars: Point sources to star images:



Small and difficult to measure effect, but observable

Control the measurement using known pointlike objects → stars

Weak Gravitational Lensing

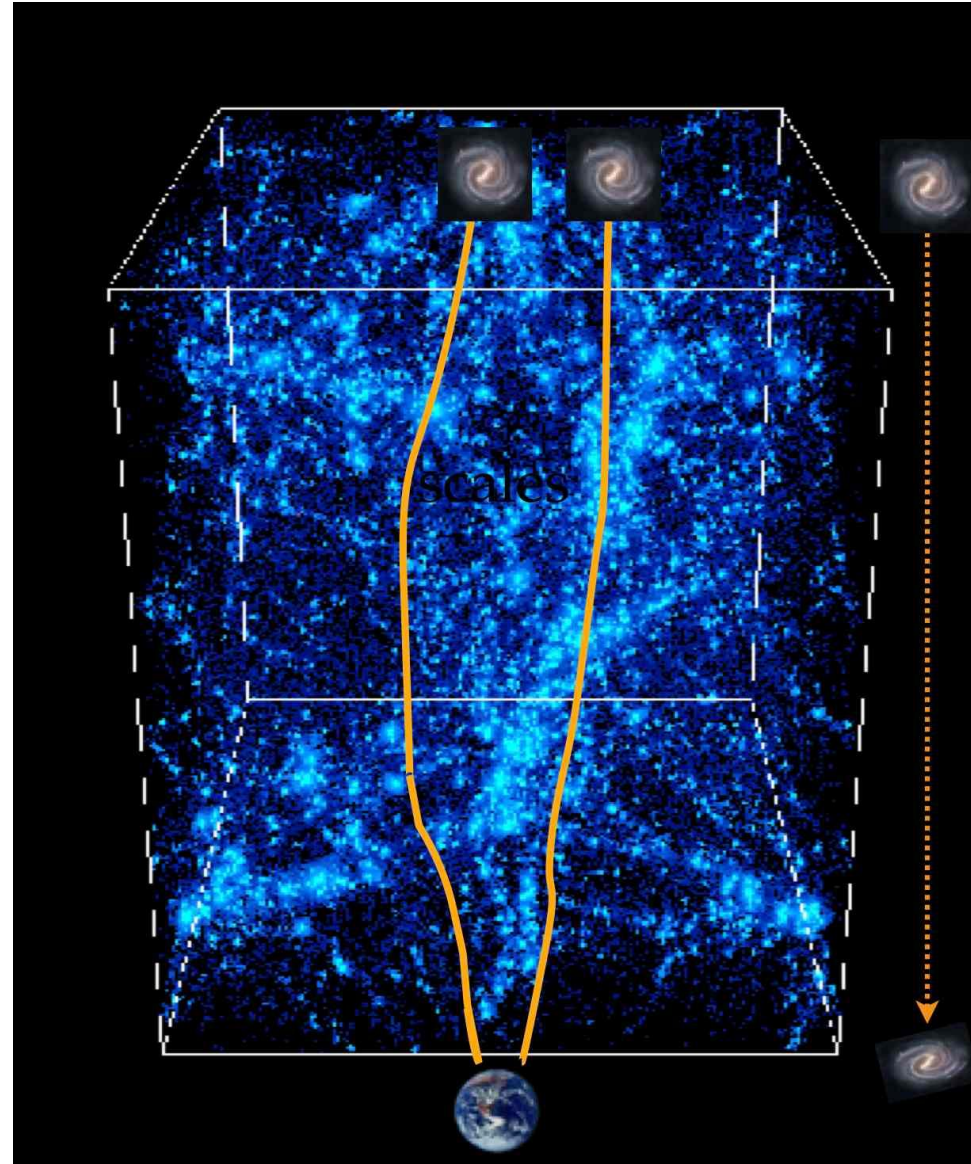
The light of distant galaxies is deflected while travelling through the inhomogeneous Universe. Information about mass distributions is imprinted on observed galaxy images

Sensitive to projected 2D mass distribution

2 effects: magnification, distortions of images

few percent change of images. Need a statistical measurement and huge surveys to have enough statistics

Coherent distortions: measure correlation

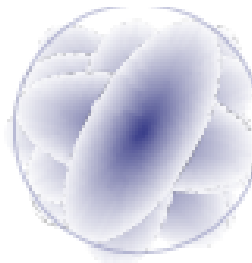


Weak Gravitational Lensing

small patch on sky filled with (elliptical) galaxies
(unrelated objects with different redshifts)

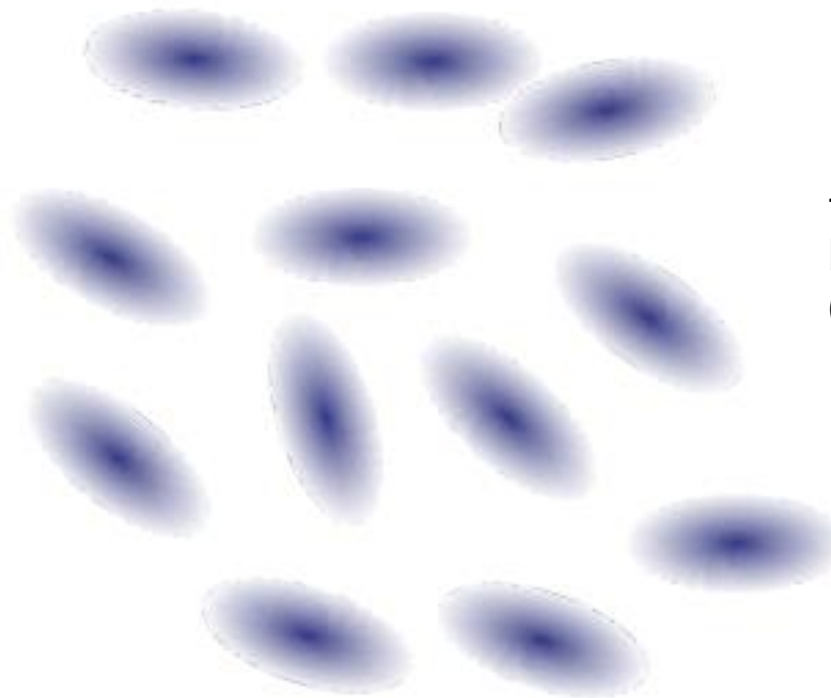


=> the average shape will be circular:



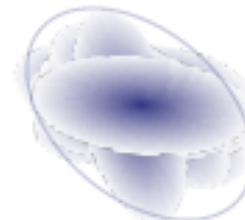
Weak Gravitational Lensing

small patch on sky filled with (elliptical) galaxies
(unrelated objects with different redshifts)

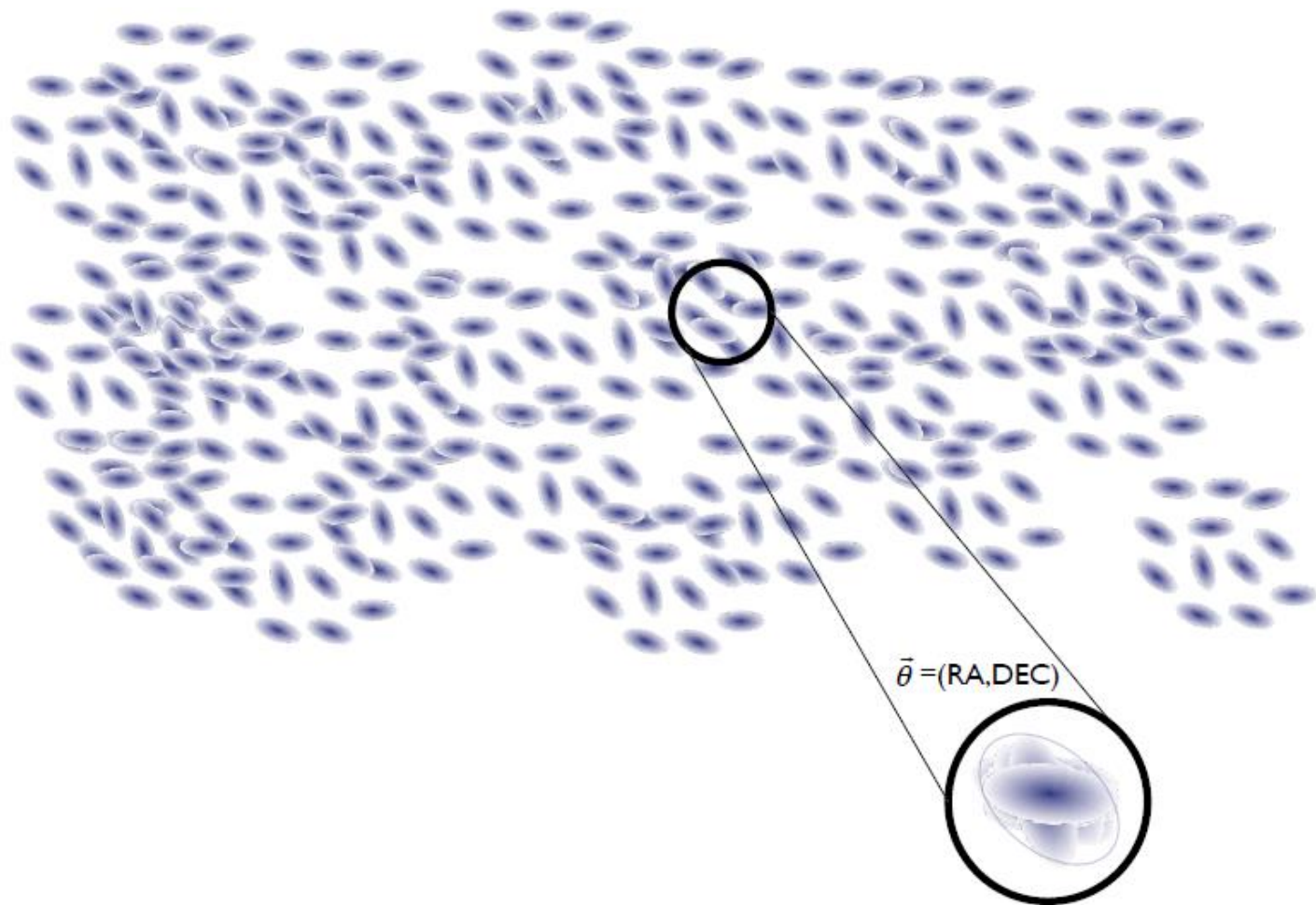


+ weak gravitational
lensing!
(lightpaths become related)

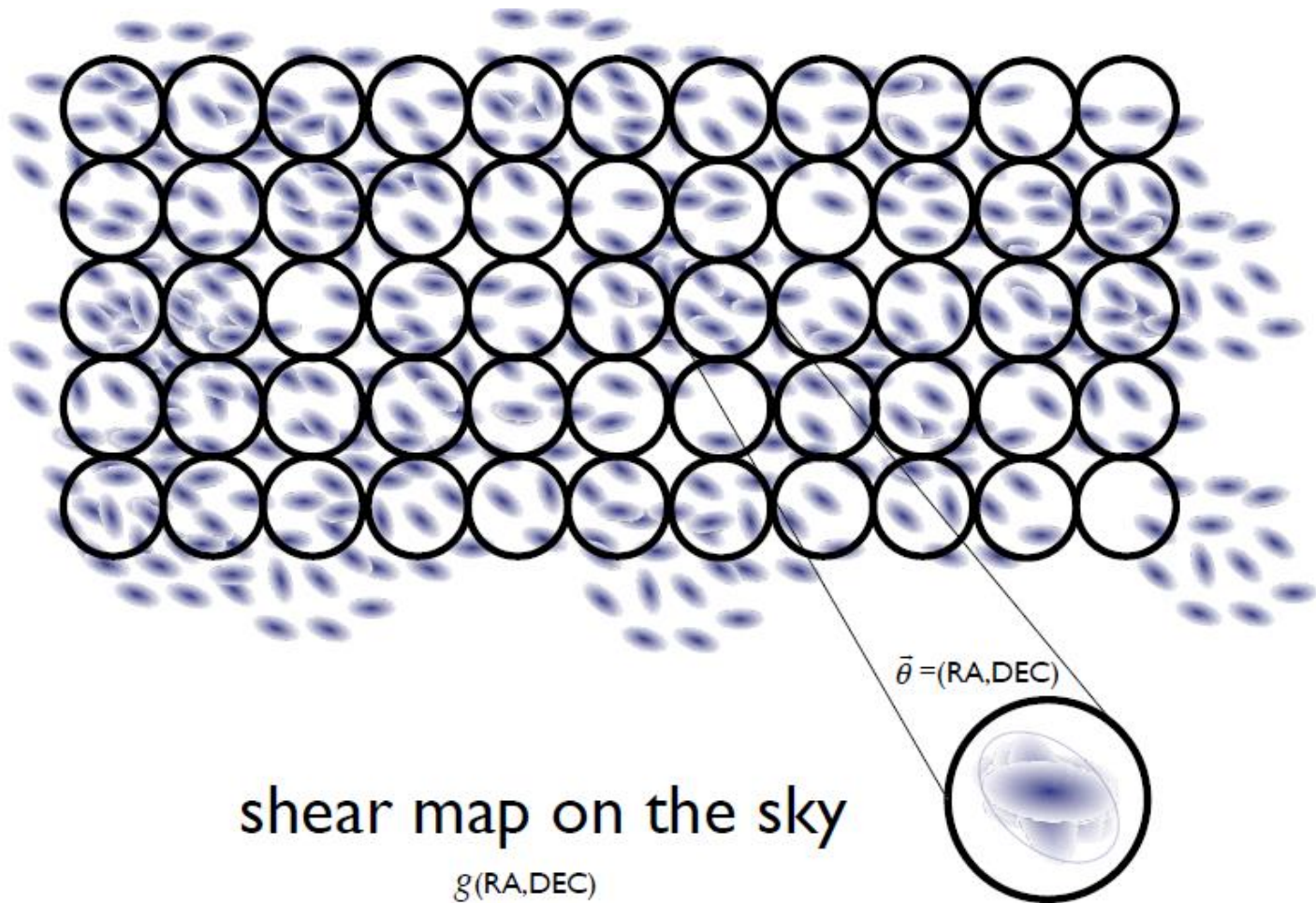
=> the average shape will be elliptical:



Weak Gravitational Lensing

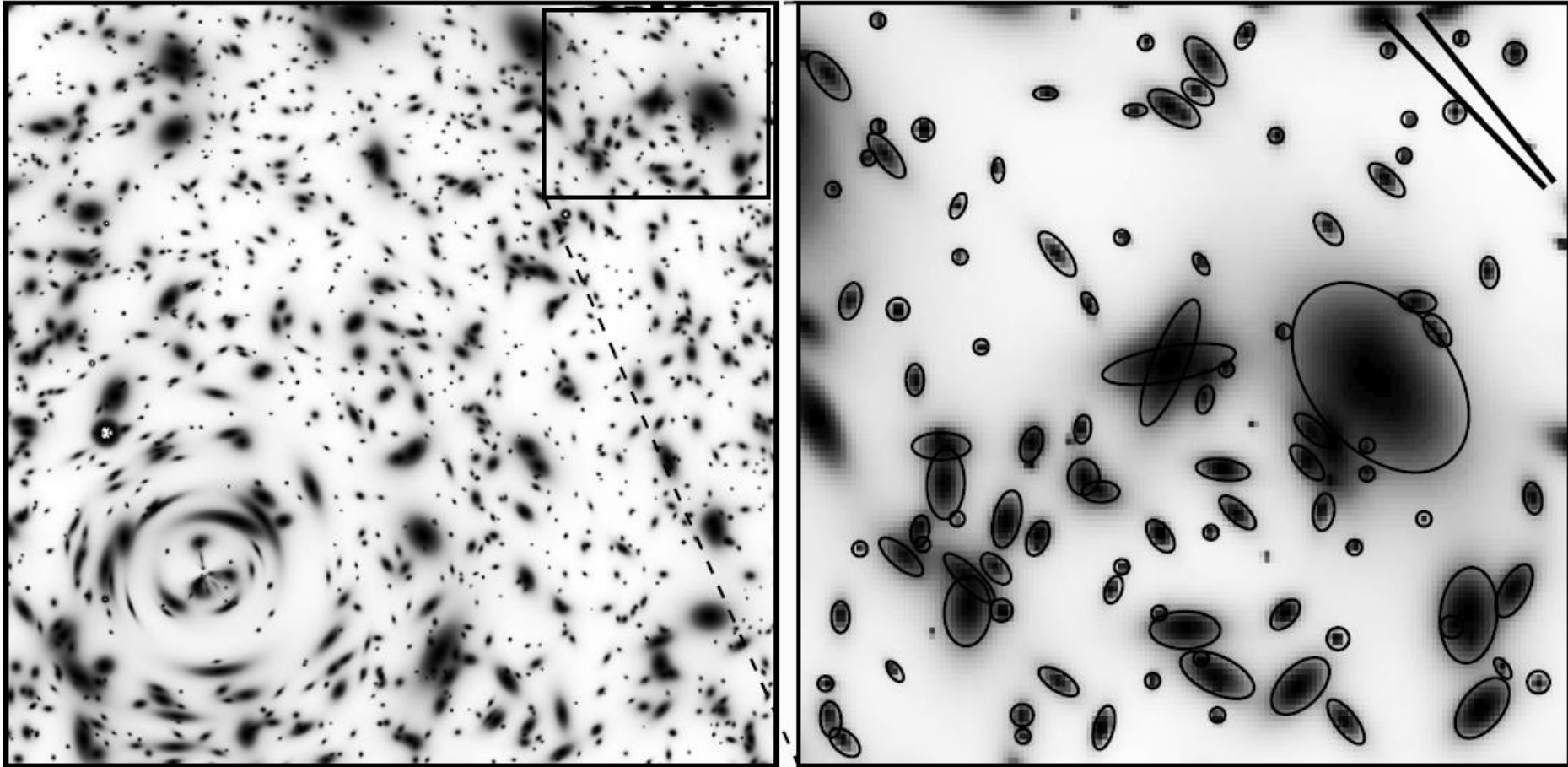


Weak Gravitational Lensing



Weak Gravitational Lensing

Ellipticity and local shear

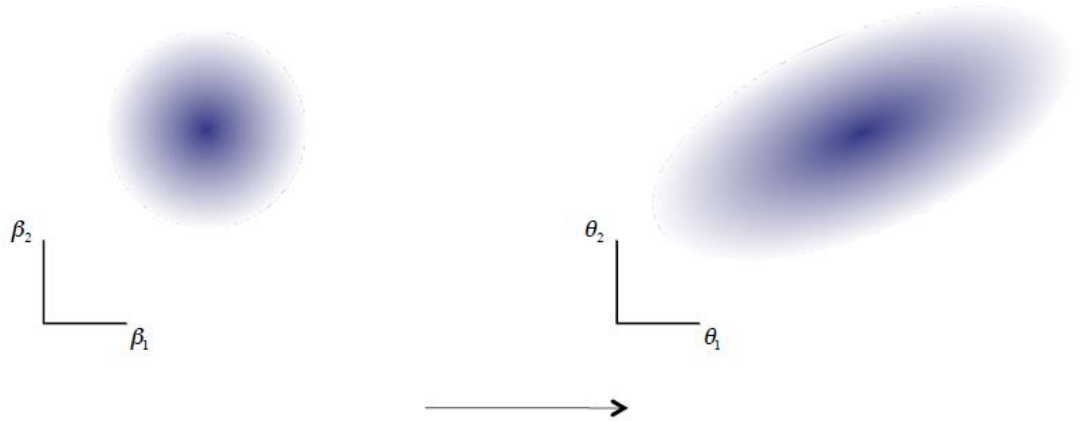
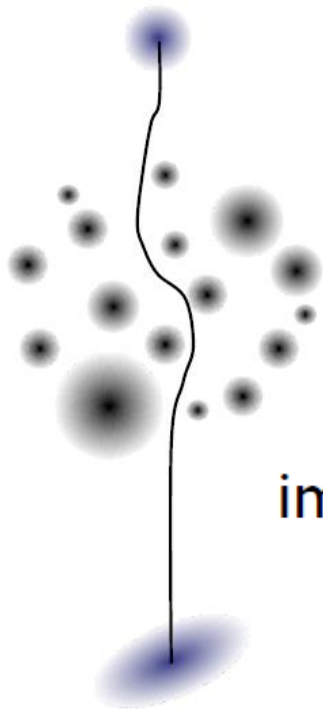


[from Y. Mellier]

Galaxy ellipticities are an estimator of the local shear.

Weak Gravitational Lensing

The distortion matrix



$$A_{ij} = (1 - \kappa) \begin{pmatrix} 1 & 0 \\ 0 & 1 \end{pmatrix} - \begin{pmatrix} \gamma_1 & \gamma_2 \\ \gamma_2 & -\gamma_1 \end{pmatrix}$$

image distortion depends on...

...cosmic structure formation

$$G(a) = \frac{5}{2} \Omega_0 \frac{\dot{a}}{a} \int_0^a \frac{1}{\dot{a}^3} da$$

...cosmic distance

$$D(z) = \frac{1}{1+z} \frac{c}{H_0} \int_0^z \frac{dz}{\left[\Omega_0 (1+z)^3 + \Omega_\Lambda \right]^{1/2}}$$

Great potential for cosmology

Weak Gravitational Lensing

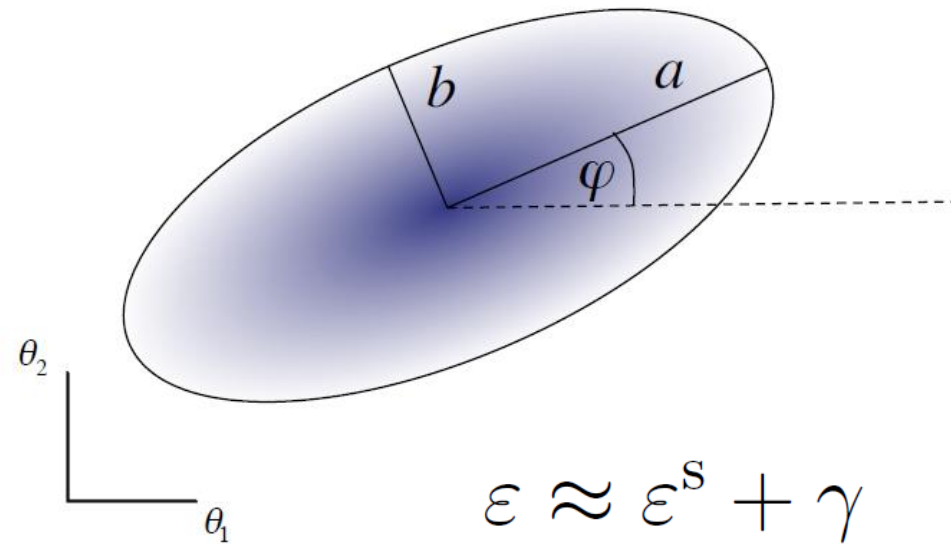
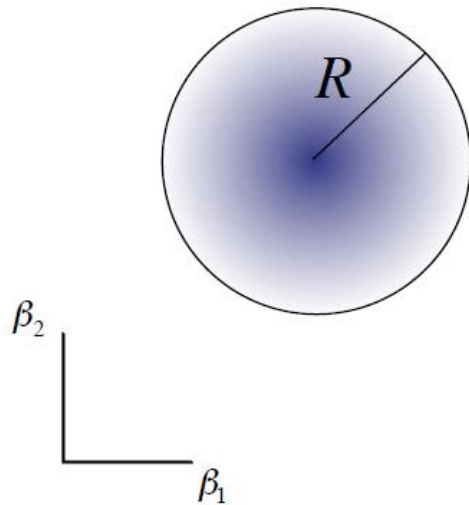
$$g = \frac{\gamma}{1 - \kappa} = \langle \varepsilon(\theta) \rangle$$

is observable!

$$\gamma = |\gamma| e^{i2\varphi}$$

$$a = \frac{R}{1 - \kappa - |\gamma|}$$

$$b = \frac{R}{1 - \kappa + |\gamma|}$$



$$\varepsilon \approx \varepsilon^s + \gamma$$

circular source \Rightarrow measuring a, b (and φ) gives reduced shear $g=|\gamma|/(1-\kappa)$

$$A_{ij} = (1 - \kappa) \begin{pmatrix} 1 & 0 \\ 0 & 1 \end{pmatrix} - \begin{pmatrix} \gamma_1 & \gamma_2 \\ \gamma_2 & -\gamma_1 \end{pmatrix}$$

If the original shape is not circular, the ellipticity does not give the reduced shear

Weak Gravitational Lensing

Weak lensing quantities are related: $\kappa(\boldsymbol{\theta}) - \kappa_0 = \frac{1}{\pi} \int \text{Re}[D^*(\boldsymbol{\theta} - \boldsymbol{\theta}')\gamma(\boldsymbol{\theta}')] d^2\theta'$

$$D(\boldsymbol{\theta} - \boldsymbol{\theta}') = \frac{((\theta_1 - \theta'_1) + i(\theta_2 - \theta'_2))^2}{|\boldsymbol{\theta} - \boldsymbol{\theta}'|^4}$$

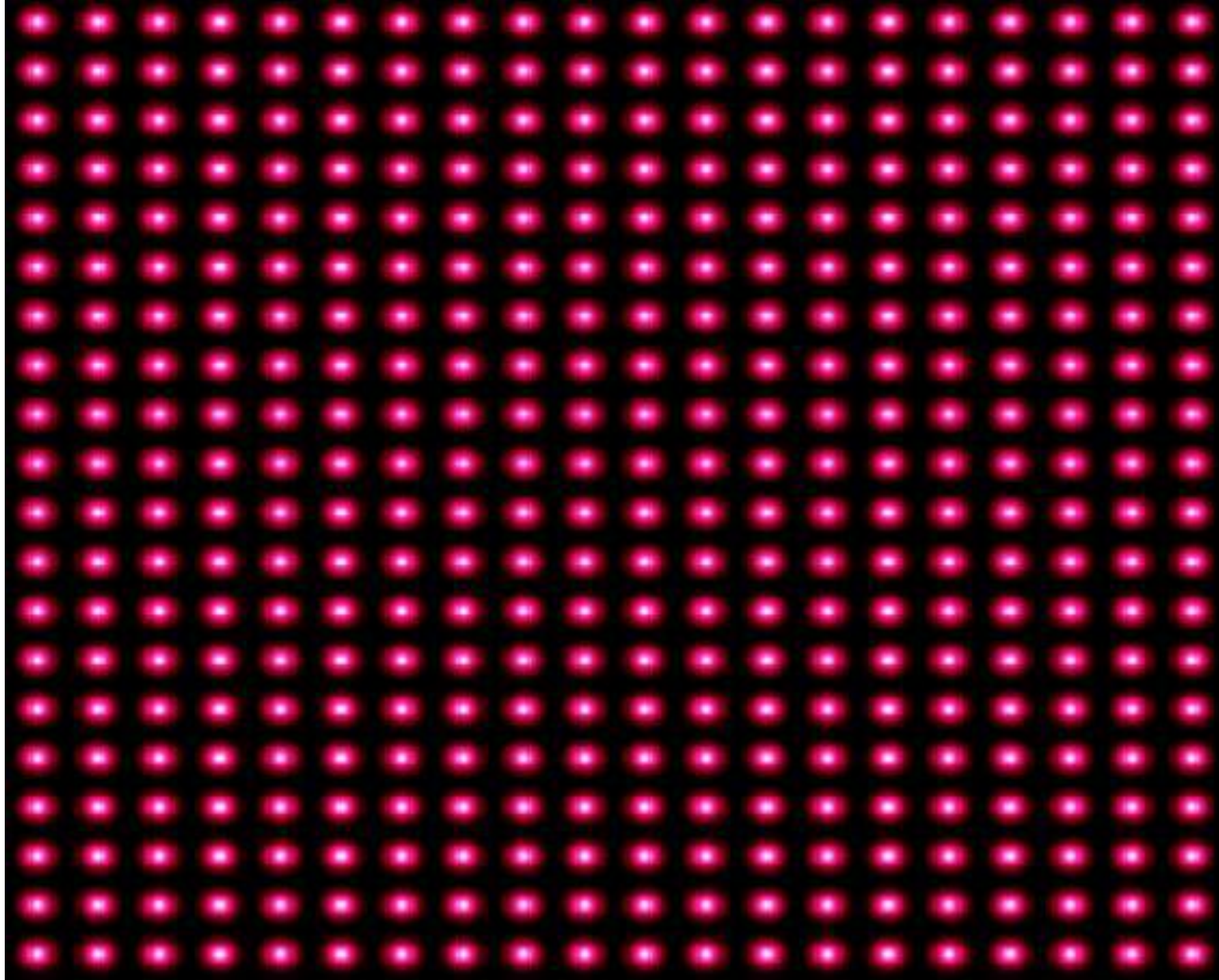
And related to cosmology: $\kappa(\boldsymbol{\theta}) = \frac{3H_0^2\Omega_0}{2c^2} \int \frac{D_{LS}D_L}{D_S} \frac{\delta(\boldsymbol{\theta}, z)}{a(z)} dz$

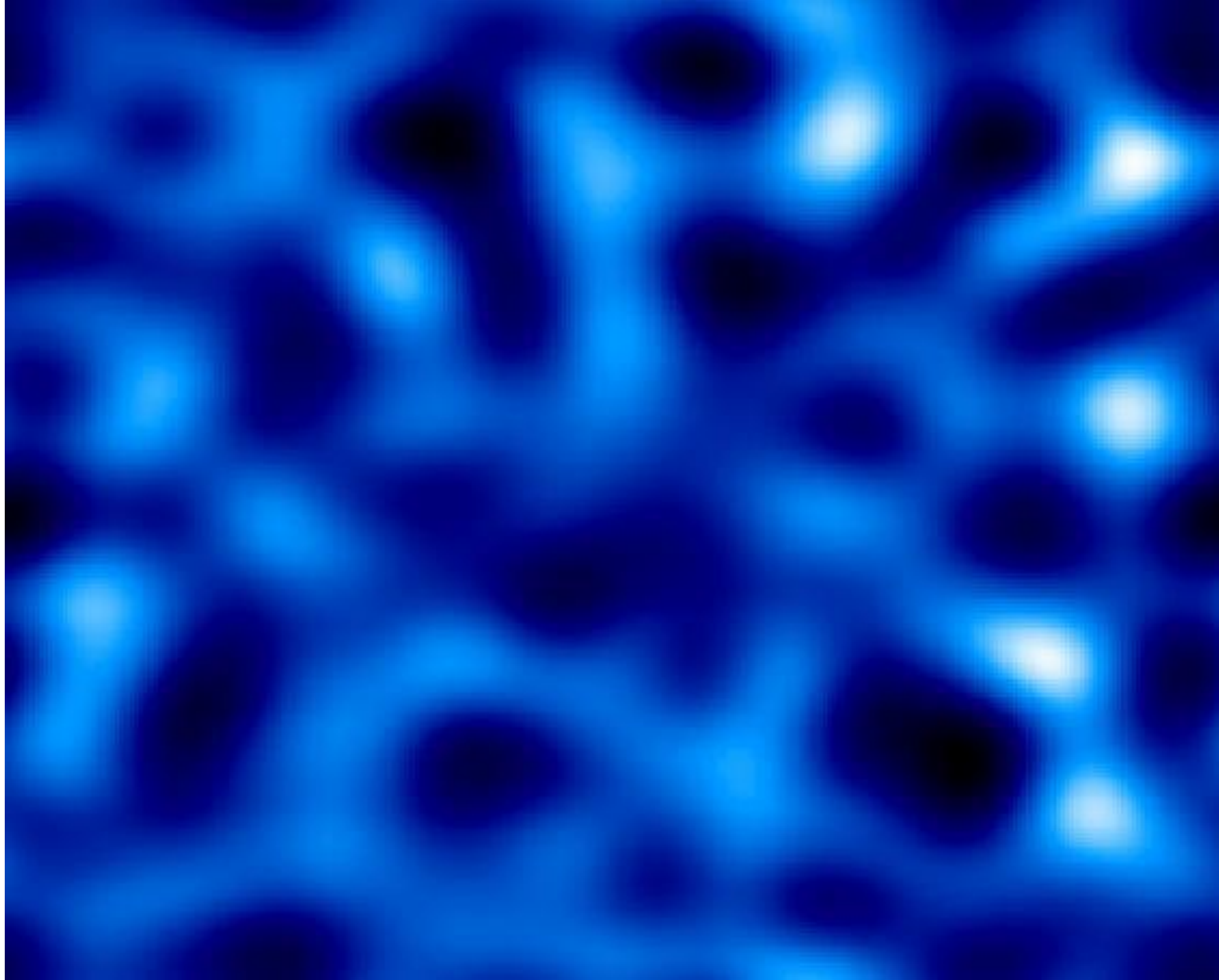
For a distribution of sources:

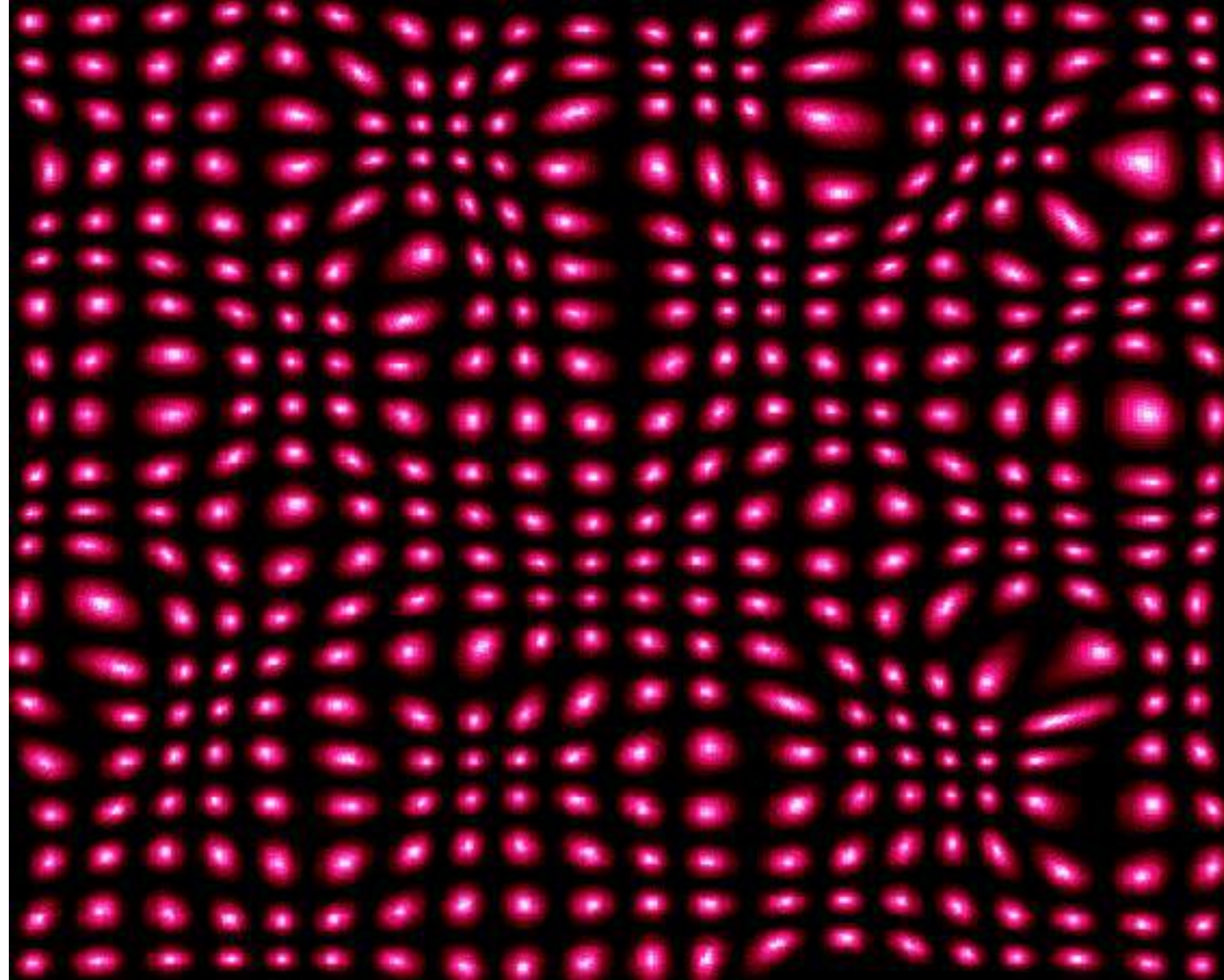
Geometry: Comoving distance
to lens, source and scale
factor

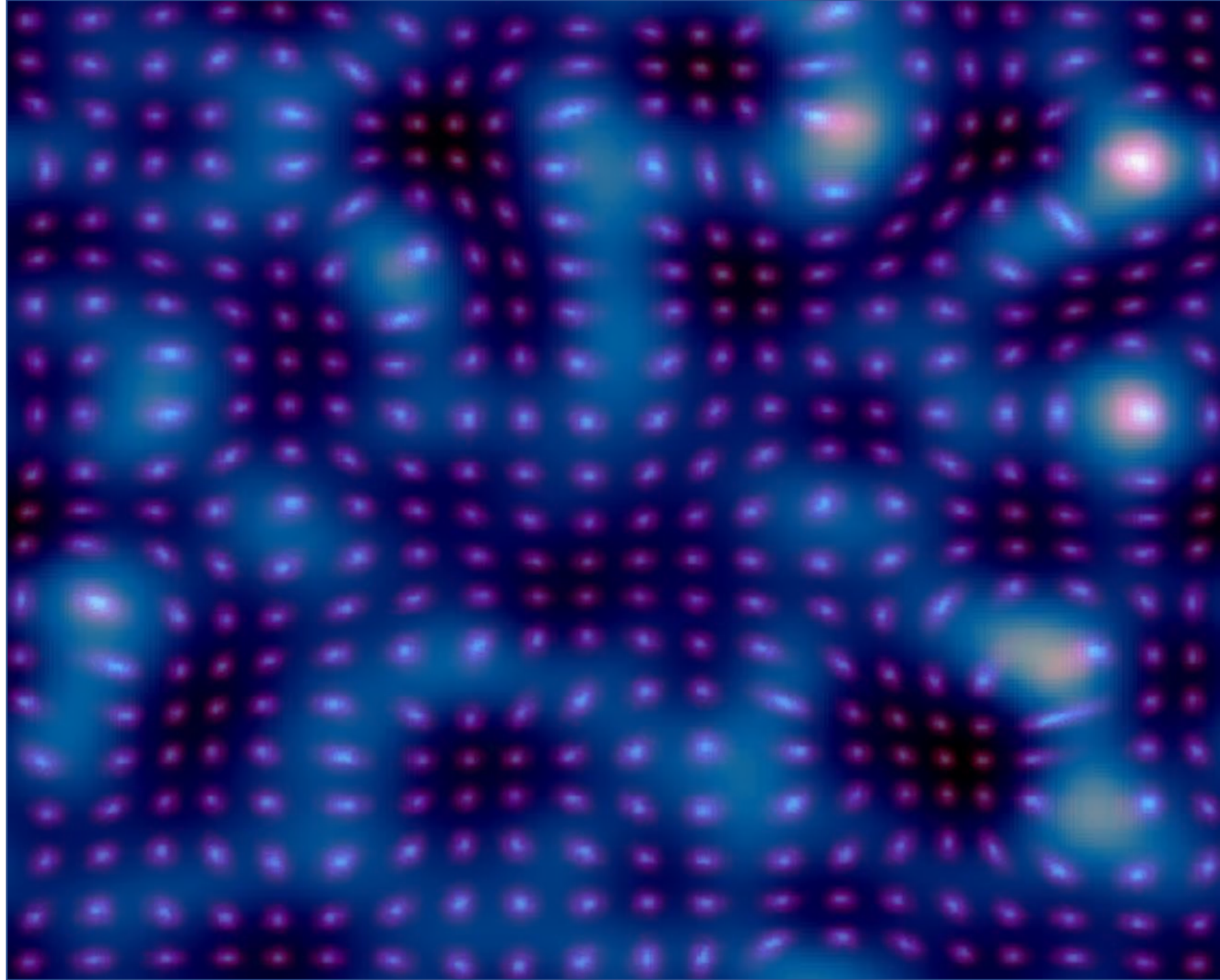
Growth of structure: Density
contrast

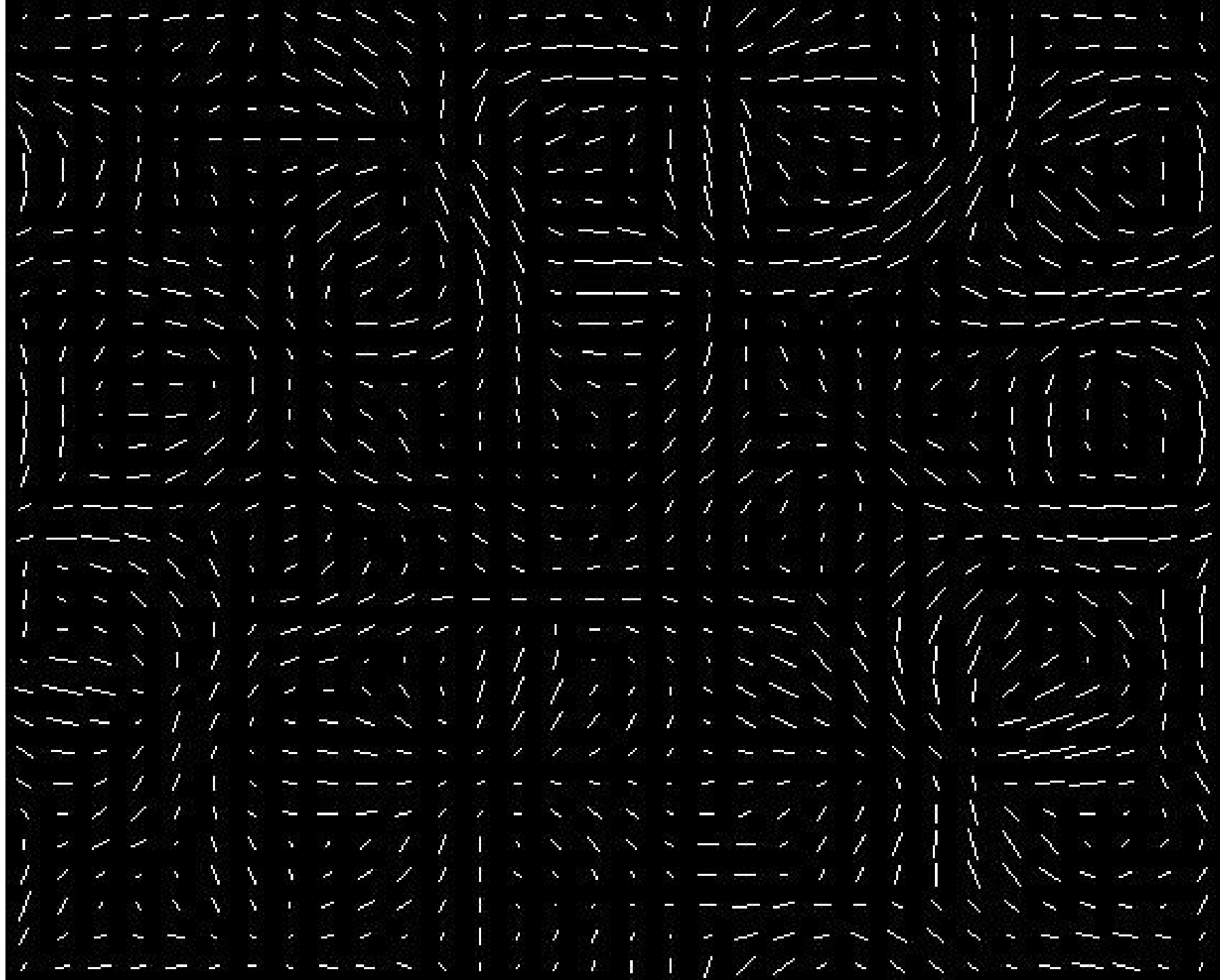
$$\kappa(\boldsymbol{\theta}) = \frac{3H_0^2\Omega_0}{2c^2} \int n_s(z_s) \int \frac{D_{LS}D_L}{D_S} \frac{\delta(\boldsymbol{\theta}, z)}{a(z)} dz dz_s$$

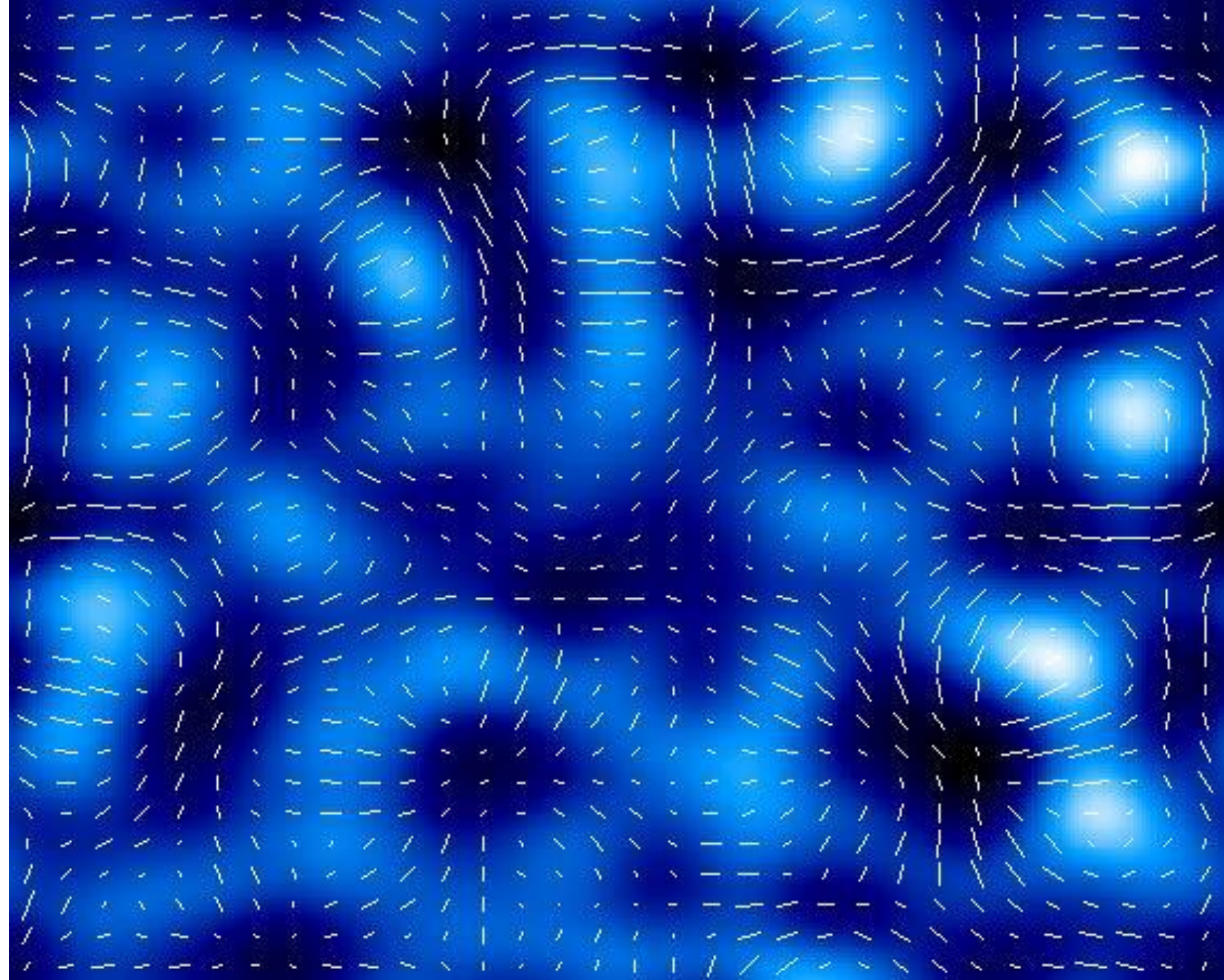


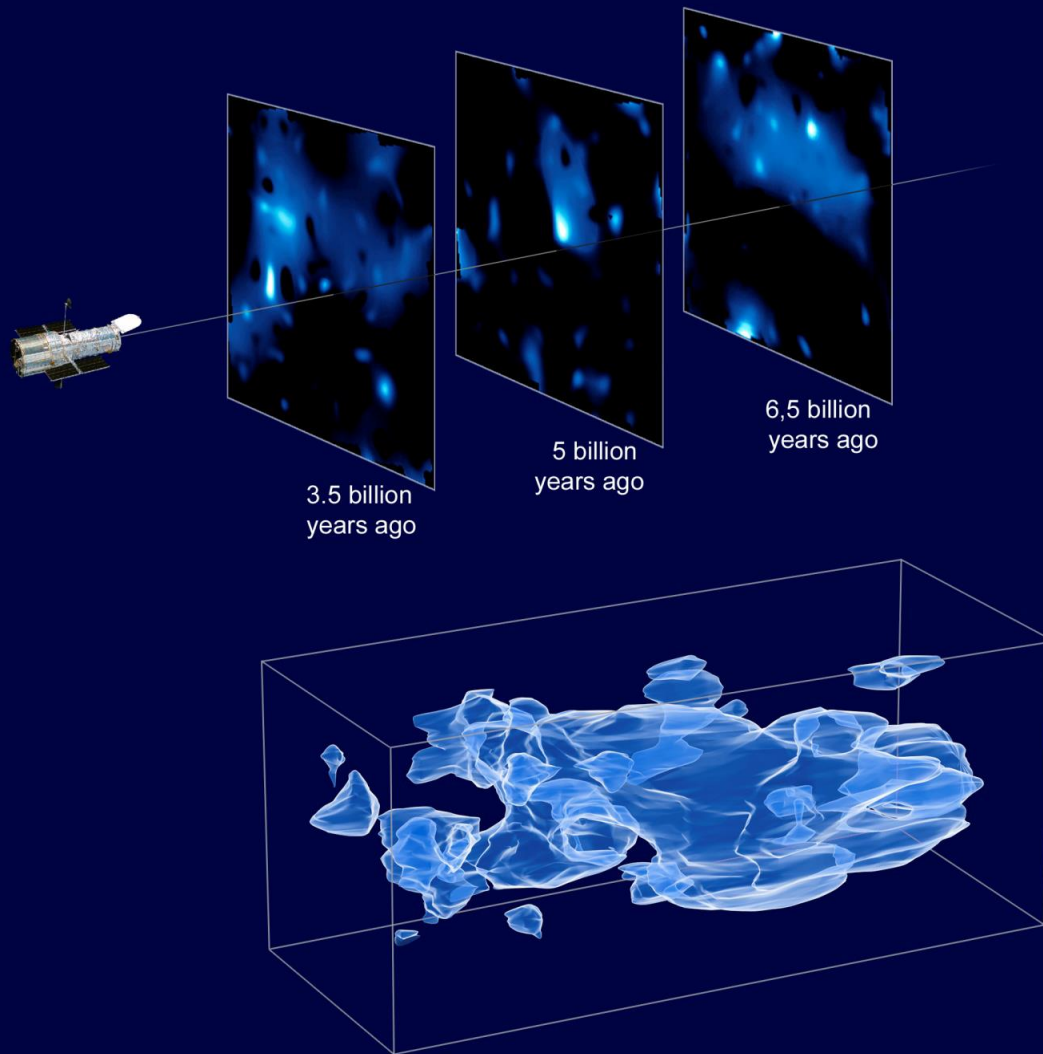












Weak Gravitational Lensing

The variance of convergence is related to the variance of the density contrast

Power spectrum of
convergence and matter

$$\begin{aligned}\langle \hat{\kappa}(\ell) \hat{\kappa}^*(\ell') \rangle &= (2\pi)^2 \delta_D(\ell - \ell') P_\kappa(\ell) \\ \langle \hat{\delta}(\mathbf{k}) \hat{\delta}^*(\mathbf{k}') \rangle &= (2\pi)^3 \delta_D(\mathbf{k} - \mathbf{k}') P_\delta(k)\end{aligned}$$

Related between them and related to cosmology (Limber's equation)

$$P_\kappa(\ell) = \int d\chi G^2(\chi) P_\delta \left(k = \frac{\ell}{\chi} \right)$$

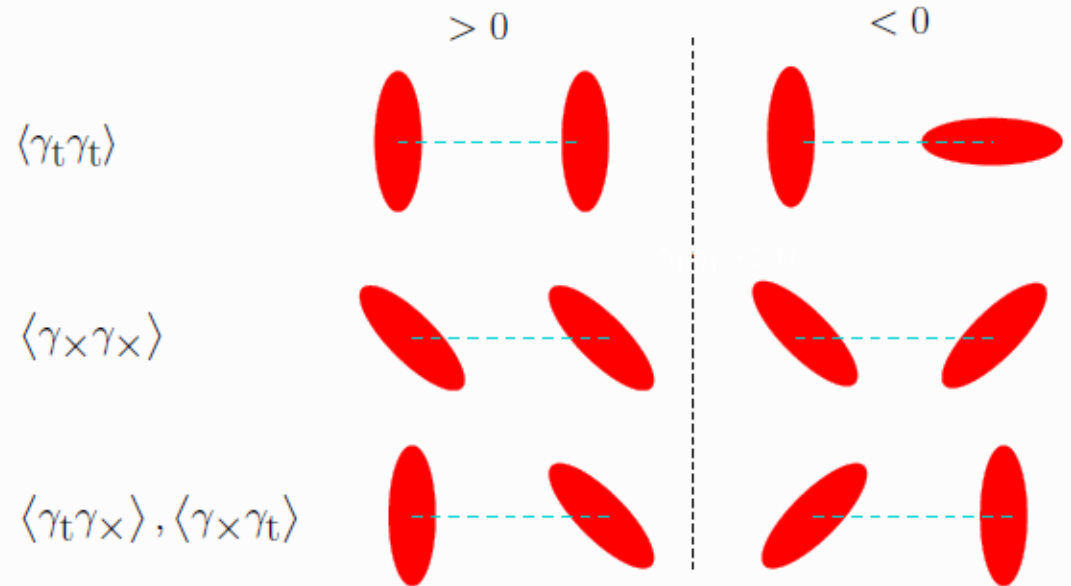
In the small angle approximation and assuming that the power spectrum varies slowly

Weak Gravitational Lensing

Cosmic shear: Correlations of shears at two points give us 4 functions

$$\gamma_t = -\Re(\gamma e^{-2i\phi})$$

$$\gamma_\times = -\Im(\gamma e^{-2i\phi})$$



Robustness test: The cross correlations must be null $\rightarrow \langle \gamma_t \gamma_\times \rangle = \langle \gamma_\times \gamma_t \rangle = 0$

If they are not, this is a clear sign of a systematic error in your analysis.

Finally the 2 correlation functions that are used for cosmic shear are defined as:

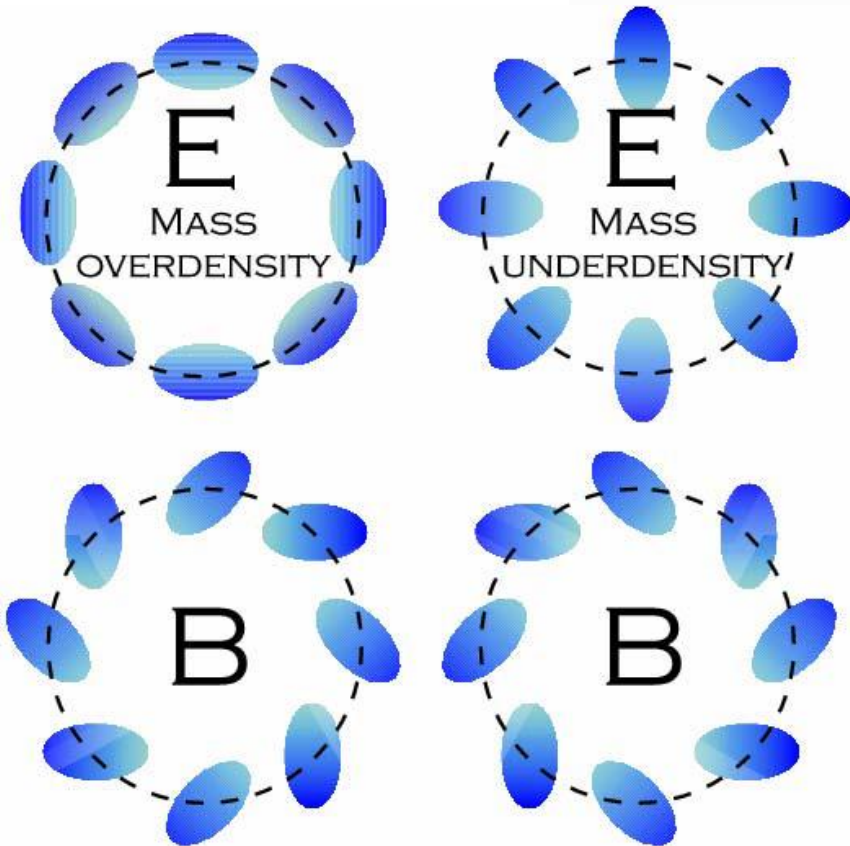
$$\xi_+(\vartheta) = \langle \gamma_t \gamma_t \rangle(\vartheta) + \langle \gamma_\times \gamma_\times \rangle(\vartheta)$$

$$\xi_-(\vartheta) = \langle \gamma_t \gamma_t \rangle(\vartheta) - \langle \gamma_\times \gamma_\times \rangle(\vartheta)$$

Weak Gravitational Lensing

The cosmic shear correlation functions are related to cosmological parameters

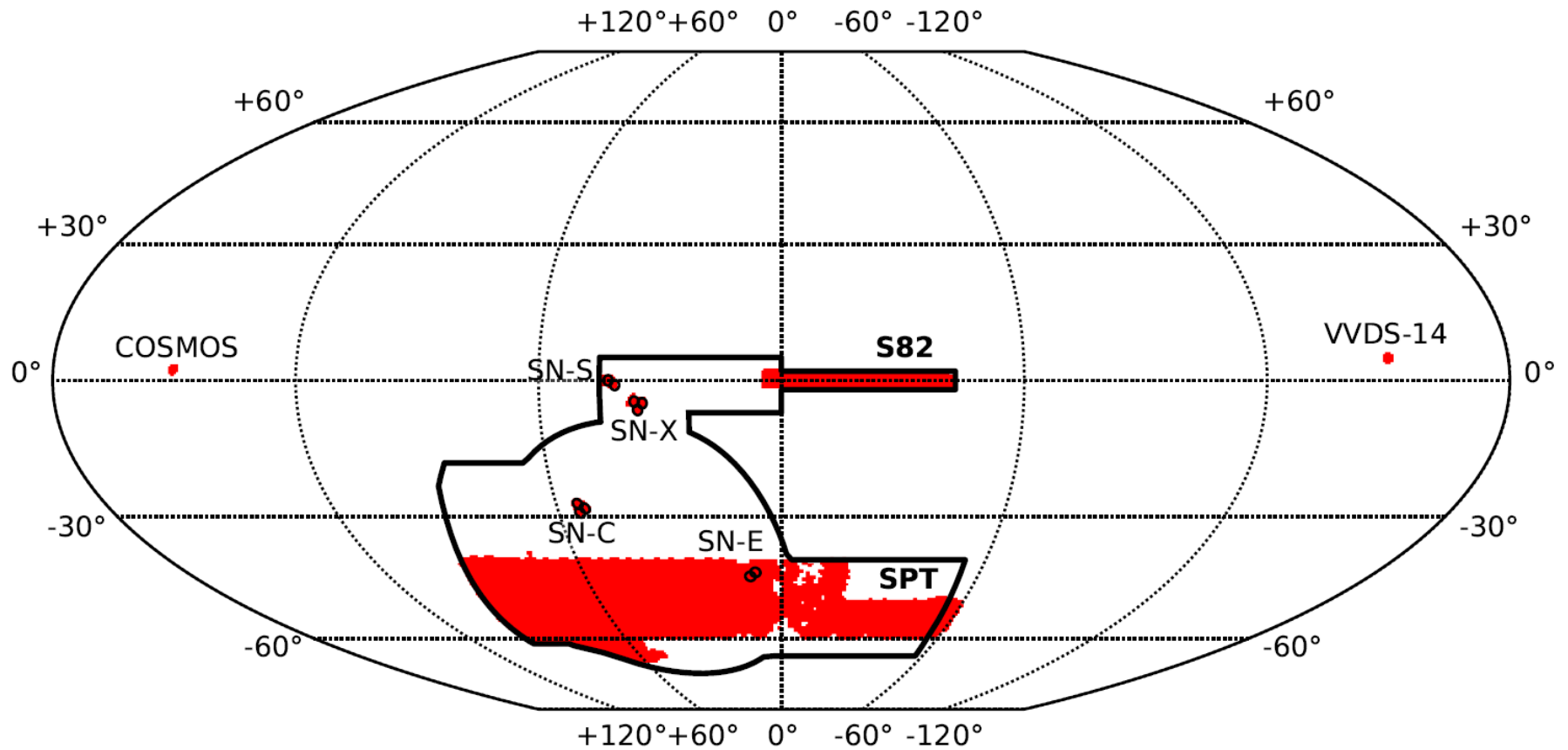
$$\xi_+(\theta) = \frac{1}{2\pi} \int_0^\infty d\ell \ell J_0(\ell\theta) P_\kappa(\ell)$$
$$\xi_-(\theta) = \frac{1}{2\pi} \int_0^\infty d\ell \ell J_4(\ell\theta) P_\kappa(\ell),$$



Tangential pattern is due to mass overdensity
Radial pattern is due to underdensities

No other patterns are possible for the shear field. A so-called B-mode is not generated

Example: Cosmology from clustering AND weak lensing from DES Y1 Data



The Dark Energy Survey



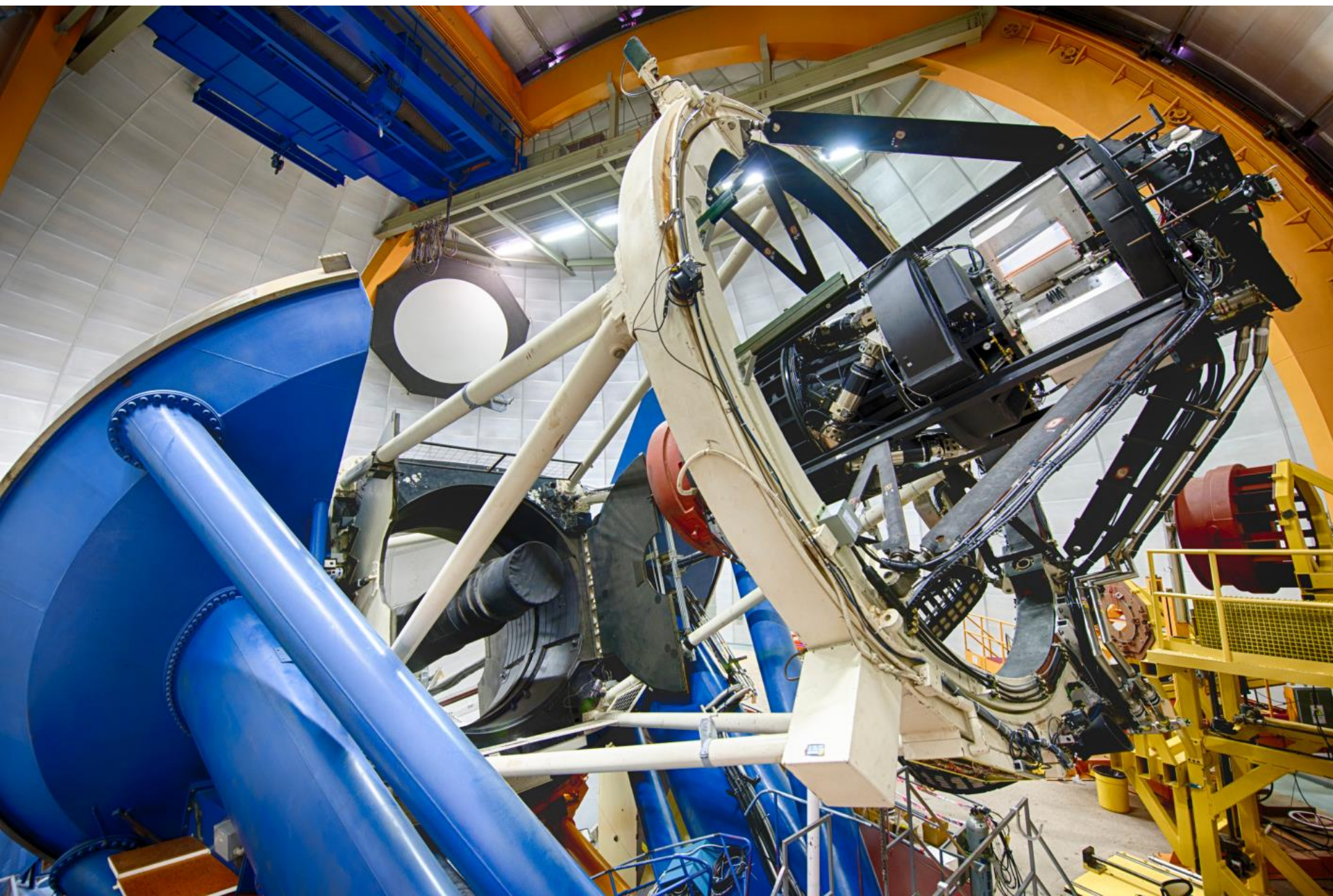
Optical/IR imaging survey with the Blanco 4m telescope at Cerro Tololo Inter-American Observatory(CTIO) in Chile

5000 sq-deg (1/8 of the sky) in grizY bands (2500 sq-deg overlapping with SPT survey) + 30 sq-deg time-domain griz (SNe)

Up to $i_{AB} \sim 24$ th magnitude at 10σ ($z \sim 1.5$)

570 Mpx camera with 3 sq-deg FoV, DECam

Installed on Blanco since 2012



NGC 1365

NGC 1365 (the Great Barred Spiral Galaxy) is a barred spiral galaxy about 56 million light-years away in the constellation Fornax. (DECam, DES Collaboration)



NGC 1566

NGC 1566 (the Spanish Dancer) is a spiral galaxy in the constellation Dorado. (DECam, DES Collaboration)



DECam

74 CCD chips (570
Mpx/image) (62 2kx4k
image, 8 2kx2k
alignment/focus, 4 2kx2k
guiding)

Red Sensitive CCDs
QE>50% @ 1000 nm
250 microns thick

3 sq-deg FoV
Excellent image quality
0.27''/pixel

Low noise electronics (<15 e
@ 250 kpx/s)



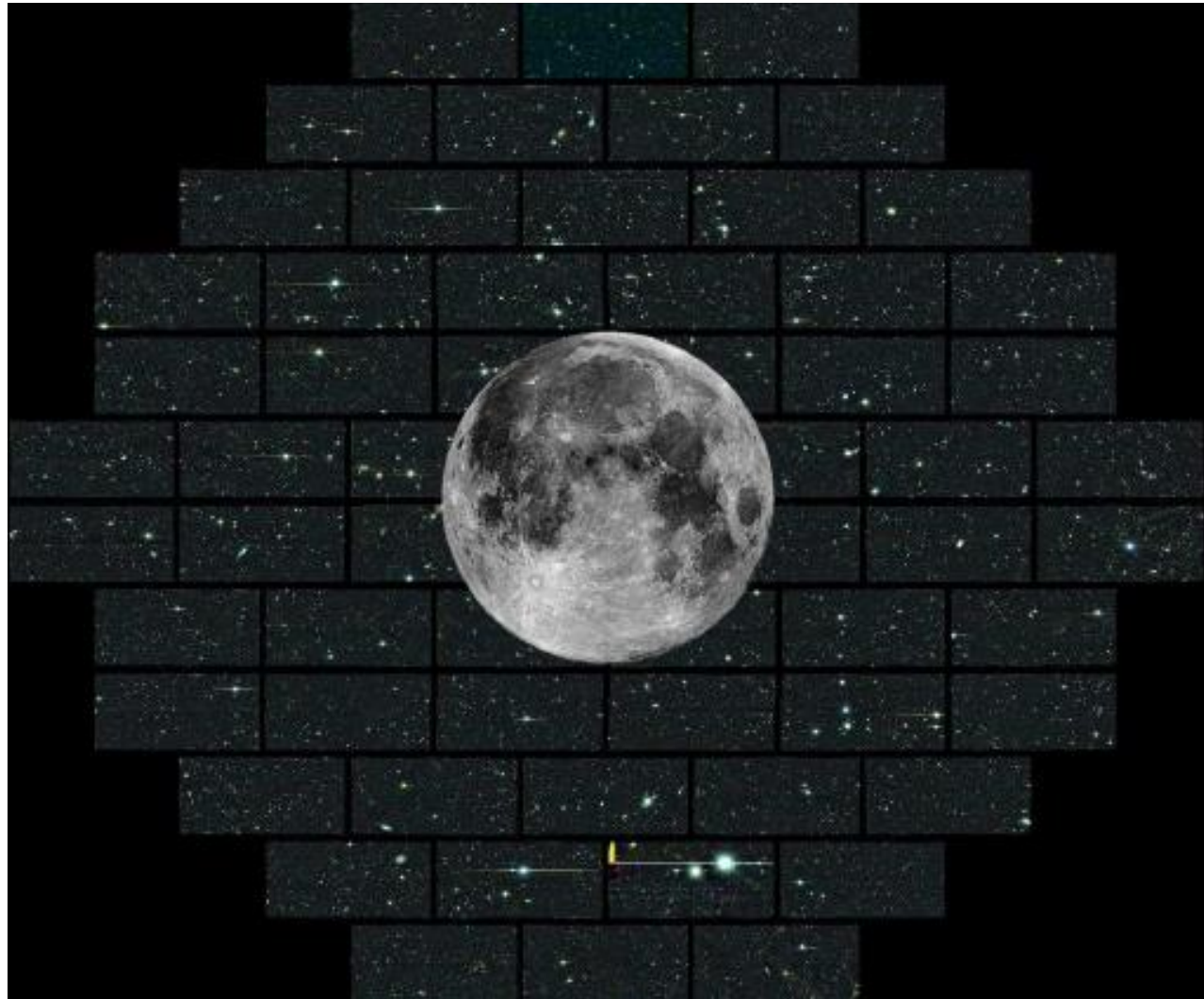
DECam

74 CCD chips (570
Mpx/image) (62 2kx4k
image, 8 2kx2k
alignment/focus, 4 2kx2k
guiding)

Red Sensitive CCDs
QE>50% @ 1000 nm
250 microns thick

3 sq-deg FoV
Excellent image quality
0.27''/pixel

Low noise electronics (<15 e
@ 250 kpx/s)



DES Science Summary

4 Probes of Dark Energy

Galaxy Clusters (dist & struct)

Tens of thousands of clusters to $z \sim 1$
Synergy with SPT, VHS

Weak Lensing (dist & struct)

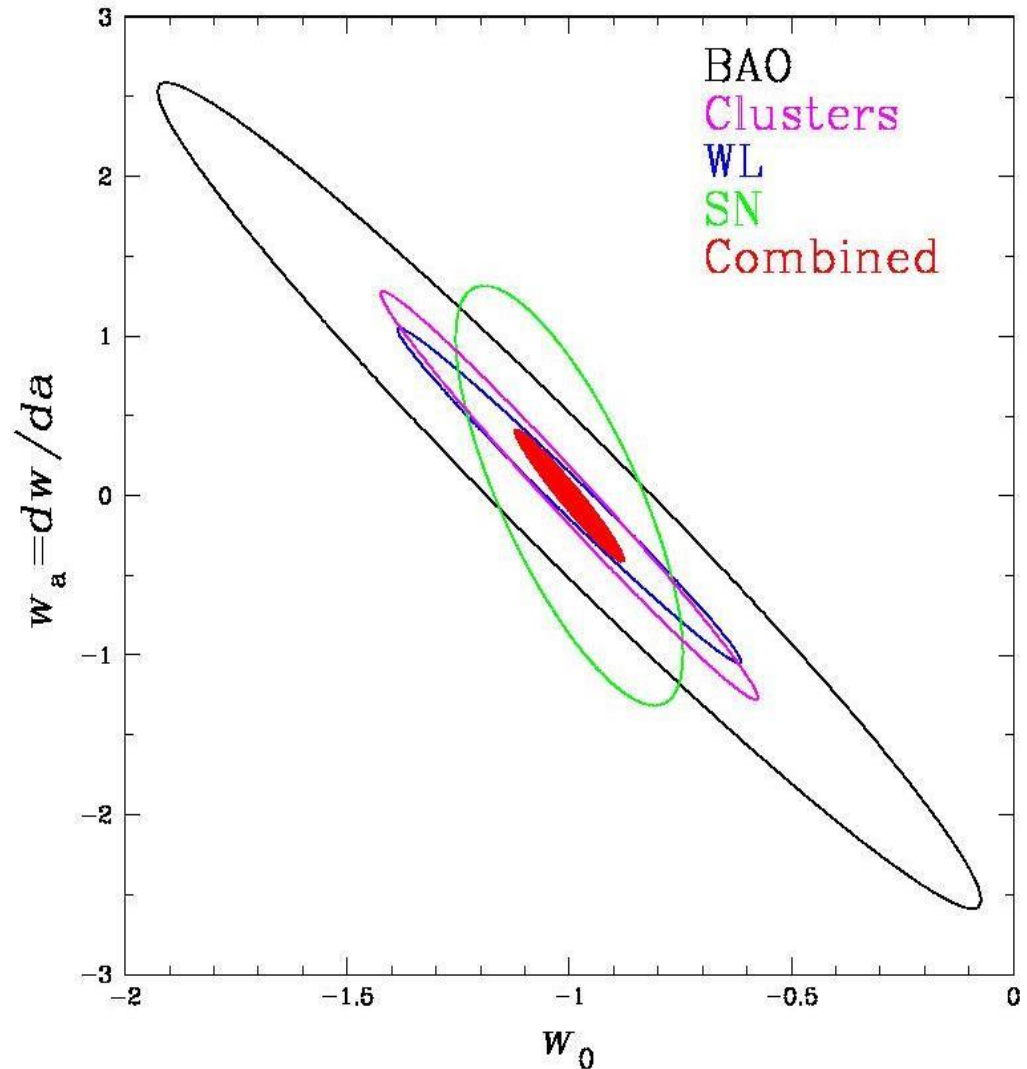
Shape and magnification measurements
of 200 million galaxies

Baryon Acoustic Oscillations (dist)

300 million galaxies to $z \sim 1.4$

Supernovae (dist)

3500 well-sampled SNe Ia to $z \sim 1$



DES Science summary

4 Probes of Dark Energy

Galaxy Clusters (dist & struct)

Tens of thousands of clusters to $z \sim 1$
Synergy with SPT, VHS

Weak Lensing (dist & struct)

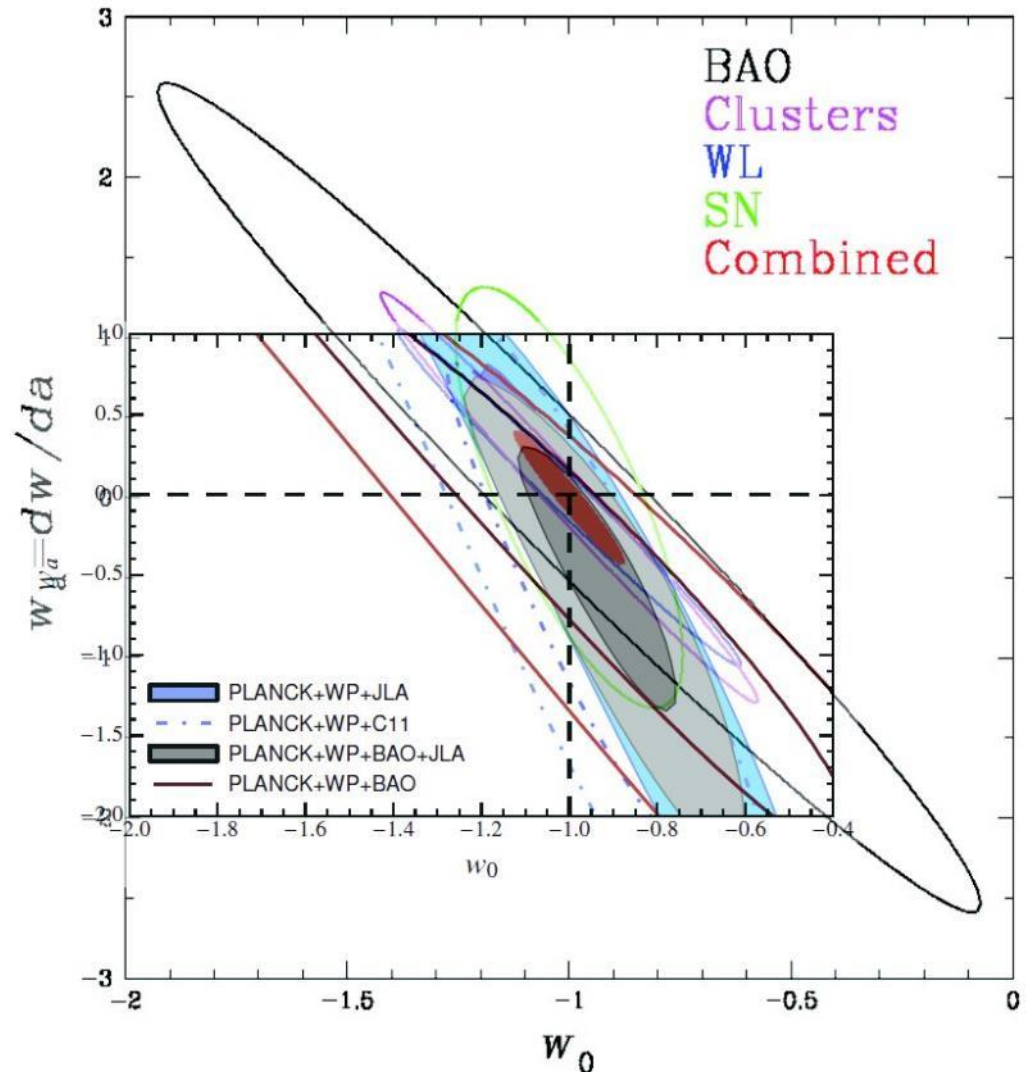
Shape and magnification measurements
of 200 million galaxies

Baryon Acoustic Oscillations (dist)

300 million galaxies to $z \sim 1.4$

Supernovae (dist)

3500 well-sampled SNe Ia to $z \sim 1$





USA: Fermilab, UIUC/NCSA, University of Chicago, LBNL, NOAO, University of Michigan, University of Pennsylvania, Argonne National Laboratory, Ohio State University, Santa Cruz/SLAC Consortium, Texas A&M University, CTIO (in Chile)

DES Collaboration

~500 scientists from
25 institutions in 7 countries

darkenergysurvey.org

Facebook.com/darkenergysurvey



DARK ENERGY
SURVEY



UK Consortium: UCL, Cambridge, Edinburgh, Portsmouth, Sussex, Nottingham



Germany: Munich



Switzerland: Zurich



Spain Consortium:
CIEMAT, ICE, IFAE

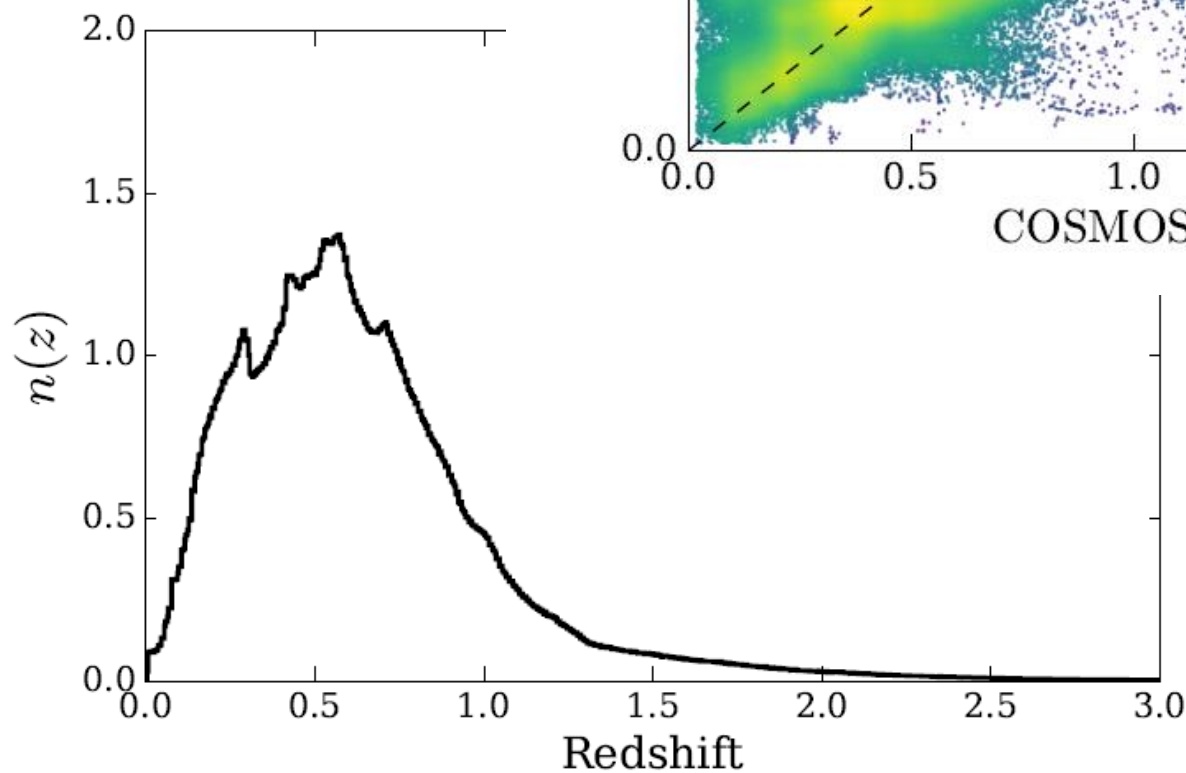
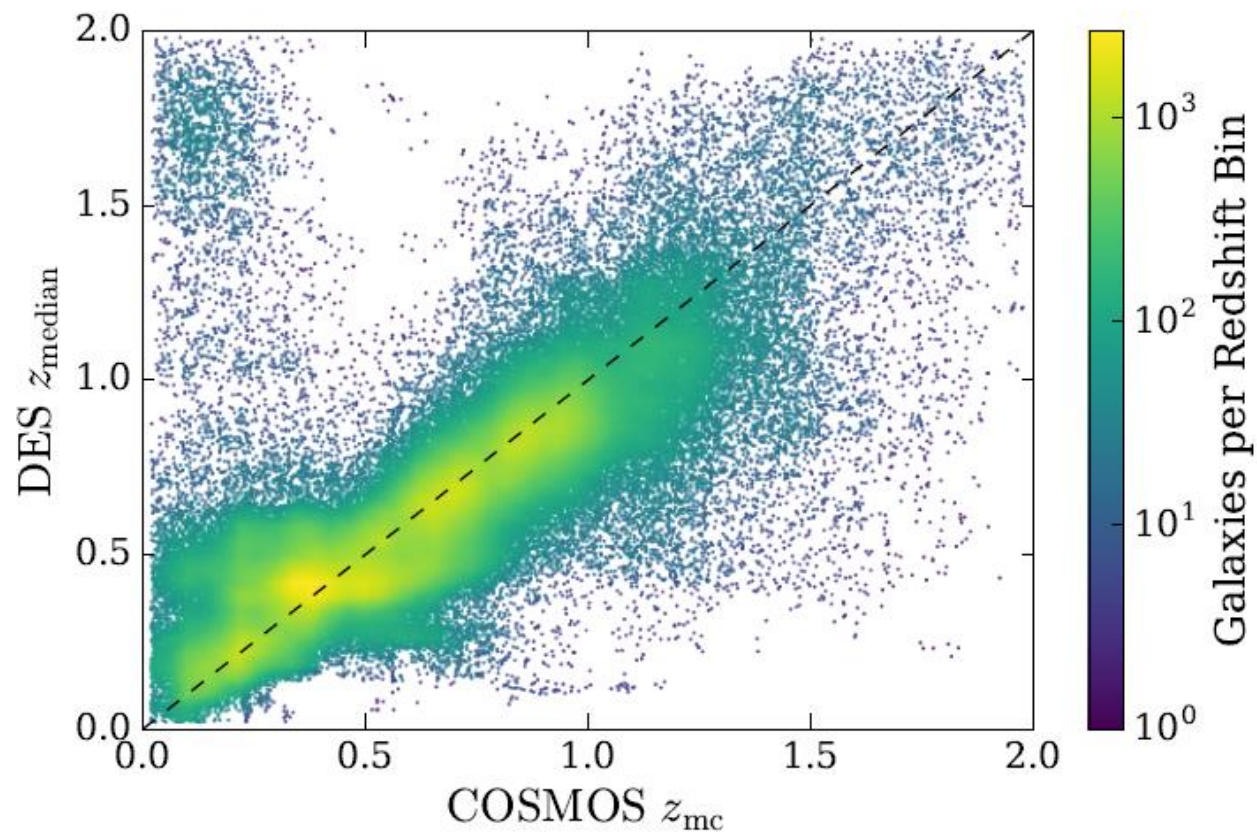


OzDES: CAASTRO, AAO, ANU, Queensland, Swinburne



Brazil Consortium:
Observatorio nacional, CBPF, Universidade Federal do Rio de Janeiro, Universidade Federal do Rio Grande do Sul

Redshift distribution of galaxies within DES Y1 data

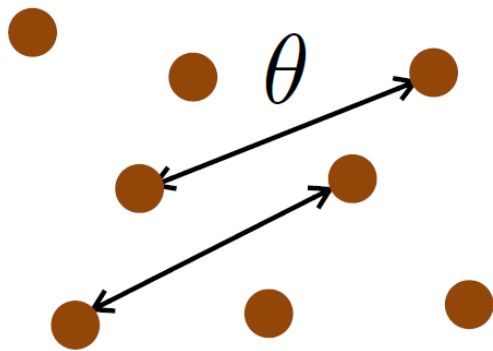
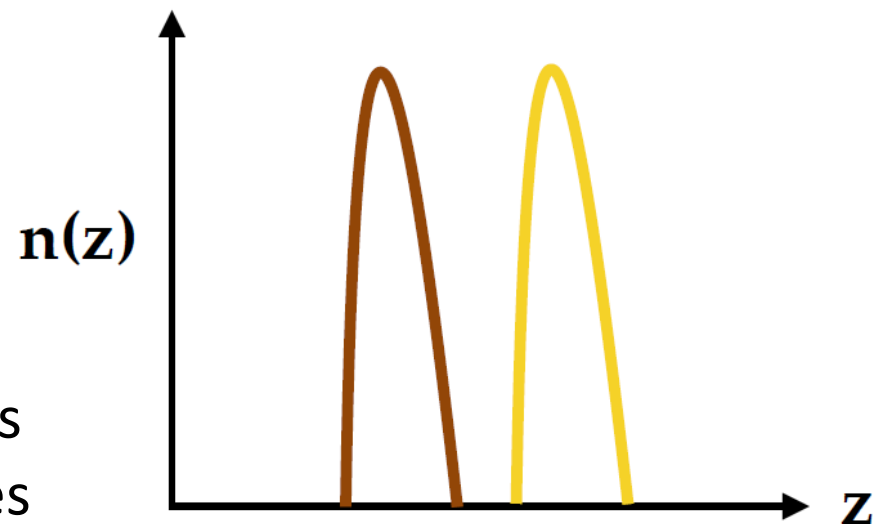


DES Y1 3x2pt Cosmology

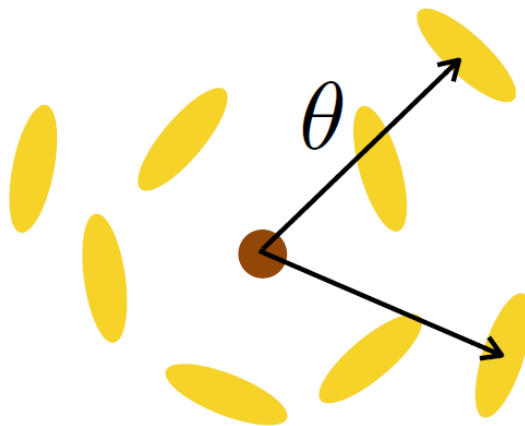
2 samples of galaxies: “**lens**” and “**sources**”

Combine the auto and cross-correlation of

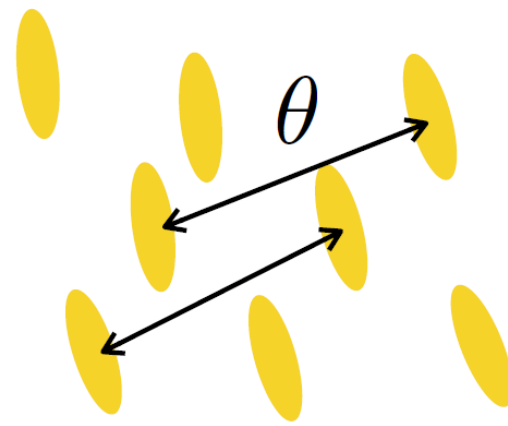
1. **positions** of the lens galaxies
2. **shapes** of the source galaxies



Galaxy clustering



Galaxy-galaxy lensing

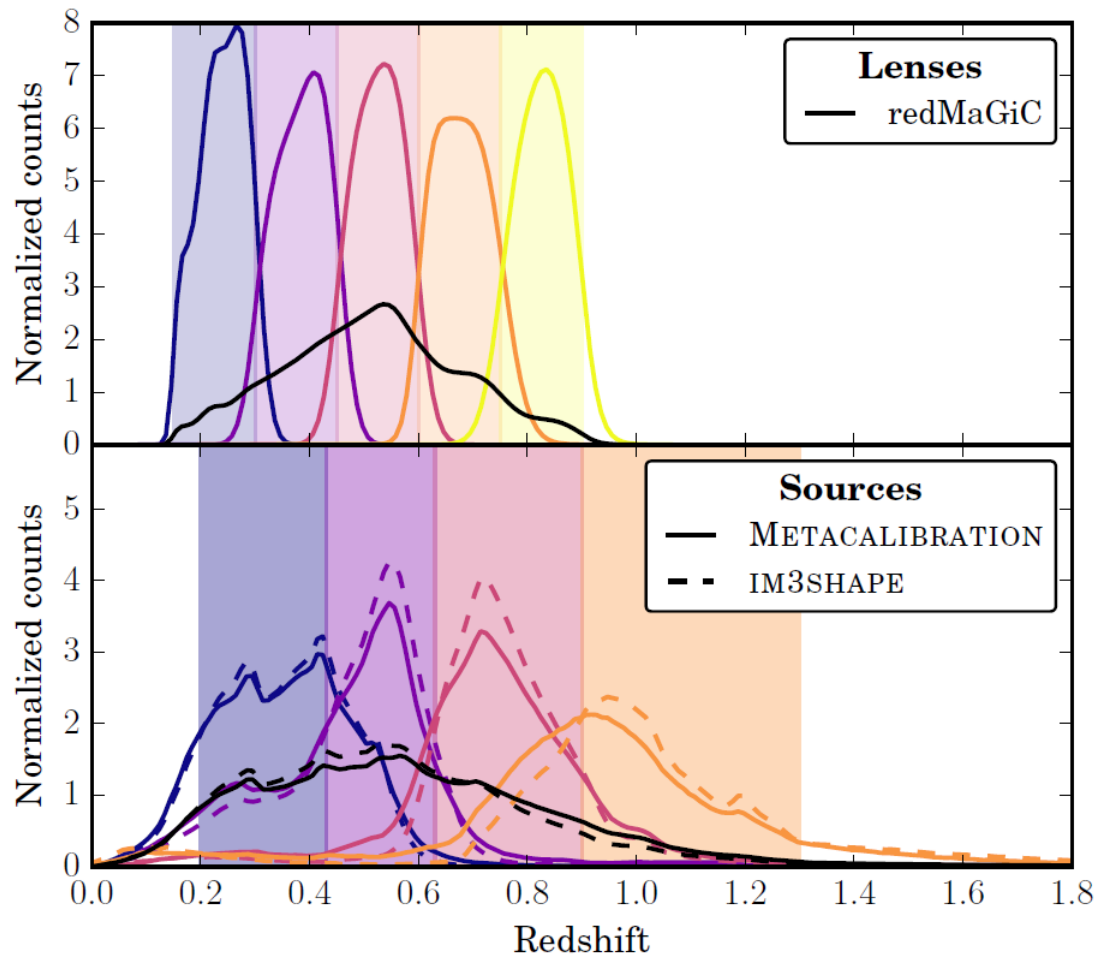


Cosmic shear

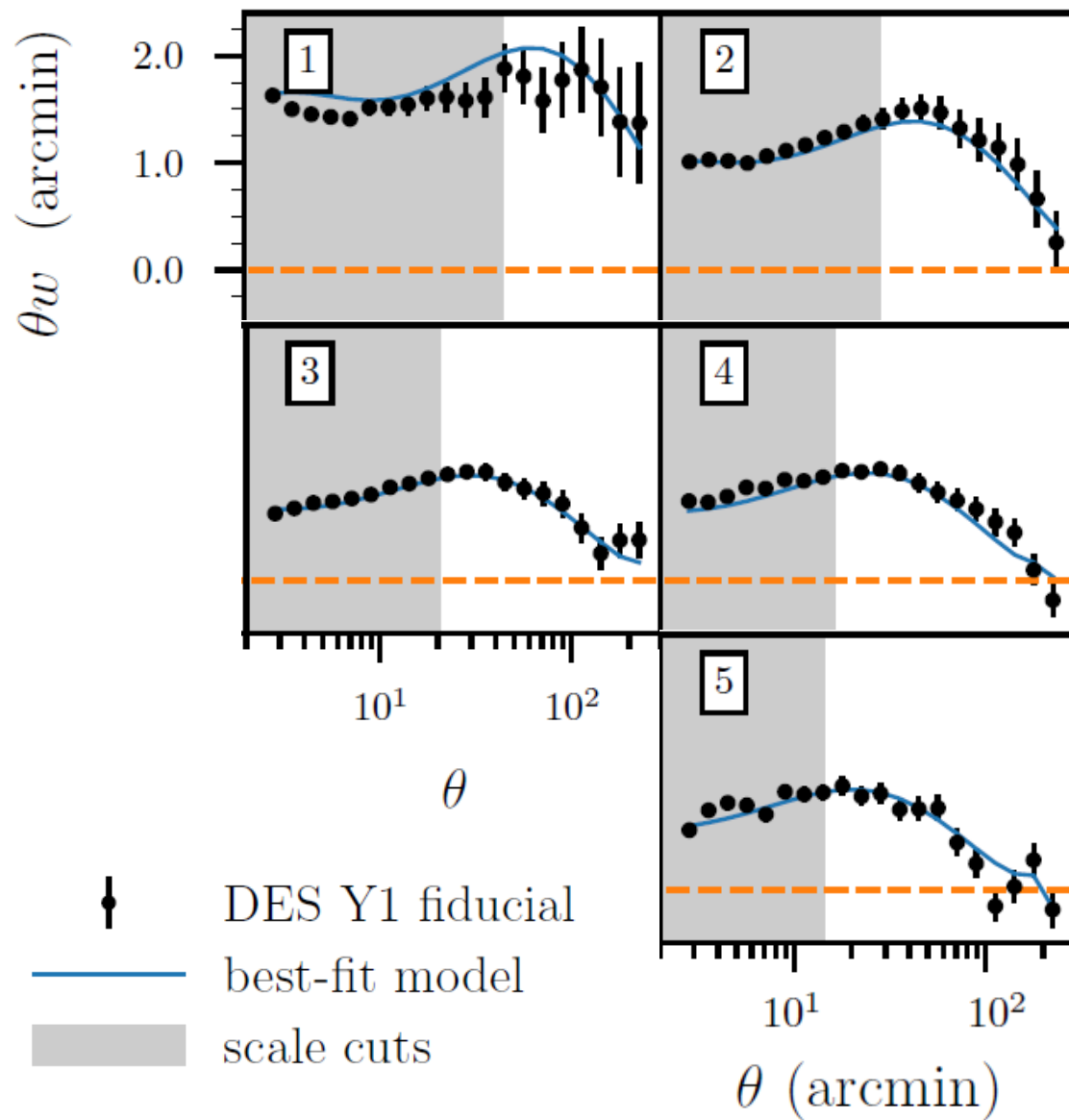
DES Y1 3x2pt Cosmology

This is a very demanding measurement:

- Manage a large dataset
- Compute correlation functions (3 types)
- These measurements are not independent → Compute and verify the covariance matrix

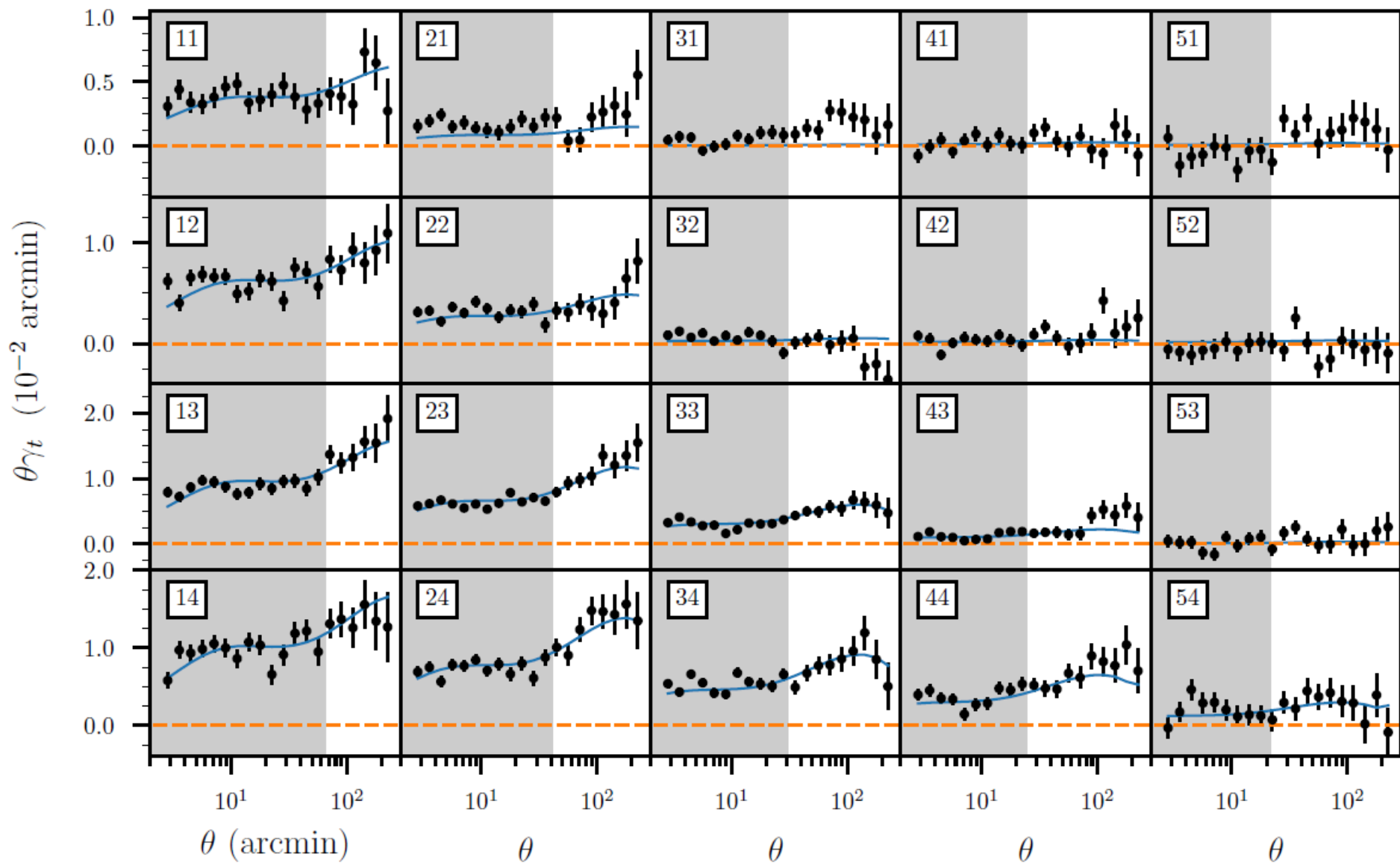
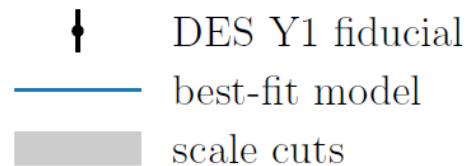


DES Y1 **3x2pt** Cosmology

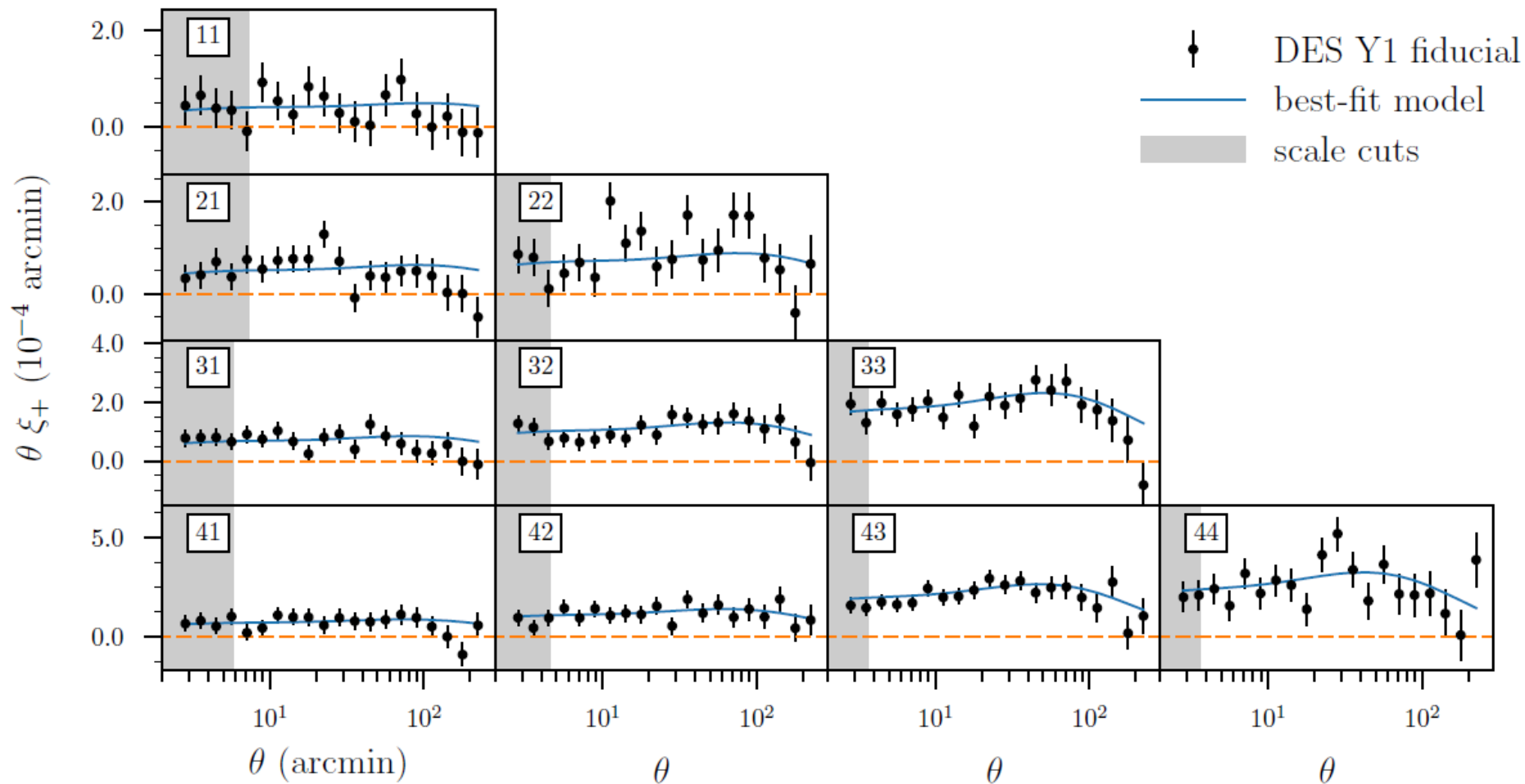


Lens density correlation functions for each redshift bin

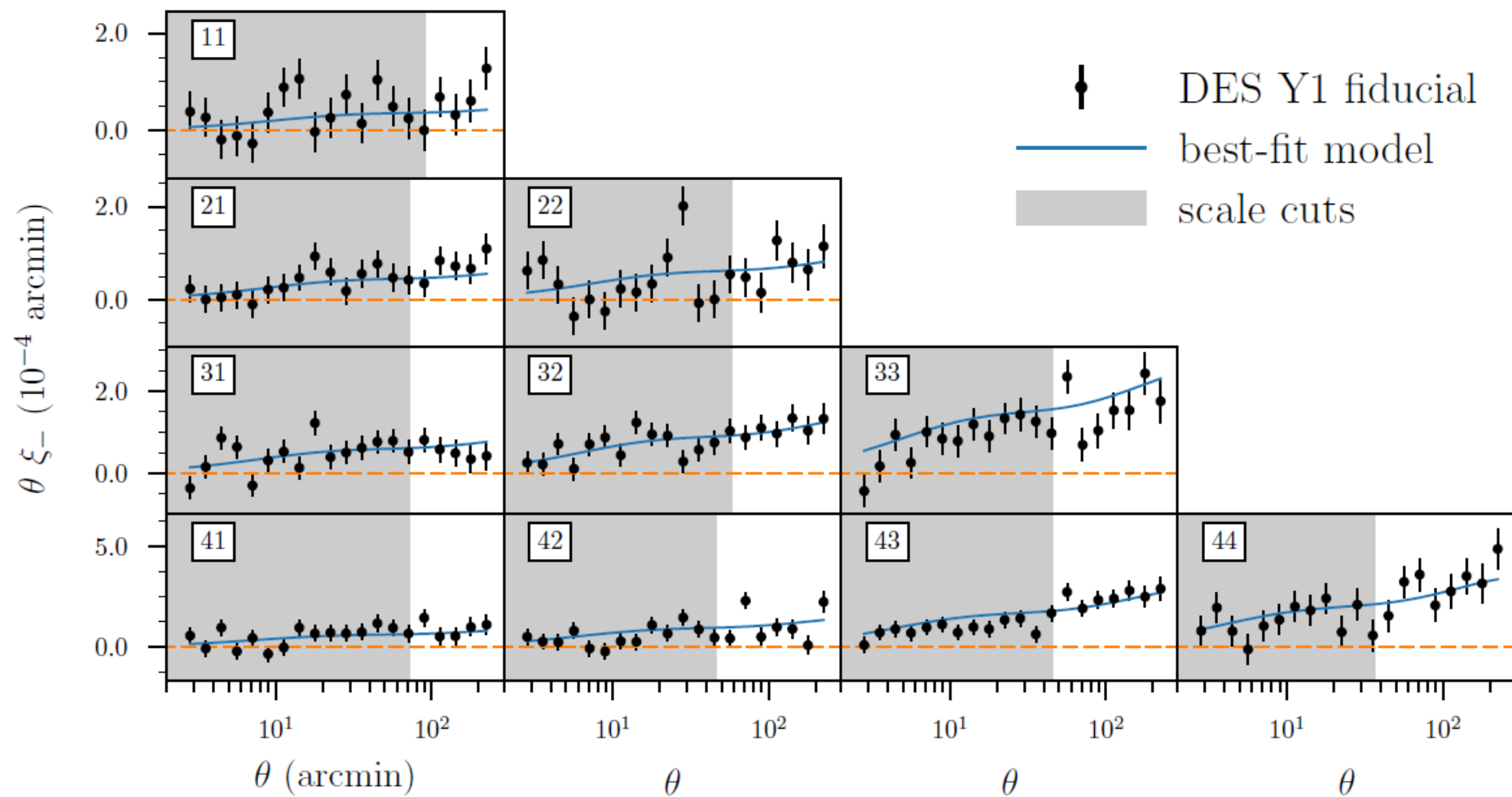
DES Y1 **3x2pt** Cosmology



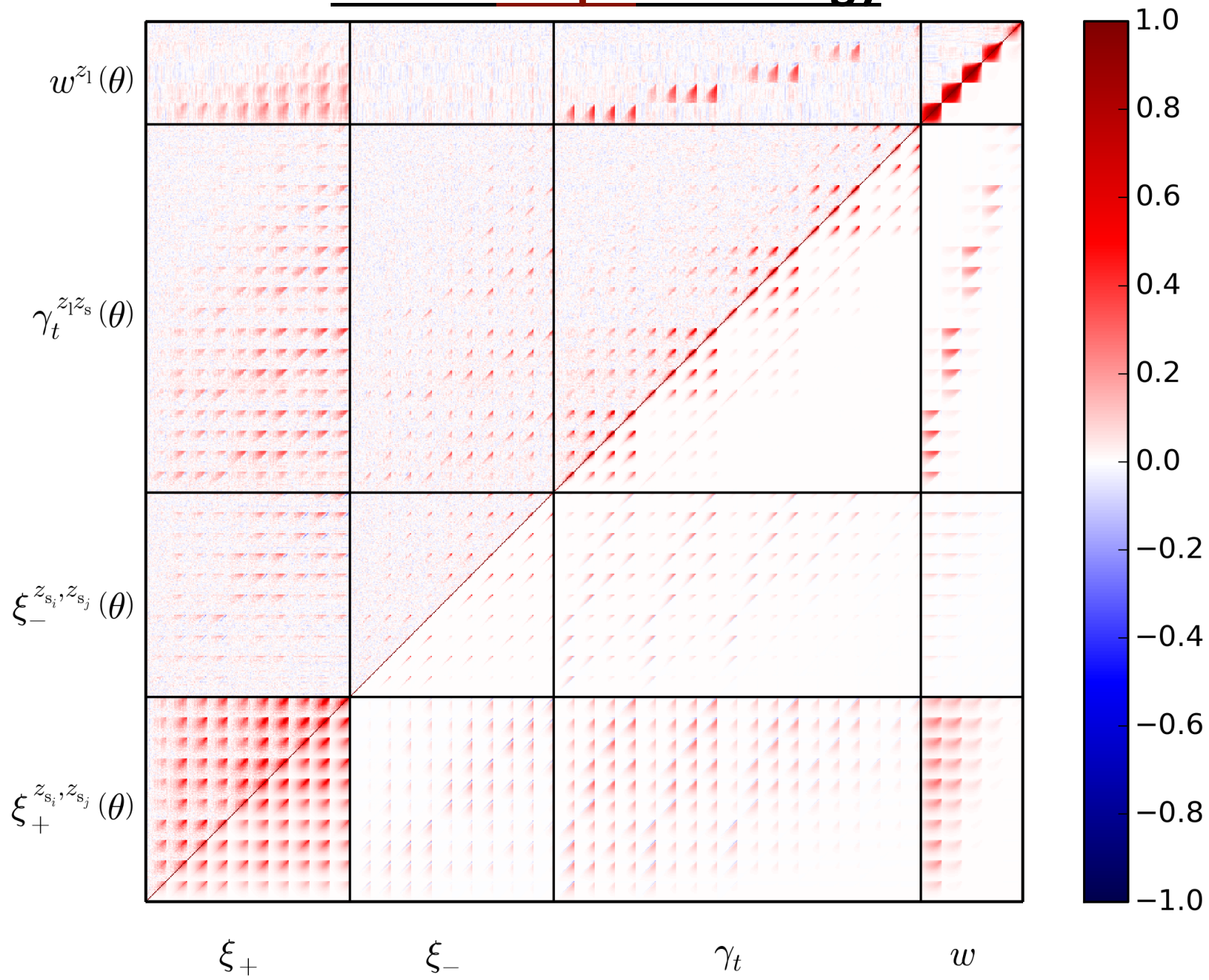
DES Y1 **3x2pt** Cosmology



DES Y1 **3x2pt** Cosmology



DES Y1 **3x2pt** Cosmology



DES Y1 **3x2pt** Cosmology

$$w^i(\theta) = (b^i)^2 \int \frac{dl l}{2\pi} J_0(l\theta) \int d\chi$$

$$\times \frac{[n_1^i(z(\chi))]^2}{\chi^2 H(z)} P_{\text{NL}} \left(\frac{l + 1/2}{\chi}, z(\chi) \right)$$

Galaxy Clustering
Correlation position-position

$$\gamma_{\text{t}}^{ij}(\theta) = b^i(1 + m^j) \int \frac{dl l}{2\pi} J_2(l\theta) \int d\chi n_1^i(z(\chi))$$

$$\times \frac{q_s^j(\chi)}{H(z)\chi^2} P_{\text{NL}} \left(\frac{l + 1/2}{\chi}, z(\chi) \right)$$

Galaxy-Glaxy Lensing
Correlation position-shape

$$q_s^i(\chi) = \frac{3\Omega_m H_0^2}{2} \frac{\chi}{a(\chi)} \int_{\chi}^{\chi(z=\infty)} d\chi' n_s^i(z(\chi')) \frac{dz}{d\chi'} \frac{\chi' - \chi}{\chi'}$$

(IV.3)

$$\xi_{+/-}^{ij}(\theta) = (1 + m^i)(1 + m^j) \int \frac{dl l}{2\pi} J_{0/4}(l\theta) \int d\chi$$

$$\times \frac{q_s^i(\chi) q_s^j(\chi)}{\chi^2} P_{\text{NL}} \left(\frac{l + 1/2}{\chi}, z(\chi) \right)$$

Cosmic Shear
Correlation shape-shape

DES Y1 3x2pt Cosmology

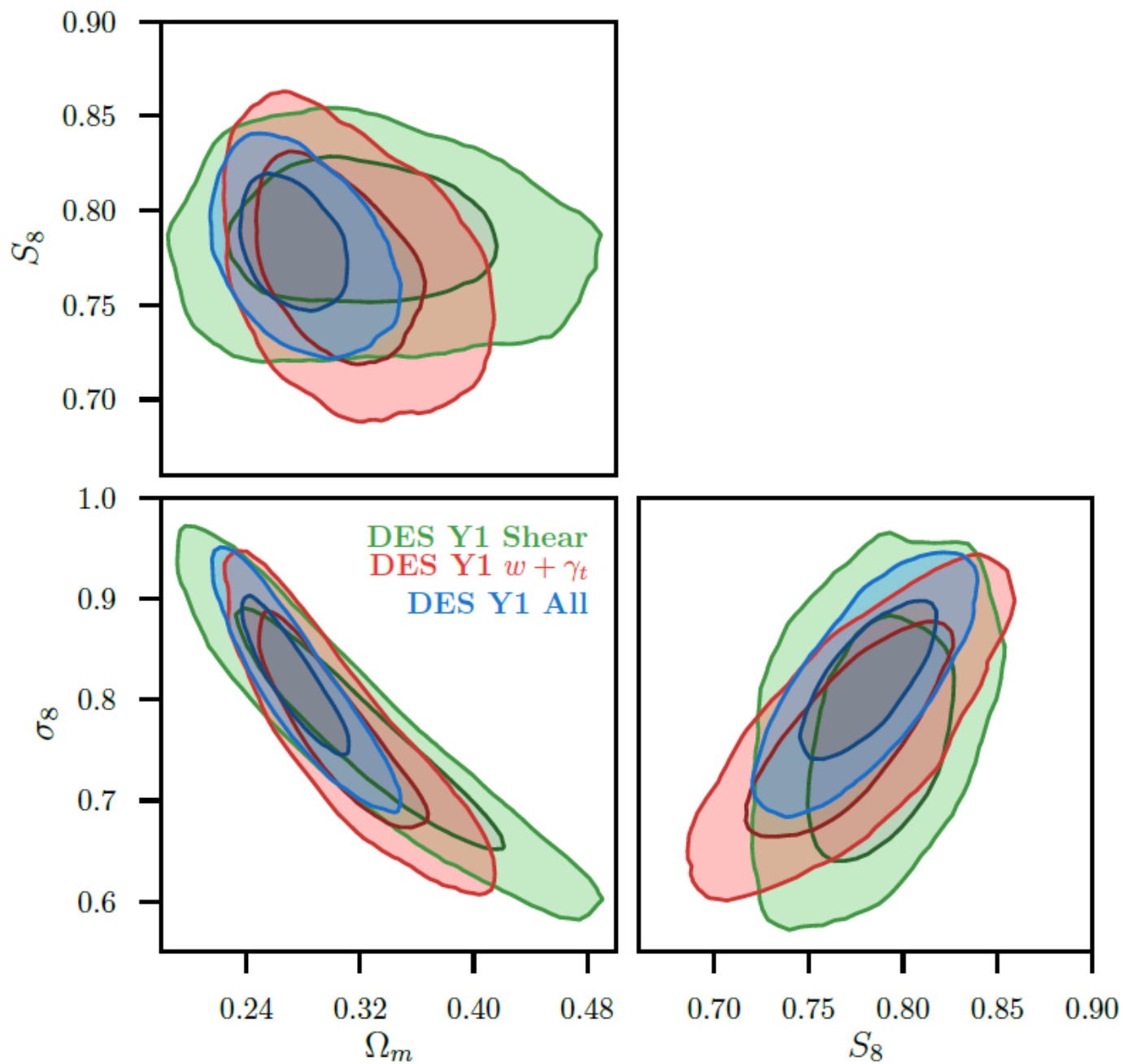
How to decide if Λ CDM (or any other theory) describes the data: The Likelihood function

$$\ln \mathcal{L}(\vec{p}) = -\frac{1}{2} \sum_{ij} [D_i - T_i(\vec{p})] C^{-1}_{ij} [D_j - T_j(\vec{p})]$$

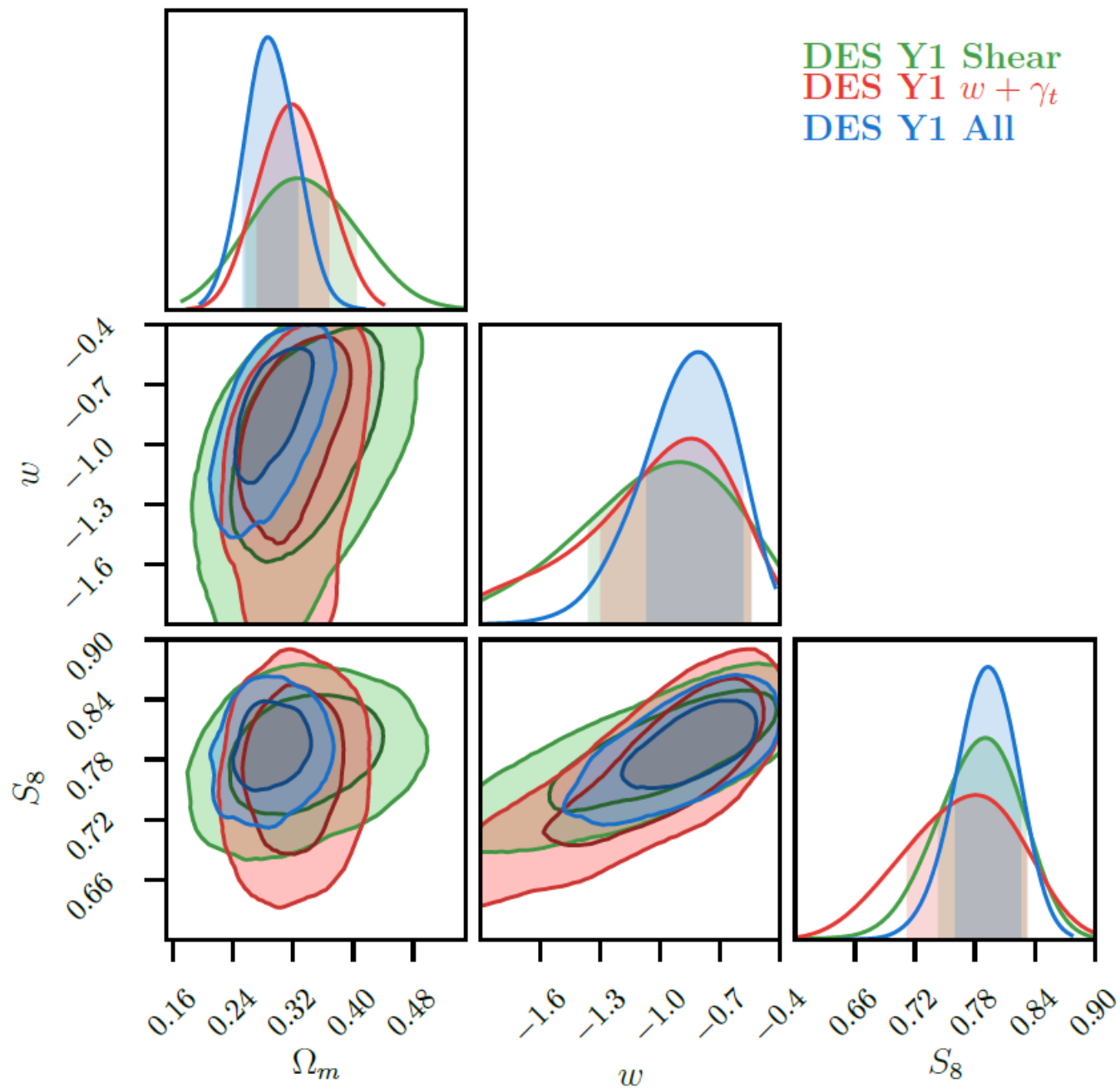
Derived Parameters: S8 to minimize correlations between original parameters

$$S_8 \equiv \sigma_8 \left(\frac{\Omega_m}{0.3} \right)^{0.5}$$

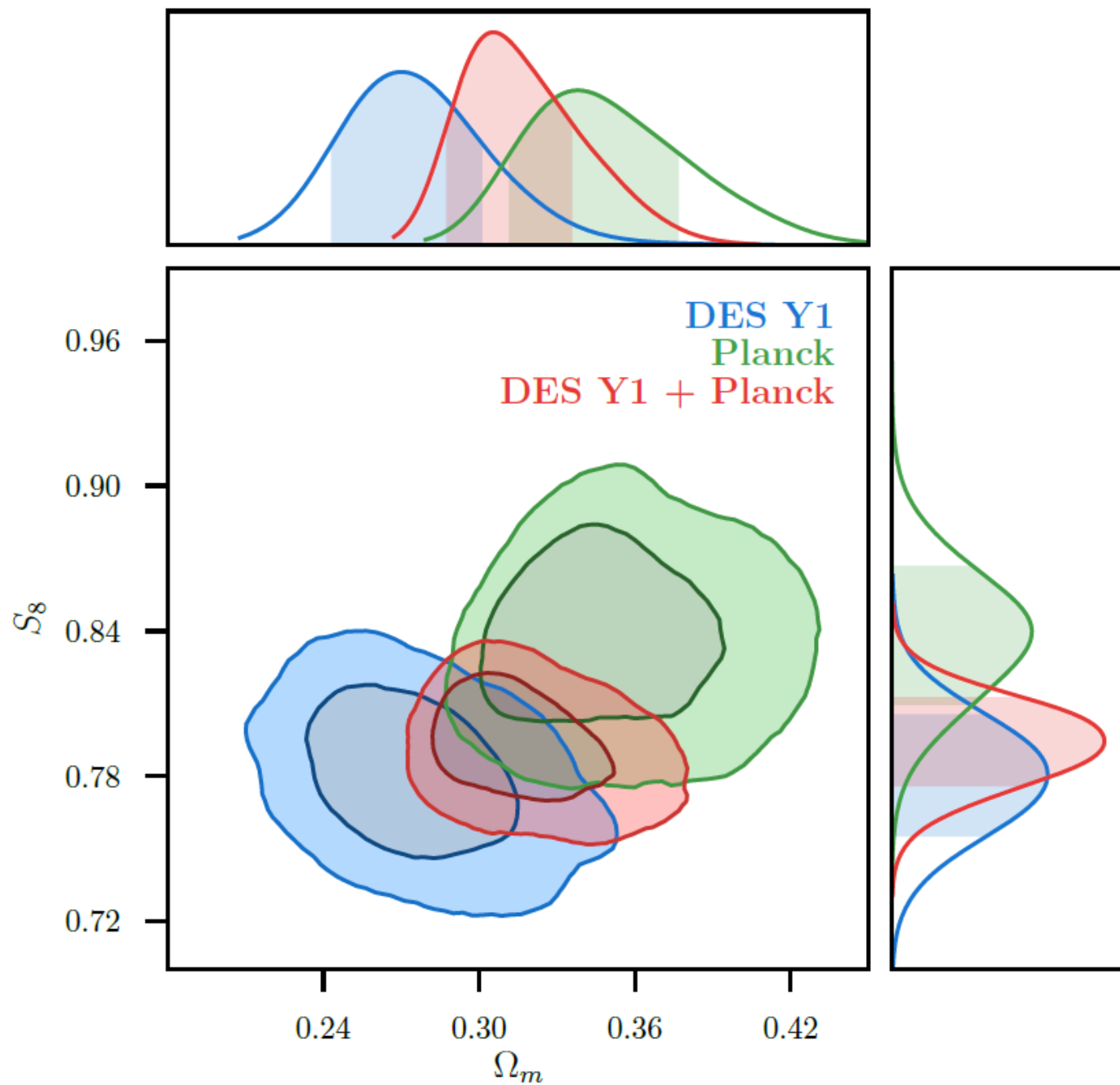
DES Y1 3x2pt Cosmology



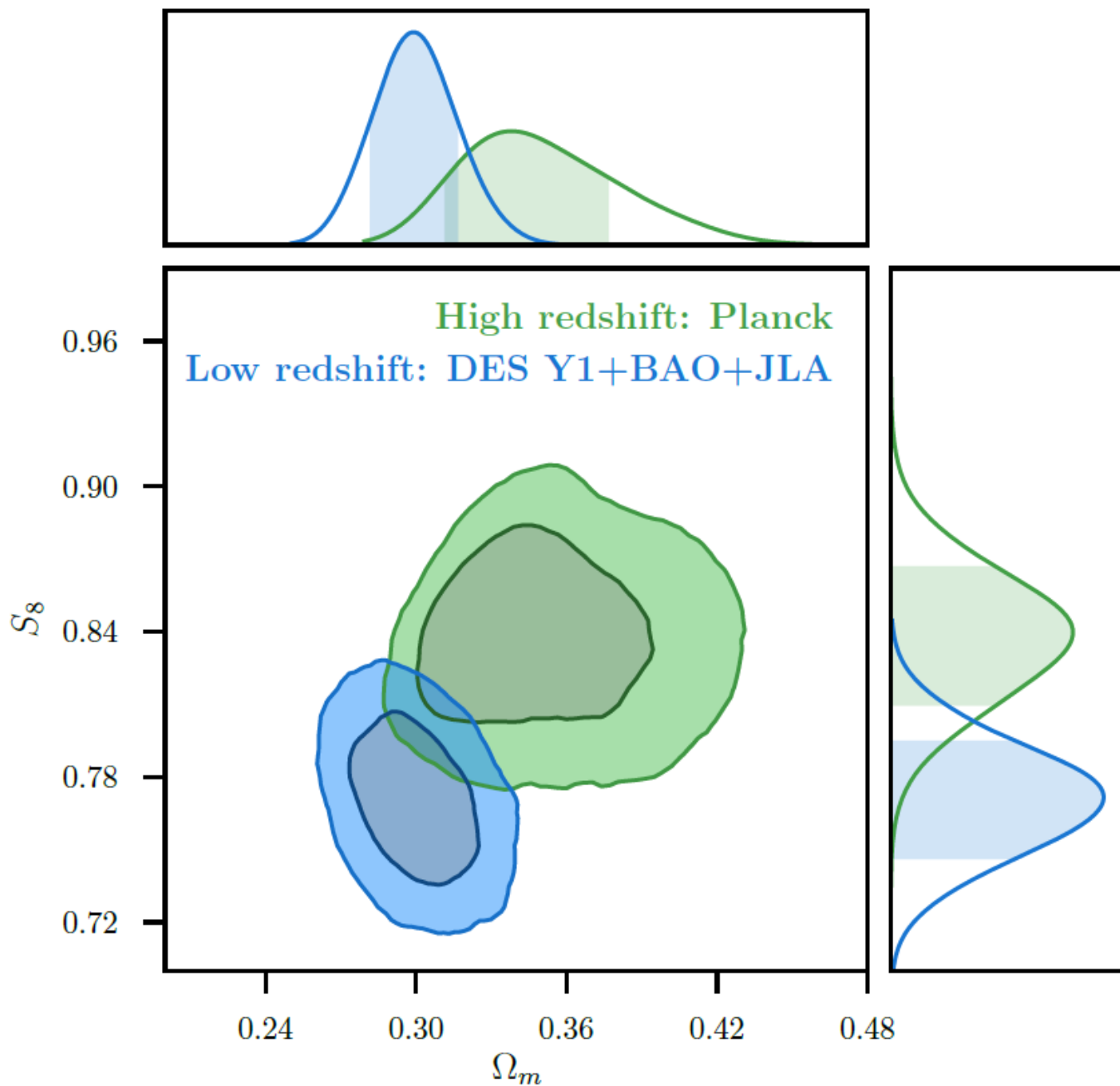
DES Y1 **3x2pt** Cosmology



DES Y1 3x2pt Cosmology

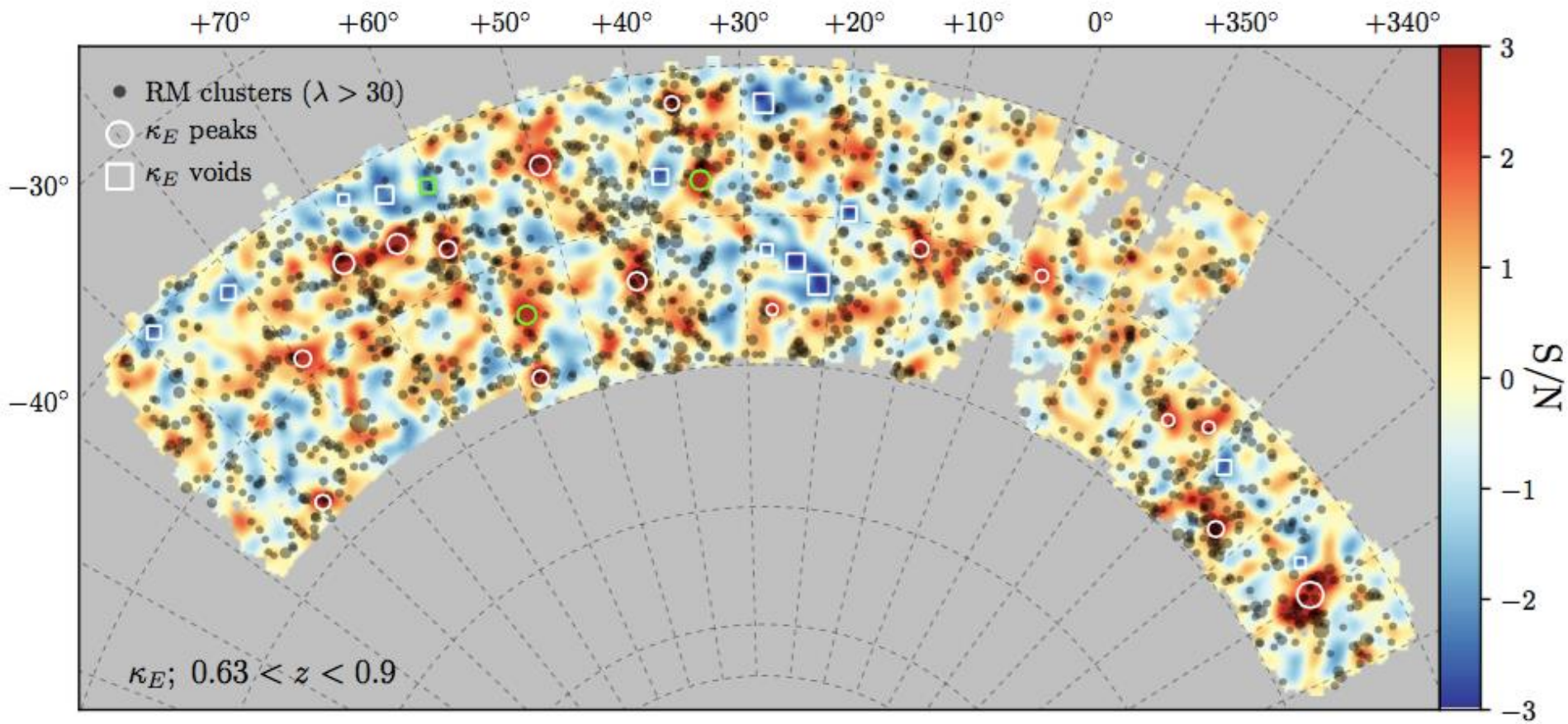


DES Y1 **3x2pt** Cosmology



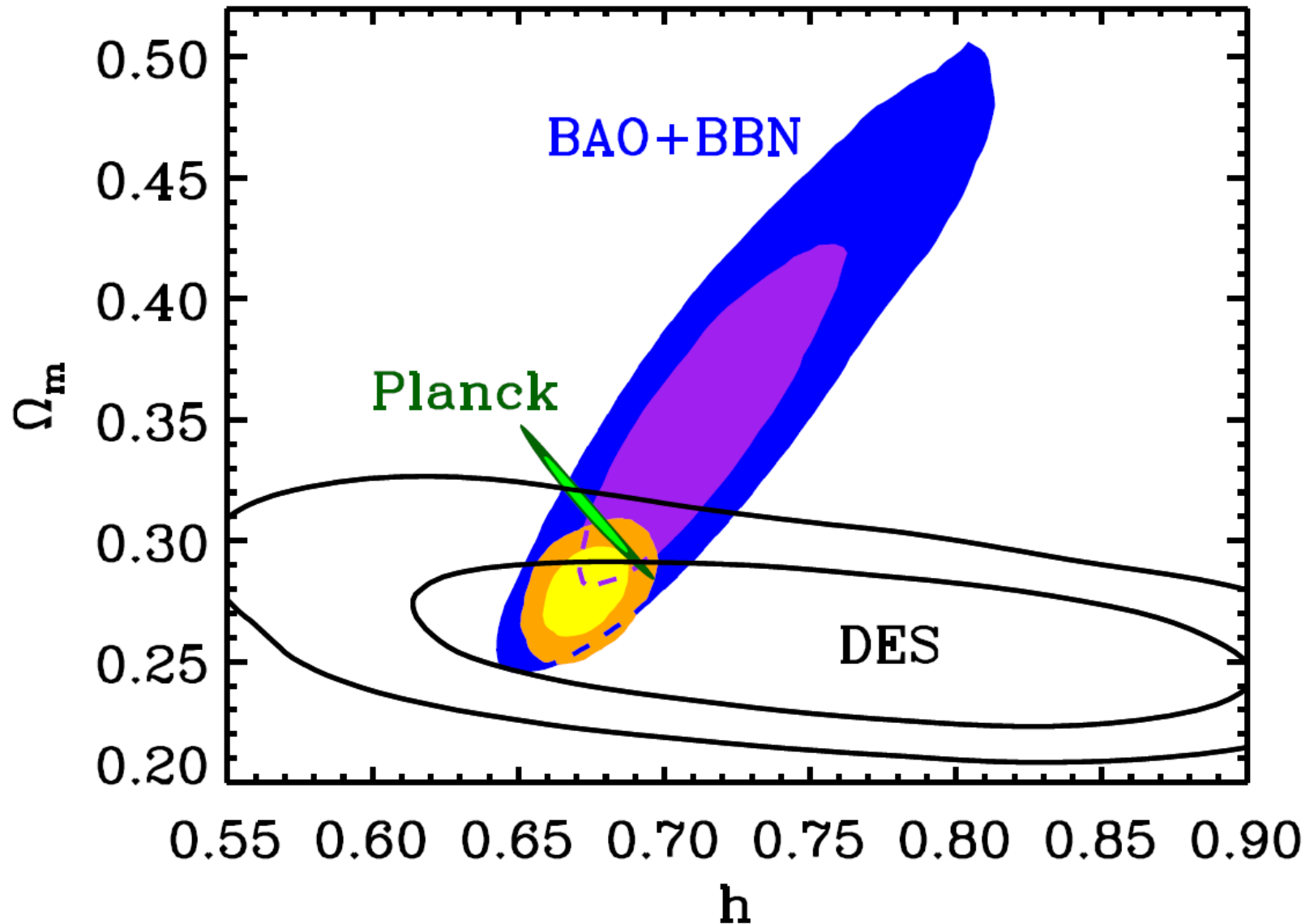
DES Y1 **3x2pt** Cosmology

Using the weak gravitational lensing it is possible to build a map of matter (all, including the dark matter) in the Universe



DES Y1 **3x2pt** Cosmology

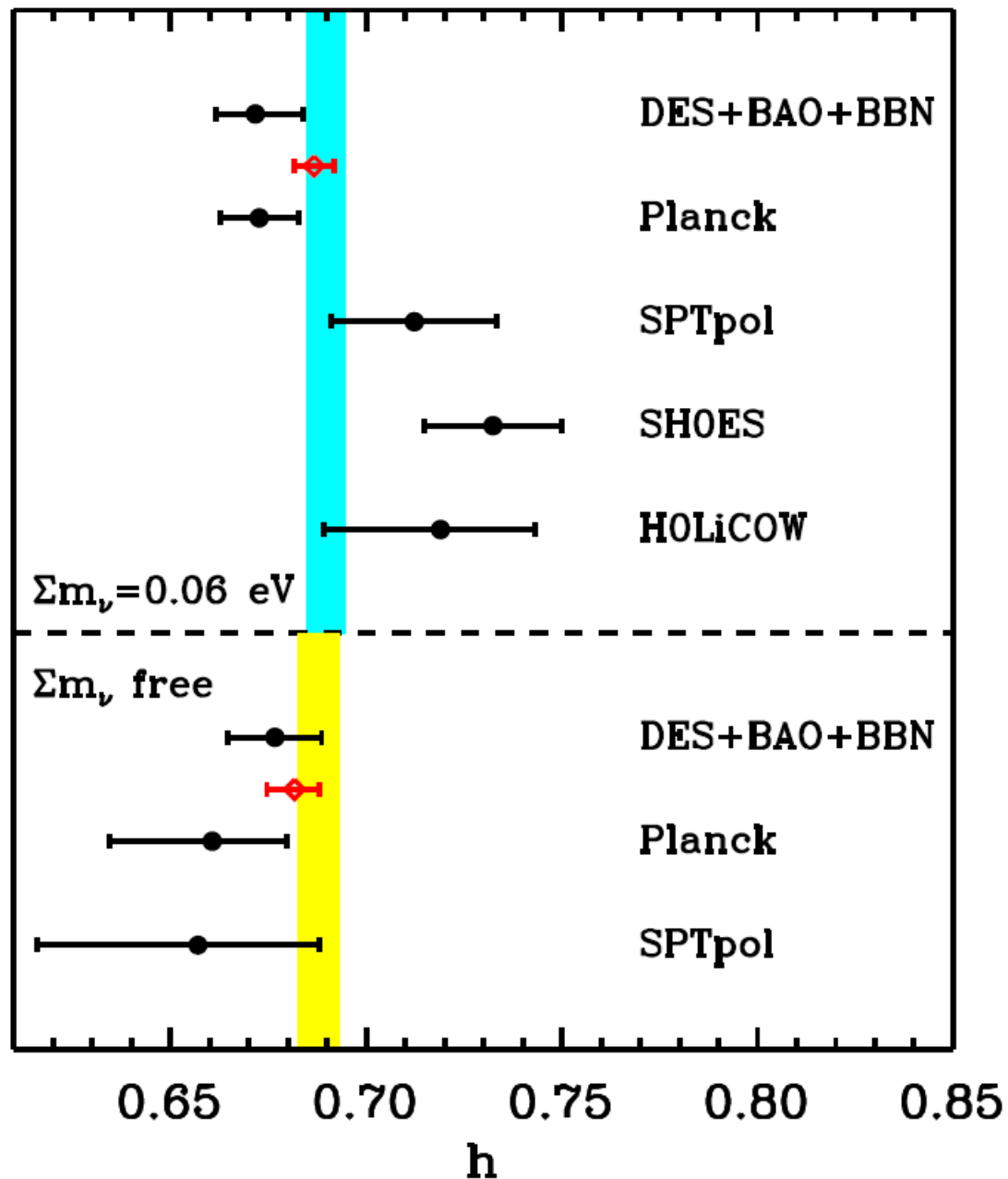
Other Results; Hubble parameter measurement combining BAO, BBN and DES 3x2pt.
Independent determination



DES Y1 3x2pt Cosmology

No significant
tensión found
in the
measurements

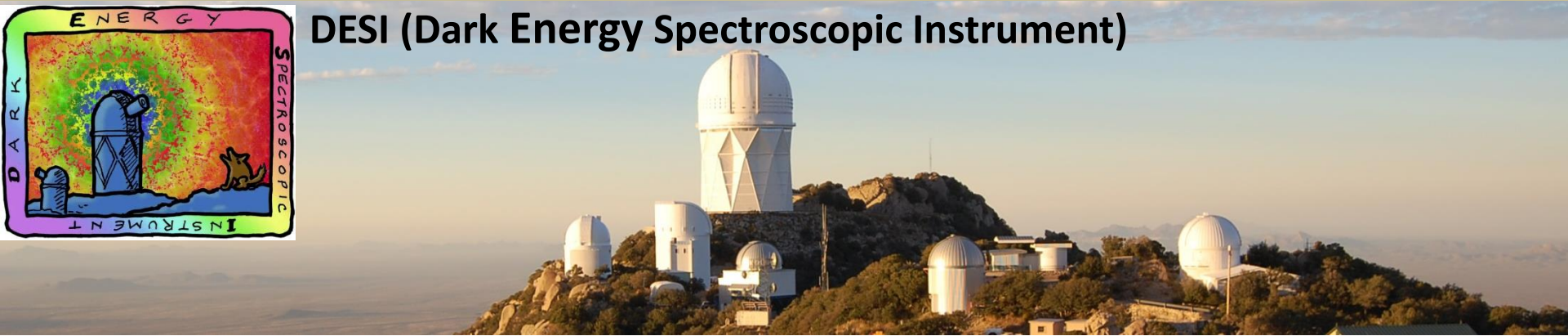
... yet?



Future Projects: DESI



DESI (Dark Energy Spectroscopic Instrument)



The DESI collaboration is building:

A new corrector for the Mayall telescope at Kitt Peak (8 deg² FOV)

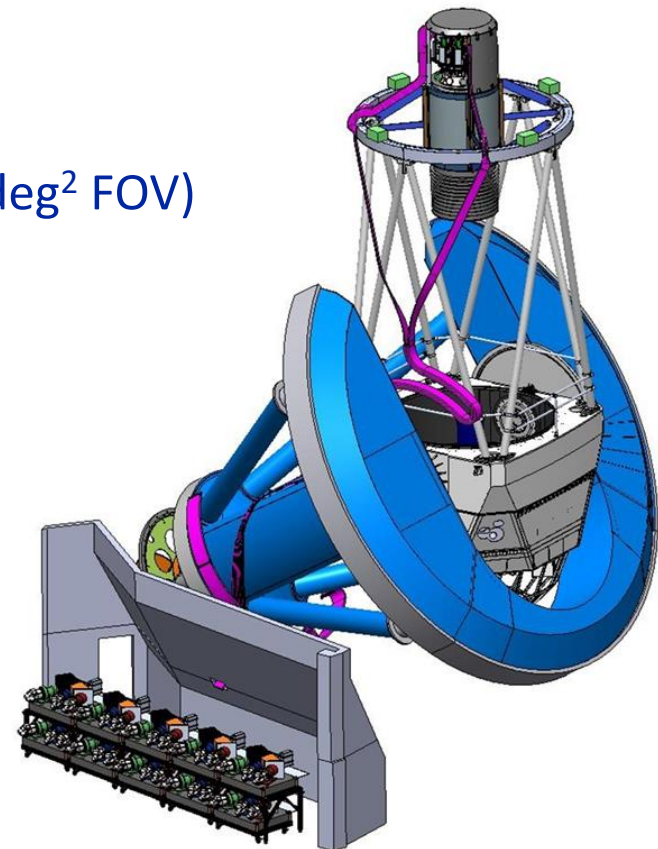
A new top ring, barrel and hexapod

A focal plane with 5000 robots fiber positioner

10 spectrographs, following the BOSS design

Instrument control and data process systems

**DESI will start the data taking in
2019**



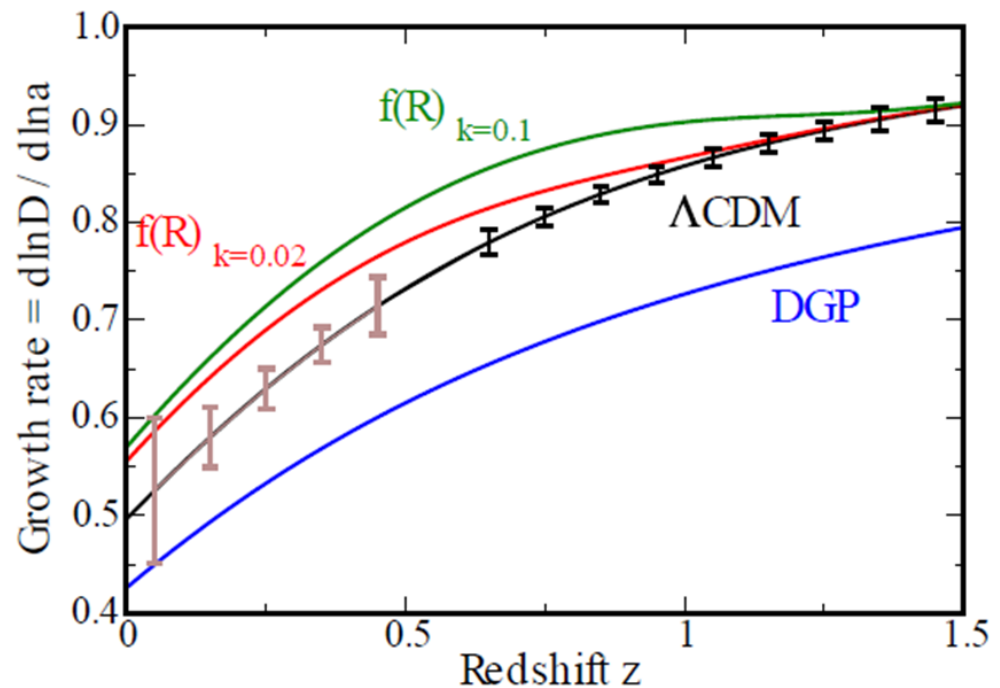
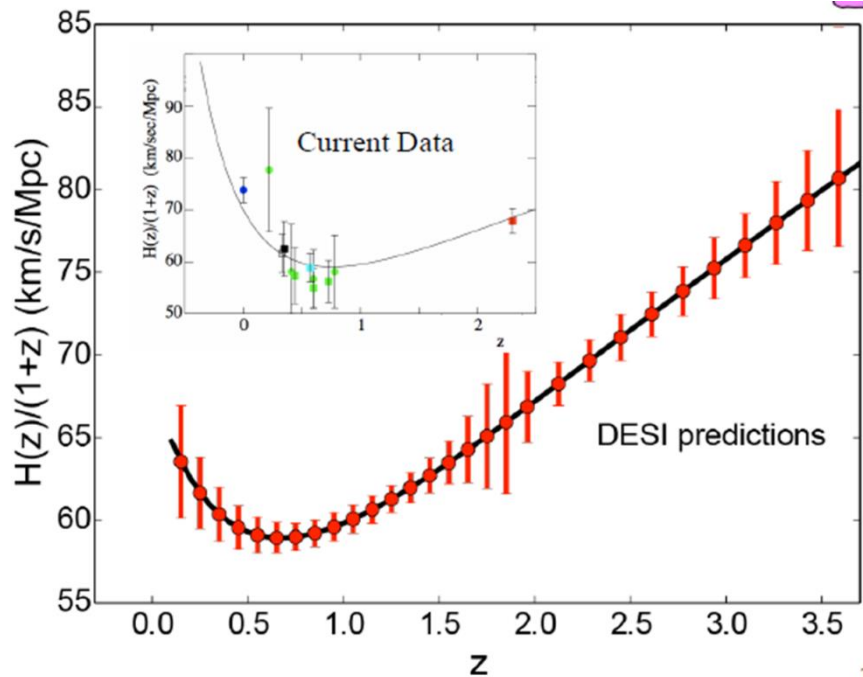
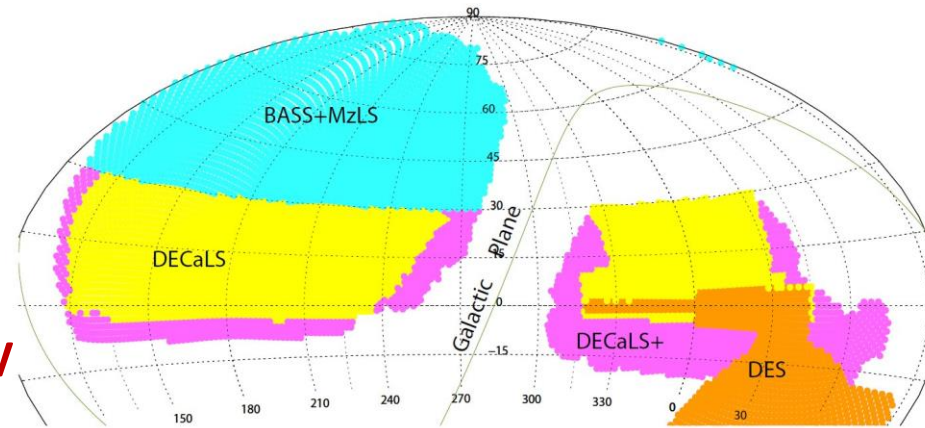
Future Projects: DESI

Scientific potential

Distances with BAO better than 0.3%

Growth factor better than 1% → GR test

Sum of neutrino masses better than 20 meV

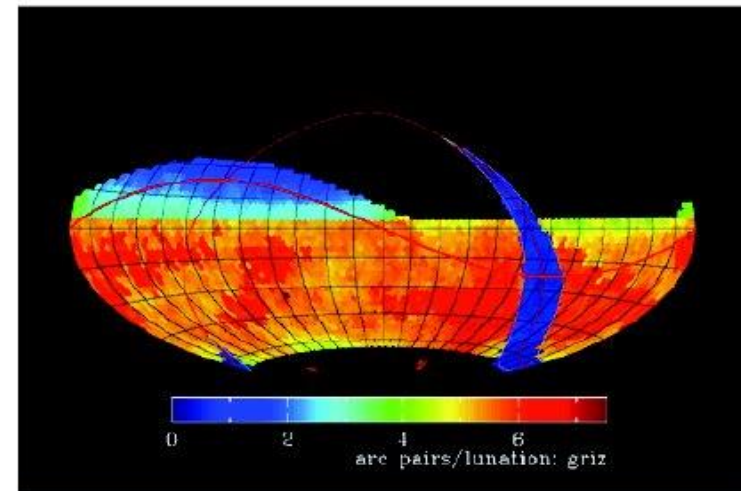
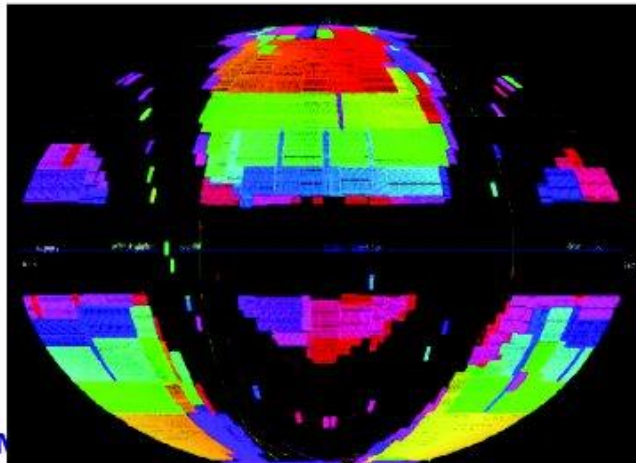


Future Projects: Euclid & LSST



FoM ~ 1500 , -4000 (all)
Main probes: WL & Galaxie clustering (BAO,RSD) (spectro))
European lead project / ESA
Participation of NASA
~ 1000 members
Space telescope / 1.2 m mirror
Launch : Q4 2020
Mission length : 6 years
1 exposure depth : 24 mag
Survey Area : 15 000 sq deg (.36 sky)
Filters : 1 Visible(550-900nm)+ 3 IR (920-2000 nm) + NIR spectroscopy (1100 – 2000 nm)

FoM > 800
Main probes : WL, CL, SN, BAO (photo)...
US lead project / NSF-DOE
Participation of France/In2P3
~ 450 Core members + 450 to come
Ground Telescope / 6.5 m effective mirror
1st light : 2021
Observation length : 10 years
1 exposure depth : 24 mag (i)
Survey Area : 20 000 sq dg (.48 sky)
Filters : 6 filters (320-1070 nm)



Conclusions

Cosmology is in a golden era

All current data are consistent with Λ CDM: ~70% cosmological constant, ~25% of dark matter (of unknown nature) and ~5% of ordinary matter

Some open problems that affect the whole picture of physics: dark energy, dark matter, inflation, baryogenesis → Require new physics

Probing the expansion history of the Universe and the growth of structure with much better precision can provide a strong boost to the current knowledge

A number of large projects are under way or planned for the future, and hopefully, will bring significant progress

Dark matter, dark energy, baryogenesis and inflation are very important questions both for cosmology and for particle physics, since the unveiling of their physical nature can bring us to a revolution in our understanding of the cosmos